(12) INTERNATIONAL APPLICATION PUBLISHED UNDER THE PATENT COOPERATION TREATY (PCT)

(19) World Intellectual Property Organization
International Bureau

(43) International Publication Date
3 November 2016 (03.11.2016)

WIPO | PCT

(10) International Publication Number
WO 2016/176665 A1

(51) International Patent Classification:
A01N 57/00 (2006.01) *A01N 57/10* (2006.01)

(21) International Application Number:
PCT/US2016/030317

(22) International Filing Date:
29 April 2016 (29.04.2016)

(25) Filing Language: English

(26) Publication Language: English

(30) Priority Data:

62/154,699	29 April 2015 (29.04.2015)	US
62/155,451	30 April 2015 (30.04.2015)	US
62/158,469	7 May 2015 (07.05.2015)	US
62/192,940	15 July 2015 (15.07.2015)	US
62/192,944	15 July 2015 (15.07.2015)	US
62/252,085	6 November 2015 (06.11.2015)	US
62/252,916	9 November 2015 (09.11.2015)	US
62/265,696	10 December 2015 (10.12.2015)	US
62/265,658	10 December 2015 (10.12.2015)	US
62/265,774	10 December 2015 (10.12.2015)	US
62/265,663	10 December 2015 (10.12.2015)	US
62/323,572	15 April 2016 (15.04.2016)	US
62/323,576	15 April 2016 (15.04.2016)	US

(71) Applicant: **RADIUS HEALTH, INC.** [US/US]; 950 Winter Street, Waltham, Massachusetts 02451 (US).

(72) Inventors: **GARNER, Fiona**; 950 Winter Street, Waltham, Massachusetts 02451 (US). **HATTERSLEY, Gary**; 14 Woodman Drive, Stow, Massachusetts 01775 (US).

(74) Agent: **WANG, Yingli**; Perkins Coie LLP, P.O. Box 1247, Seattle, Washington 98111-1247 (US).

(81) Designated States *(unless otherwise indicated, for every kind of national protection available)*: AE, AG, AL, AM, AO, AT, AU, AZ, BA, BB, BG, BH, BN, BR, BW, BY, BZ, CA, CH, CL, CN, CO, CR, CU, CZ, DE, DK, DM, DO, DZ, EC, EE, EG, ES, FI, GB, GD, GE, GH, GM, GT, HN, HR, HU, ID, IL, IN, IR, IS, JP, KE, KG, KN, KP, KR, KZ, LA, LC, LK, LR, LS, LU, LY, MA, MD, ME, MG, MK, MN, MW, MX, MY, MZ, NA, NG, NI, NO, NZ, OM, PA, PE, PG, PH, PL, PT, QA, RO, RS, RU, RW, SA, SC, SD, SE, SG, SK, SL, SM, ST, SV, SY, TH, TJ, TM, TN, TR, TT, TZ, UA, UG, US, UZ, VC, VN, ZA, ZM, ZW.

(84) Designated States *(unless otherwise indicated, for every kind of regional protection available)*: ARIPO (BW, GH, GM, KE, LR, LS, MW, MZ, NA, RW, SD, SL, ST, SZ, TZ, UG, ZM, ZW), Eurasian (AM, AZ, BY, KG, KZ, RU, TJ, TM), European (AL, AT, BE, BG, CH, CY, CZ, DE, DK, EE, ES, FI, FR, GB, GR, HR, HU, IE, IS, IT, LT, LU, LV, MC, MK, MT, NL, NO, PL, PT, RO, RS, SE, SI, SK, SM, TR), OAPI (BF, BJ, CF, CG, CI, CM, GA, GN, GQ, GW, KM, ML, MR, NE, SN, TD, TG).

Declarations under Rule 4.17:

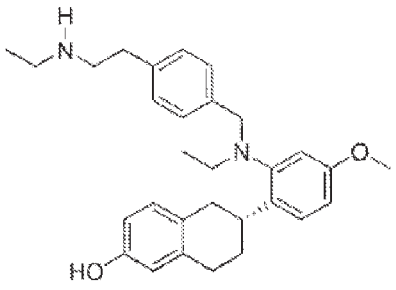
— *as to applicant's entitlement to apply for and be granted a patent (Rule 4.17(ii))*

— *as to the applicant's entitlement to claim the priority of the earlier application (Rule 4.17(iii))*

Published:

— *with international search report (Art. 21(3))*

(54) **Title**: METHODS OF TREATING CANCER



(I)

(57) **Abstract**: Disclosed herein are methods of inhibiting tumor growth or producing tumor regression in a subject having a drug-resistant estrogen receptor alpha positive cancer or a mutant estrogen receptor alpha positive cancer. The methods entail administering to the subject a therapeutically effective amount of RAD 1901 having the structure (I) or a salt or solvate thereof.

WO 2016/176665 A1

METHODS FOR TREATING CANCER

CROSS-REFERENCE TO RELATED APPLICATIONS

[0001] This application claims the benefit of U.S. Provisional Application No. 62/154,699, filed April 29, 2015, U.S. Provisional Application No. 62/155,451, filed April 30, 2015, U.S. Provisional Application No. 62/252,085, filed November 6, 2015, U.S. Provisional Application No. 62/265,696, filed December 10, 2015, U.S. Provisional Application No. 62/158,469, filed May 7, 2015, U.S. Provisional Application No. 62/252,916, filed November 9, 2015, U.S. Provisional Application No. 62/265,774, filed December 10, 2015, U.S. Provisional Application No. 62/192,940, filed July 15, 2015, U.S. Provisional Application No. 62/265,658, filed December 10, 2015, U.S. Provisional Application No. 62/323,572, filed April 15, 2016, U.S. Provisional Application No. 62/192,944, filed July 15, 2015, U.S. Provisional Application No. 62/265,663, filed December 10, 2015, and U.S. Provisional Application No. 62/323,576, filed April 15, 2016, all of which are incorporated herein by reference in their entireties.

BACKGROUND

[0002] Breast cancer is divided into three subtypes based on expression of three receptors: estrogen receptor (ER), progesterone receptor (PR), and human epidermal growth factor receptor-2 (Her2). Overexpression of ERs is found in many breast cancer patients. ER-positive (ER+) breast cancers comprise two-thirds of all breast cancers. Other than breast cancer, estrogen and ERs are associated with, for example, ovarian cancer, colon cancer, prostate cancer and endometrial cancer.

[0003] ERs can be activated by estrogen and translocate into the nucleus to bind to DNA, thereby regulating the activity of various genes. See, e.g., Marino et al., "Estrogen Signaling Multiple Pathways to Impact Gene Transcription," *Curr. Genomics* 7(8): 497-508 (2006); and Heldring et al., "Estrogen Receptors: How Do They Signal and What Are Their Targets," *Physiol. Rev.* 87(3): 905-931 (2007).

[0004] Agents that inhibit estrogen production, such as aromatase inhibitors (AIs, e.g., letrozole, anastrozole and aromasin), or those that directly block ER activity, such as selective estrogen receptor modulators (SERMs, e.g., tamoxifen, toremifene, droloxifene, idoxifene, raloxifene, lasofoxifene, arzoxifene, miproxifene, levormeloxifene, and EM-652 (SCH 57068)) and selective estrogen receptor degraders (SERDs, e.g., fulvestrant, TAS-108 (SR16234), ZK191703, RU58668, GDC-0810 (ARN-810), GW5638/DPC974, SRN-927, ICI182782 and

AZD9496), have been used previously or are being developed in the treatment of ER-positive breast cancers.

[0005] SERMs and AIs are often used as a first-line adjuvant systemic therapy for ER-positive breast cancer. Tamoxifen is currently used for both early and advanced ER-positive breast cancer in pre- and post-menopausal women. However, tamoxifen may have serious side effects such as blood clotting and stroke. Tamoxifen may cause bone thinning in pre-menopausal women, although it may prevent bone loss in post-menopausal women. As tamoxifen acts as a partial agonist on the endometrium, it also increases risk of endometrial cancer.

[0006] AIs suppress estrogen production in peripheral tissues by blocking the activity of aromatase, which turns androgen into estrogen in the body. However, AIs cannot stop the ovaries from making estrogen. Thus, AIs are mainly used to treat post-menopausal women. Furthermore, as AIs are much more effective than tamoxifen with fewer serious side effects, AIs may also be used to treat pre-menopausal women with their ovarian function suppressed. See, e.g., Francis et al., "Adjuvant Ovarian Suppression in Premenopausal Breast Cancer," the *N. Engl. J. Med.*, 372:436-446 (2015).

[0007] While initial treatment with these agents may be successful, many patients eventually relapse with drug-resistant breast cancers. Mutations affecting the ER have emerged as one potential mechanism for the development of this resistance. See, e.g., Robinson et al., "Activating ESR1 mutations in hormone-resistant metastatic breast cancer," *Nat Genet.* 45:1446–51 (2013). Mutations in the ligand-binding domain (LBD) of ER are found in 21% of metastatic ER-positive breast tumor samples from patients who received at least one line of endocrine treatment. Jeselsohn, et al., "ESR1 mutations—a mechanism for acquired endocrine resistance in breast cancer," *Nat. Rev. Clin. Oncol.*, 12:573-83 (2015).

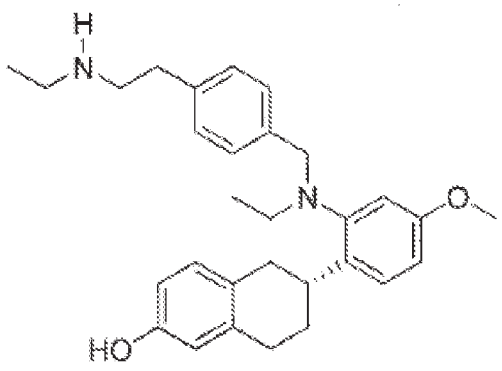
[0008] Fulvestrant is currently the only SERD approved for the treatment of ER-positive metastatic breast cancers with disease progression following antiestrogen therapy. Despite its clinical efficacy, the utility of fulvestrant has been limited by the amount of drug that can be administered in a single injection and by reduced bioavailability. Imaging studies using 18F-fluoroestradiol positron emission tomography (FES-PET) suggest that even at the 500 mg dose level, some patients may not have complete ER inhibition, and insufficient dosing may be a reason for therapy failure.

[0009] Another challenge associated with estrogen-directed therapies is that they may have undesirable effects on uterine, bone, and other tissues. The ER directs transcription of estrogen-responsive genes in a wide variety of tissues and cell types. These effects can be particularly pronounced as endogenous levels of estrogen and other ovarian hormones diminish during menopause. For example, tamoxifen can cause bone thinning in pre-menopausal women and increase the risk of endometrial cancer because it acts as a partial agonist on the endometrium. In post-menopausal women, AIs can cause more bone loss and more broken bones than tamoxifen. Patients treated with fulvestrant may also be exposed to the risk of osteoporosis due to its mechanism of action.

[0010] Therefore, there remains a need for more durable and effective ER-targeted therapies to overcome some of the challenges associated with current endocrine therapies and to combat the development of resistance.

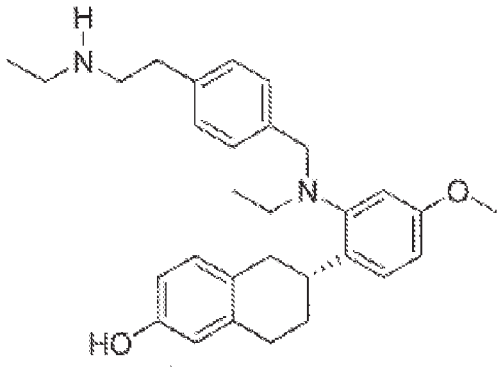
BRIEF SUMMARY OF THE INVENTION

[0011] In one aspect, the disclosure relates to a method of inhibiting tumor growth or producing tumor regression in a subject having a drug-resistant estrogen receptor alpha positive cancer. The method entails administering to the subject a therapeutically effective amount of RAD1901 having the structure:



or a salt or solvate thereof.

[0012] In another aspect, the disclosure relates to a method of inhibiting tumor growth or producing tumor regression in a subject having a mutant estrogen receptor alpha positive cancer. The method entails administering to the subject a therapeutically effective amount of RAD1901 having the structure:



or a salt or solvate thereof.

[0013] In some embodiments, the cancer is selected from the group consisting of breast cancer, uterine cancer, ovarian cancer, and pituitary cancer. In some embodiments, the cancer is a metastatic cancer. In some embodiments, the cancer is positive for the mutant estrogen receptor alpha comprising one or more mutations selected from the group consisting of $Y537X_1$, $L536X_2$, P535H, V534E, S463P, V392I, E380Q and combinations thereof, wherein X_1 is S, N, or C, D538G; and X_2 is R or Q. For example, the mutation is Y537S.

[0014] In some embodiments, the tumor is resistant to a drug selected from the group consisting of anti-estrogens, aromatase inhibitors, and combinations thereof. For example, the anti-estrogen is tamoxifen or fulvestrant, and the aromatase inhibitor is aromasin.

BRIEF DESCRIPTION OF DRAWINGS AND TABLES

[0015] Figure 1: RAD1901 inhibited tumor growth in various patient-derived xenograft (PDx) models regardless of ESR1 status and prior endocrine therapy. Percentage of tumor growth inhibition (TGI) in PDx models treated with RAD1901 is shown.

[0016] Figures 2A-E: RAD1901 demonstrated dose-dependent inhibition of tumor growth and tumor regression in wild-type (WT) ERα MCF-7 mouse xenograft models (PR+, Her2-). (Figure 2A): Box and whisker plots showed the day 40 tumor volume by group in MCF-7 mouse xenograft models treated with vehicle control, RAD1901 (0.3, 1, 3, 10, 30, and 60 mg/kg p.o., q.d.), tamoxifen (TAM) (1 mg/dose, s.c., q.o.d.), and fulvestrant (FUL) (0.5 mg/dose, s.c., q.d.); (Figure 2B): Median tumor volumes over time in MCF-7 mouse xenograft models treated with vehicle control, RAD1901 (60, 90, and 120 mg/kg, p.o. q.d.), tamoxifen (1 mg/dose, s.c., q.o.d.), and fulvestrant (0.5 mg/dose, s.c., q.d.) (Figure 2C): Tumor volumes from individual animals at day 42 in MCF-7 mouse xenograft models treated with vehicle control, RAD1901 (60, 90, and

120 mg/kg, p.o., q.d.), tamoxifen (1 mg/dose, s.c., q.o.d.), and fulvestrant (0.5 mg/dose, s.c., q.d.); (Figure 2D): Median tumor volumes over time in MCF-7 mouse xenograft models treated with vehicle control, RAD1901 (RAD) (0.3, 1, 3, 10, 30, and 60 mg/kg p.o., q.d.), tamoxifen (1 mg/dose, s.c., q.o.d.), and fulvestrant (0.5 mg/dose, s.c., q.d.); (Figure 2E): Percent group mean body weight changes from Day 1 in MCF-7 mouse xenograft models treated with vehicle control, RAD1901 (RAD) (0.3, 1, 3, 10, 30, and 60 mg/kg p.o., q.d.), tamoxifen (1 mg/dose, s.c., q.o.d.), and fulvestrant (0.5 mg/dose, s.c., q.d.).

[0017] Figures 3A-B: RAD1901 demonstrated tumor growth inhibition and tumor regression in WT ERα MCF-7 xenograft models (PR+, Her2-). (Figure 3A): Tumor growth of MCF-7 xenograft models treated with vehicle control, RAD1901 (30 and 60 mg/kg, p.o., o.d.) and fulvestrant (3 mg/dose, s.c., qwk); (Figure 3B): Change in individual tumor size from baseline to end of study in MCF-7 xenograft models treated with vehicle control, RAD1901 (30 and 60 mg/kg, p.o., o.d.) and fulvestrant (3 mg/dose, s.c., qwk).

[0018] Figures 4A-B: RAD1901 demonstrated tumor growth inhibition and tumor regression in WT ERα PDx-4 models (PR+, Her2-, treatment naïve). (Figure 4A): Tumor growth of PDx-4 models treated with vehicle control, RAD1901 (30, 60 and 120 mg/kg, p.o., o.d.) and fulvestrant (3 mg/dose, s.c., qwk); (Figure 4B): Change in individual tumor size from baseline to end of study in PDx-4 models treated with vehicle control, RAD1901 (30, 60, 120 mg/kg, p.o., o.d.) and fulvestrant (3 mg/dose, s.c., qwk).

[0019] Figure 5: Efficacy of RAD1901 sustained at least two months after RAD1901 treatment ended while estradiol treatment continued in WT ERα PDx-4 models (PR+, Her2-, treatment naïve). Tumor growth of PDx-4 models treated with vehicle control, RAD1901 (30 mg/kg, p.o., q.d.), and fulvestrant (1 mg/dose, s.c., qwk).

[0020] Figure 6: RAD1901 demonstrated tumor growth inhibition in WT ERα PDx-2 models (PR+, Her2+, treatment naïve). Tumor growth of PDx-2 models treated with vehicle control, RAD1901 (60 mg/kg, p.o., q.d.), fulvestrant (3 mg/dose, s.c., qwk).and a combination of (60 mg/kg, p.o., q.d.) and fulvestrant (3 mg/dose, s.c., qwk). n = 8-10/group.

[0021] Figures 7A-B: RAD1901 demonstrated tumor growth inhibition and tumor regression in WT ERα PDx-11 models (PR+, Her2+, previously treated with aromatase inhibitor, fulvestrant, and chemotherapy). (Figure 7A): Tumor growth of PDx-11 models treated with vehicle control, RAD1901 (60 mg/kg, p.o., q.d.), and fulvestrant (3 mg/dose, s.c., qwk); (Figure

7B): Change in individual tumor size from baseline to end of study in PDx-11 models treated with vehicle control, RAD1901 (60 mg/kg, p.o., q.d.), and fulvestrant (3 mg/dose, s.c., qwk). n = 8-10/group.

[0022] Figure 8: RAD1901 demonstrated tumor growth inhibition and tumor regression at various doses in WT ERα PDx-12 models (PR+, Her2+, , treatment naïve). Tumor growth of PDx-11 models treated with vehicle control, RAD1901 (30, and 60 mg/kg, p.o., q.d.), and fulvestrant (1 mg/dose, s.c., qwk).

[0023] Figures 9A-C: RAD1901 demonstrated tumor growth inhibition in mutant (Y537S) ERα PDx-5 models (PR+, Her2+, prior treatment with aromatase inhibitor). (Figure 9A): Tumor growth of PDx-11 models treated with vehicle control, RAD1901 (60, 120 mg/kg, p.o., q.d.), and fulvestrant (3 mg/dose, s.c., qwk); (Figure 9B): Change in individual tumor size from baseline to day 17 in PDx-5 models treated with vehicle control, RAD1901 (60, 120 mg/kg, p.o., q.d.), and fulvestrant (3 mg/dose, s.c., qwk); (Figure 9C): Change in individual tumor size from baseline to day 56 in PDx-5 models treated with RAD1901 (60, 120 mg/kg, p.o., q.d.).

[0024] Figures 10A-B: RAD1901 demonstrated tumor growth inhibition and tumor regression in mutant (Y537S) ERα PDx-6 models (PR+, Her2:1+, previously treated with tamoxifen, aromatase inhibitor, and fulvestrant). (Figure 10A): Tumor growth of PDx-6 models treated with vehicle control, RAD1901 (30, 60, and 120 mg/kg p.o., q.d.), tamoxifen (1 mg/dose, s.c., q.o.d.), and fulvestrant (1 mg/dose, s.c., qwk); (Figure 10B): Change in individual tumor size from baseline to end of study in PDx-6 models treated with vehicle control, RAD1901 (30, 60, and 120 mg/kg p.o., q.d.), and fulvestrant (1 mg/dose, s.c., qwk).

[0025] Figure 11: Pharmacokinetic analysis of fulvestrant in nude mice. The plasma concentration of fulvestrant at 1 mg/dose (solid diamond), 3 mg/dose (solid circle), and 5 mg/dose (solid triangle) is shown. The nude mice were dosed subcutaneously with fulvestrant on Day 1 and the second dose on Day 8. The plasma concentration of fulvestrant was monitored at the indicated time points for up to 168 hours after the second dose.

[0026] Figure 12: Effect of RAD1901 and fulvestrant (Faslodex) on mouse survival in an intracranial MCF-7 tumor model.

[0027] Figure 13: Phase 1 study of RAD1901 treatment for ER+ advanced breast cancer.

[0028] Figures 14A-B: Prior treatment history and RAD1901 treatment of subjects enrolled in a Phase 1 study of RAD1901 treatment for ER+ advanced breast cancer. (Figure 14A): Prior cancer treatment; (Figure 14B): RAD1901 treatment.

[0029] Figures 15A-C: A representative image of FES-PET scan of the uterus of a subject treated with 200 and 500 mg RAD1901 p.o., q.d., and change of the ER engagement after the RAD1901 treatments. (Figure 15A): Transversal view of uterus CT scan before 200 mg RAD1901 treatment (a) and after (c), and transversal view of uterus FES-PET scan before the RAD1901 treatment (b) and after (d); (Figure 15B): Sagittal view of uterus CT scan before 500 mg RAD1901 treatment (top (a) panel) and after (bottom (a) panel), sagittal view of uterus FES-PET scan before the RAD1901 treatment (top (b) panel) and after (bottom (b) panel), transversal view of uterus CT scan before the RAD1901 treatment (top (c) panel) and after (bottom (c) panel), transversal view of uterus FES-PET scan before the RAD1901 treatment (top (d) panel) and after (bottom (d) panel); (Figure 15C): % change of ER engagement after the RAD1901 treatments of Subjects 1-3 (200 mg) and Subjects 4-7 (500 mg) compared to baseline (before RAD1901 treatment).

[0030] Figures 16A-B: A representative image of FES-PET scan of the uterus (Figure 16A) and pituitary (Figure 16B) before (Baseline) and after (Post-treatment) RAD1901 treatment (500 mg). (a) Lateral cross-section; (b) longitude cross-section; and (c) longitude cross-section.

[0031] Figures 17A-B: RAD1901 treatment resulted in complete ER degradation and inhibited ER signaling in MCF-7 cell lines (Figure 17A) and T47D cell lines (Figure 17B) *in vitro*. The ER expression was shown in both cell lines treated with RAD1901 and fulvestrant at various concentrations of 0.001 μM, 0.01 μM, 0.1 μM and 1 μM, respectively. ER signaling was shown by three ER target genes tested: *PGR*, *GREB1* and *TFF1*.

[0032] Figures 18A-C: RAD1901 treatment resulted in ER degradation and abrogation of ER signaling in MCF-7 xenograft models. (Figure 18A): Western blot showing PR and ER expression in the MCF-7 xenograft models treated with vehicle control, RAD1901 at 30 and 60 mg/kg, and fulvestrant at 3mg/dose, 2 hour or 8 hour after the last dose; (Figure 18B): ER protein expression in the MCF-7 xenograft models treated with vehicle control, RAD1901 at 30 and 60 mg/kg, and fulvestrant at 3mg/dose, 2 hour after the last dose; (Figure 18C): PR protein expression in the MCF-7 xenograft models treated with vehicle control, RAD1901 at 30 and 60 mg/kg, and fulvestrant at 3mg/dose, 8 hour after last dose.

[0033] Figures 19A-C: RAD1901 treatment resulted in a rapid decrease in PR in MCF-7 xenograft models. (Figure 19A): Western blot showing PR expression in MCF-7 xenograft models treated with vehicle control and RAD1901 at 30, 60, and 90 mg/kg, at 8 hours or 12 hours after single dose; (Figure 19B): Western blot showing PR expression in MCF-7 xenograft models treated with vehicle control and RAD1901 at 30, 60, and 90 mg/kg, at 4 hours or 24 hours after the 7th dose; (Figure 19C): Dose-dependent decrease in PR expression in MCF-7 xenograft models treated with RAD1901 at 30, 60, and 90 mg/kg.

[0034] Figures 20A-B: RAD1901 treatment resulted in a rapid decrease in proliferation in MCF-7 xenograft models. (Figure 20A): A representative photograph of a sectioned tumor harvested from MCF-7 xenograft models treated with vehicle control and RAD1901 at 90 mg/kg, 8 hours after single dose and 24 hours after the 4th dose, stained for proliferation marker Ki-67; (Figure 20B): Histogram showing decrease of proliferation marker Ki-67 in MCF-7 xenograft models treated with vehicle control and RAD1901 at 90 mg/kg, 8 hours after single dose and 24 hours after the 4th dose.

[0035] Figure 21: RAD1901 treatment at 30, 60, and 120 mg/kg decreased Ki67 more significantly than fulvestrant (1 mg/animal) in end of study tumors of PDx-4 models four hours on the last day of a 56 day efficacy study.

[0036] Figure 22: RAD1901 treatment at 60 and 120 mg/kg resulted in reduced ER signaling *in vivo* in PDx-5 models with decreased PR expression.

[0037] Figures 23A-D: Effect of RAD1901 on uterine tissue in newly weaned female Sprague-Dawley rats. (Figure 23A): Uterine wet weights of rats euthanized 24 hours after the final dose; (Figure 23B): Epithelial height in tissue sections of the uterus; (Figure 23C): Representative sections of Toluidine Blue O-stained uterine tissue at 400x magnification, arrows indicate uterine epithelium; (Figure 23D): Total RNA extracted from uterine tissue and analyzed by quantitative RT-PCR for the level of complement C3 expression relative to the 18S ribosomal RNA housekeeping gene.

[0038] Figure 24: Plasma pharmacokinetic results of RAD1901 at 200, 500, 750, and 1000 mg/kg after dosing on Day 7.

[0039] Figure 25: 3ERT (I).

[0040] Figure 26: 3ERT (II).

[0041] Figure 27: Superimpositions of the ERα LBD-antagonist complexes summarized in Table 13.

[0042] Figures 28A-B: Modeling of (Figure 28A) RAD1901-1R5K; and (Figure 28B) GW5-1R5K.

[0043] Figures 29 A-B: Modeling of (Figure 29A) RAD1901-1SJ0; and (Figure 29B) E4D-1SJ0.

[0044] Figures 30 A-B: Modeling of (Figure 30A) RAD1901-2JFA; and (Figure 30B) RAL-2JFA.

[0045] Figures 31 A-B: Modeling of (Figure 31A) RAD1901-2BJ4; and (Figure 31B) OHT-2BJ4.

[0046] Figures 32 A-B: Modeling of (Figure 32A) RAD1901-2IOK; and (Figure 32B) IOK-2IOK.

[0047] Figure 33: Superimpositions of the RAD1901 conformations resulted from IFD analysis with 1R5K and 2OUZ.

[0048] Figure 34: Superimpositions of the RAD1901 conformations resulted from IFD analysis with 2BJ4 and 2JFA.

[0049] Figure 35A-B: Superimpositions of the RAD1901 conformations resulted from IFD analysis with 2BJ4, 2JFA and 1SJ0.

[0050] Figures 36A-C: IFD of RAD1901 with 2BJ4.

[0051] Figures 37A-C: Protein Surface Interactions of RAD1901 docked in 2BJ4 by IFD.

[0052] Figures 38A-C: IFD of Fulvestrant with 2BJ4.

[0053] Figures 39A-B: IFD of Fulvestrant and RAD1901 with 2BJ4.

[0054] Figures 40A-B: Superimposions of IFD of Fulvestrant and RAD1901 with 2BJ4.

[0055] Figure 41: RAD1901 in vitro binding assay with ERα constructs of WT and LBD mutant.

[0056] Figure 42: Estrogen Receptor.

[0057] Table 1. Key baseline demographics of Phase 1 study of RAD1901 for the treatment of ER+ advanced breast cancer.

[0058] Table 2. Treatment related AEs in a Phase 1 study of RAD1901 for the treatment of ER+ advanced breast cancer.

[0059] Table 3. RAD1901 levels in plasma, tumor and brain of mice implanted with MCF7 cells after treated for 40 days. *BLQ: below the limit quantitation.

[0060] Table 4. SUV for uterus, muscle, and bone for a human subject treated with 200 mg dose PO one/day for six days.

[0061] Table 5. SUV for uterus, muscle, and bone for human subjects (n=4) treated with 500 mg dose PO one/day for six days.

[0062] Table 6. Effect of RAD1901 on BMD in ovariectomized rats. Adult female rats underwent either sham or ovariectomy surgery before treatment initiation with vehicle, E2 (0.01 mg/kg) or RAD1901 (3 mg/kg) once daily (n=20 per treatment group). BMD was measured by dual emission x-ray absorptiometry at baseline and after 4 weeks of treatment. Data are expressed as mean ± SD. *$P < 0.05$ versus the corresponding OVX+Veh control. BMD, bone mineral density; E2, beta estradiol; OVX, ovariectomized; Veh, vehicle.

[0063] Table 7. Effect of RAD1901 on femur microarchitecture in ovariectomized rats. aAdult female rats underwent either sham or ovariectomy surgery before treatment initiation with vehicle, E2 (0.01 mg/kg) or RAD1901 (3 mg/kg) once daily (n=20 per treatment group). After 4 weeks, Bone microarchitecture was evaluated using microcomputed tomography. Data are expressed as mean ± SD. *$P < 0.05$ versus the corresponding OVX+Veh control. ABD, apparent bone density; BV/TV, bone volume density; ConnD, connectivity density; E2, beta estradiol; OVX, ovariectomized; TbN, trabecular number; TbTh, trabecular thickness; TbSp, trabecular spacing; Veh, vehicle.

[0064] Table 8. Key baseline demographics of Phase 1 dose escalation study of RAD1901.

[0065] Table 9. Most frequent (>10%) treatment related AEs in a Phase 1 dose escalation study of RAD1901. AEs graded as per CTCAE v4.0. Any patient with multiple scenarios of a same preferred term was counted only once to the most severe grade. *>10% of patients in the total active group who had any related TEAEs. n= number of subjects with at least one treatment-related AE in a given category.

[0066] Table 10. Pharmacokinetic parameters in a Phase 1 dose escalation study of RAD1901 (Day 7).

[0067] Table 11. Frequency of LBD mutations.

[0068] Table 12. Differences of ER-α LBD-antagonist complexes in residue poses versus 3ERT.

[0069] Table 13. Evaluation of structure overlap of ER-α LBD-antagonist complexes by RMSD calculations.

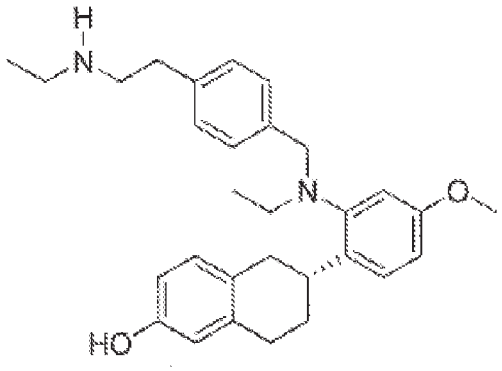
[0070] Table 14. Analysis of ligand binding in ER-α LBD-antagonist complexes.

[0071] Table 15. Model evaluation for RAD1901 docking.

[0072] Table 16. Induced Fit Docking Score of RAD1901 with 1R5K, 2IFA, 2BJ4 and 2OUZ.

DETAILED DESCRIPTION OF THE INVENTION

[0073] As set forth in the Examples section below, RAD1901 (structure below) was found to inhibit tumor growth and/or drive tumor regression in breast cancer xenograft models, regardless of ESR1 status and prior endocrine therapy (Example I(A)). The xenograft models treated had tumor expressing WT or mutant (e.g., Y537S) ERα, with high or low Her2 expression, and with or without prior endocrine therapy (e.g., tamoxifen (tam), AI, chemotherapy (chemo), Her2 inhibitors (Her2i, e.g., trastuzumab, lapatinib), bevacizumab, and/or rituximab) (Fig. 1). And, in all cases RAD1901 inhibited tumor growth. WT ER PDx models and Mutant ER PDx models may have different level of responsiveness to fulvestrant treatment. However, RAD1901 was found to inhibit tumor growth regardless of whether the PDx models were responsive to fulvestrant treatment. Thus, RAD1901 may be used as a fulvestrant replacement to treat breast cancer responsive to fulvestrant with improved tumor growth inhibition, and also to treat breast cancer less effectively treated by fulvestrant as well. For example, RAD1901 caused tumor regression in WT ER+ PDx models with varied responsiveness to fulvestrant treatment (e.g., MCF-7 cell line xenograft models, PDx-4, PDx-2 and PDx-11 models responsive to fulvestrant treatment, and PDx-12 models hardly responsive to fulvestrant treatment), and mutant (e.g., Y537S) ER+ PDx models with varied level of responsiveness to fulvestrant treatment (e.g., PDx-6 models responsive to fulvestrant treatment, and PDx-5 models hardly responsive to fulvestrant treatment). RAD1901 showed sustained efficacy in inhibiting tumor growth after treatment ended while estradiol treatment continued (e.g., PDx-4 model). The results provided herein also show that RAD1901 can be delivered to brain (Example II), and said delivery improved mouse survival in an intracranial tumor model expressing wild-type ERα (MCF-7 xenograft model, Example I(B)). RAD1901 is a powerful anti-ER+ breast cancer therapy.



RAD1901.

[0074] RAD1901 is also likely to cause fewer side effects compared to other endocrine therapies (e.g. other SERMs such as tamoxifen and SERDs such as fulvastrant). For example, tamoxifen may increase risk of endometrial cancer. Tamoxifen may also cause bone thinning in pre-menopausal women. Fulvestrant may also increase the risk of bone loss in treated patients. RAD1901 is unlikely to have similar side effect. RAD1901 was found to preferentially accumulate in tumor with a RAD1901 level in tumor v. RAD1901 level in plasma (T/P ratio) of up to about 35 (Example II). Standardized uptake values (SUV) for uterus, muscle and bone were calculated for human subjects treated with RAD1901 at a dose of about 200 mg up to about 500 mg q.d. (Example III(A)). Post-dose uterine signals were close to levels from "non-target tissues" (tissues that do not express estrogen receptor), suggesting a complete attenuation of FES-PET uptake post RAD1901 treatment. Almost no change was observed in pre- versus post-treatment PET scans in tissues that did not significantly express estrogen receptor (e.g., muscles, bones) (Example III(A)). RAD1901 treatments antagonized estradiol stimulation of uterine tissues in ovariectomized (OVX) rats (Example IV(A)), and largely preserved bone quality of the treated subjects. Thus, RAD1901 treatment is not likely to impair bone structure of patients like other endocrine therapies may. For example, OVX rats treated with RAD1901 showed maintained BMD and femur microarchitecture (Example IV(A)). Thus, the RAD1901 treatment may be especially useful for patients having osteoporosis or a higher risk of osteoporosis.

[0075] Furthermore, RAD1901 was found to degrade wild-type ERα and abrogate ER signaling *in vivo* in MCF-7 cell line xenograft models, and showed a dose-dependent decrease in PR in these MCF-7 cell line xenograft models (Example III(B)). RAD1901 decreased proliferation in MCF-7 cell line xenograft models and PDx-4 models as evidenced by decrease in

proliferation marker Ki67 in tumors harvested from the treated subjects. RAD1901 also decreased ER signaling *in vivo* in a Mutant ER PDx model that was hardly responsive to fulvestrant treatment (Example III(B)).

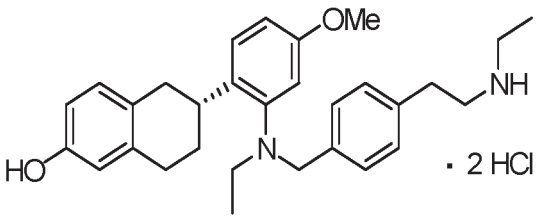
[0076] The unexpected efficacy of RAD1901 to tumors hardly responsive to fulvestrant treatments and in tumors expressing mutant ERα may be due to the unique interactions between RAD1901 and ERα. Structural models of ERα bound to RAD1901 and other ERα-binding compounds were analyzed to obtain information about the specific binding interactions (Example V). Computer modeling showed that RAD1901-ERα interactions are not likely to be affected by mutants of LBD of ERα, e.g., Y537X mutant wherein X was S, N, or C; D538G; and S463P, which account for about 81.7% of LBD mutations found in a recent study of metastatic ER positive breast tumor samples from patients who received at least one line of endocrine treatment (Table 11, Example V). This resulted in identification of specific residues in the C-terminal ligand-binding domains of ERα that are critical to binding, information that can be used to develop compounds that bind and antagonize not only wild-type ERα but also certain mutations and variants thereof.

[0077] Based on these results, methods are provided herein for inhibiting growth or producing regression of an ERα positive cancer or tumor in a subject in need thereof by administering to the subject a therapeutically effective amount of RAD1901 or a solvate (e.g., hydrate) or salt thereof. In certain embodiments, administration of RAD1901or a salt or solvate (e.g., hydrate) thereof has additional therapeutic benefits in addition to inhibiting tumor growth, including for example inhibiting cancer cell proliferation or inhibiting ERα activity (e.g., by inhibiting estradiol binding or by degrading ERα). In certain embodiments, the method does not provide negative effects to muscles, bones, breast, and uterus.

[0078] Provided herein are also methods of modulating and degrading ERα and mutant ERα, methods of treating conditions associated with ERα and mutant ERα activity or expression, compounds for use in these methods, and complexes and crystals of said compounds bound to ERα and mutant ERα.

[0079] In certain embodiments of the tumor growth inhibition or tumor regression methods provided herein, methods are provided for inhibiting growth or producing regression of an ERα-positive tumor in a subject in need thereof by administering to the subject a therapeutically

effective amount of RAD1901 or a salt or solvate (e.g., hydrate) thereof. In certain of these embodiments, the salt thereof is RAD1901 dihydrochloride having the structure:



RAD1901 dihydrochloride.

[0080] "Inhibiting growth" of an ERα-positive tumor as used herein may refer to slowing the rate of tumor growth, or halting tumor growth entirely.

[0081] "Tumor regression" or "regression" of an ERα-positive tumor as used herein may refer to reducing the maximum size of a tumor. In certain embodiments, administration of RAD1901 or a solvate (e.g., hydrate) or salt thereof may result in a decrease in tumor size versus baseline (i.e., size prior to initiation of treatment), or even eradication or partial eradication of a tumor. Accordingly, in certain embodiments the methods of tumor regression provided herein may be alternatively be characterized as methods of reducing tumor size versus baseline.

[0082] "Tumor" as used herein is malignant tumor, and is used interchangeably with "cancer."

[0083] Tumor growth inhibition or regression may be localized to a single tumor or to a set of tumors within a specific tissue or organ, or may be systemic (i.e., affecting tumors in all tissues or organs).

[0084] As RAD1901 is known to preferentially bind ERα versus estrogen receptor beta (ERβ), unless specified otherwise, estrogen receptor, estrogen receptor alpha, ERα, ER, wild-type ERα, and ESR1 are used interchangeably herein. "Estrogen receptor alpha" or "ERα" as used herein refers to a polypeptide comprising, consisting of, or consisting essentially of the wild-type ERα amino acid sequence, which is encoded by the gene *ESR1*. A tumor that is "positive for estrogen receptor alpha," "ERα-positive," "ER+," or "ERα+" as used herein refers to a tumor in which one or more cells express at least one isoform of ERα. In certain embodiments, these cells overexpress ERα. In certain embodiments, the patient has one or more cells within the tumor expressing one or more forms of estrogen receptor beta. In certain embodiments, the ERα-positive tumor and/or cancer is associated with breast, uterine, ovarian, or pituitary cancer. In certain of these embodiments, the patient has a tumor located in breast, uterine, ovarian, or pituitary tissue. In those embodiments where the patient has a tumor located in the breast, the

tumor may be associated with luminal breast cancer that may or may not be positive for HER2, and for HER2+ tumors, the tumors may express high or low HER2 (e.g., Fig. 1). In other embodiments, the patient has a tumor located in another tissue or organ (e.g., bone, muscle, brain), but is nonetheless associated with breast, uterine, ovarian, or pituitary cancer (e.g., tumors derived from migration or metastasis of breast, uterine, ovarian, or pituitary cancer). Accordingly, in certain embodiments of the tumor growth inhibition or regression methods provided herein, the tumor being targeted is a metastatic tumor and/or the tumor has an overexpression of ER in other organs (e.g., bones and/or muscles). In certain embodiments, the tumor being targeted is a brain tumor and/or cancer. In certain embodiments, the tumor being targeted is more sensitive to RAD1901 treatment than treatment with another SERD (e.g., fulvestrant, TAS-108 (SR16234), ZK191703, RU58668, GDC-0810 (ARN-810), GW5638/DPC974, SRN-927, ICI182782 and AZD9496), Her2 inhibitors (e.g., trastuzumab, lapatinib, ado-trastuzumab emtansine, and/or pertuzumab), chemo therapy (e.g., abraxane, adriamycin, carboplatin, cytoxan, daunorubicin, doxil, ellence, fluorouracil, gemzar, helaven, lxempra, methotrexate, mitomycin, micoxantrone, navelbine, taxol, taxotere, thiotepa, vincristine, and xeloda), aromatase inhibitor (e.g., anastrozole, exemestane, and letrozole), selective estrogen receptor modulators (e.g., tamoxifen, raloxifene, lasofoxifene, and/or toremifene), angiogenesis inhibitor (e.g., bevacizumab), and/or rituximab.

[0085] In certain embodiments of the tumor growth inhibition or regression methods provided herein, the methods further comprise a step of determining whether a patient has a tumor expressing ERα prior to administering RAD1901 or a solvate (e.g., hydrate) or salt thereof. In certain embodiments of the tumor growth inhibition or regression methods provided herein, the methods further comprise a step of determining whether the patient has a tumor expressing mutant ERα prior to administering RAD1901 or a solvate (e.g., hydrate) or salt thereof. In certain embodiments of the tumor growth inhibition or regression methods provided herein, the methods further comprise a step of determining whether a patient has a tumor expressing ERα that is responsive or non-responsive to fulvestrant treatment prior to administering RAD1901 or a solvate (e.g., hydrate) or salt thereof. These determinations may be made using any method of expression detection known in the art, and may be performed *in vitro* using a tumor or tissue sample removed from the subject.

[0086] In addition to demonstrating the ability of RAD1901 to inhibit tumor growth in tumors expressing wild-type ERα, the results provided herein show that RAD1901 exhibited the unexpected ability to inhibit the growth of tumors expressing a mutant form of ERα, namely Y537S ERα (Example I(A)). Computer modeling evaluations of examples of ERα mutations showed that none of these mutations were expected to impact the ligand binding domain nor specifically hinder RAD1901 binding (Example V(A)), e.g., ERα having one or more mutants selected from the group consisting of ERα with Y537X mutant wherein X is S, N, or C, ERα with D538G mutant, and ERα with S463P mutant. Based on these results, methods are provided herein for inhibiting growth or resulting in regression of a tumor that is positive for ERα having one or more mutants within the ligand-binding domain (LBD), selected from the group consisting of $Y537X_1$ wherein X_1 is S, N, or C, D538G, $L536X_2$ wherein X_2 is R or Q, P535H, V534E, S463P, V392I, E380Q, especially Y537S ERα, in a subject with cancer by administering to the subject a therapeutically effective amount of RAD1901 or a solvate (e.g., hydrate) or salt thereof. "Mutant ERα" as used herein refers to ERα comprising one or more substitutions or deletions, and variants thereof comprising, consisting of, or consisting essentially of an amino acid sequence with at least 80%, at least 85%, at least 90%, at least 95%, at least 97%, at least 98%, at least 99%, or at least 99.5% identity to the amino acid sequence of ERα.

[0087] In addition to inhibiting breast cancer tumor growth in an animal xenograft model, the results disclosed herein show that RAD1901 exhibits significant accumulation within tumor cells, and is capable of penetrating the blood-brain barrier (Example II). The ability to penetrate the blood-brain barrier was confirmed by showing that RAD1901 administration significantly prolonged survival in a brain metastasis xenograft model (Example I(B)). Accordingly, in certain embodiments of the tumor growth inhibition or regression methods provided herein, the ERα-positive tumor being targeted is located in the brain or elsewhere in the central nervous system. In certain of these embodiments, the ERα-positive tumor is primarily associated with brain cancer. In other embodiments, the ERα-positive tumor is a metastatic tumor that is primarily associated with another type of cancer, such as breast, uterine, ovarian, or pituitary cancer, or a tumor that has migrated from another tissue or organ. In certain of these embodiments, the tumor is a brain metastases, such as breast cancer brain metastases (BCBM). In certain embodiments of the methods disclosed herein, RAD1901 or salts or solvates thereof accumulate in one or more cells within a target tumor.

[0088] In certain embodiments of the methods disclosed herein, RAD1901 or a solvate (e.g., hydrate) or salt thereof preferably accumulate in tumor at a T/P (RAD1901 concentration in tumor/RAD1901 concentration in plasma) ratio of about 15 or higher, about 18 or higher, about 19 or higher, about 20 or higher, about 25 or higher, about 28 or higher, about 30 or higher, about 33 or higher, about 35 or higher, or about 40 or higher.

[0089] The results provided herein show that RAD1901 administration protects against bone loss in ovariectomized rats (Example IV(A)). Accordingly, in certain embodiments of the tumor growth inhibition or regression methods provided herein, administration of RAD1901 or a solvate (e.g., hydrate) or salt thereof does not have undesirable effects on bone, including for example undesirable effects on bone volume density, bone surface density, bone mineral density, trabecular number, trabecular thickness, trabecular spacing, connectivity density, and/or apparent bone density of the treated subject. RAD1901 can be particularly useful for patients having osteoporosis or a higher risk of osteoporosis. Tamoxifen may be associated with bone loss in pre-menopausal women, and fulvestrant may impair the bone structures due to its mechanism of action. RAD1901 can be particularly useful for pre-menopausal women and/or tumors resistant to tamoxifen or antiestrogen therapy.

[0090] The results provided herein show that RAD1901 antagonized estradiol stimulation of uterine tissues in ovariectomized rats (Example IV(A)). Furthermore, in human subjects treated with RAD1901 at a dosage of 200 mg or up to 500 mg q.d., standardized uptake value (SUV) for uterus, muscle, and bone tissues that did not significantly express ER showed hardly any changes in signals pre- and post-treatment (Example III(A)). Accordingly, in certain embodiments, such administration also does not result in undesirable effects on other tissues, including for example uterine, muscle, or breast tissue.

[0091] A therapeutically effective amount of RAD1901 for use in the methods disclosed herein is an amount that, when administered over a particular time interval, results in achievement of one or more therapeutic benchmarks (e.g., slowing or halting of tumor growth, cessation of symptoms, etc.). Ideally, the therapeutically effective amount does not exceed the maximum tolerated dosage at which 50% or more of treated subjects experience nausea or other toxicity reactions that prevent further drug administrations. A therapeutically effective amount may vary for a subject depending on a variety of factors, including variety and extent of the symptoms,

sex, age, body weight, or general health of the subject, administration mode and salt or solvate type, variation in susceptibility to the drug, the specific type of the disease, and the like.

[0092] Examples of therapeutically effective amounts of RAD1901 for use in the methods disclosed herein include, without limitation, about 150 to about 1,500 mg, about 200 to about 1,500 mg, about 250 to about 1,500 mg, or about 300 to about 1,500 mg dosage q.d. for subjects having resistant ER-driven tumors or cancers; about 150 to about 1,500 mg, about 200 to about 1,000 mg or about 250 to about 1,000 mg or about 300 to about 1,000 mg dosage q.d. for subjects having both wild-type ER driven tumors and/or cancers and resistant tumors and/or cancers; and about 300 to about 500 mg, about 300 to about 550 mg, about 300 to about 600 mg, about 250 to about 500 mg, about 250 to about 550 mg, about 250 to about 600 mg, about 200 to about 500 mg, about 200 to about 550 mg, about 200 to about 600 mg, about 150 to about 500 mg, about 150 to about 550 mg, or about 150 to about 600 mg dosage q.d. for subjects having majorly wild-type ER driven tumors and/or cancers. In certain embodiments, the dosage of RAD1901 or a solvate (e.g., hydrate) or salt thereofthereof for use in the presently disclosed methods general for an adult subject may be approximately 200 mg, 400 mg, 500 mg, 30 mg to 2,000 mg, 100 mg to 1,500 mg, or 150 mg to 1,500 mg p.o., q.d.. This daily dosage may be achieved via a single administration or multiple administrations.

[0093] Dosing of RAD1901 in the treatment of breast cancer including resistant strains as well as instances expressing mutant receptor(s) are in the range of 100 mg to 1,000 mg per day. For example, RAD1901 may be dosed at 100, 200, 300, 400, 500, 600, 700, 800, 900 or 1,000 mg per day. In particular, 200 mg, 400 mg, 500 mg, 600 mg, 800 mg and 1,000 mg per day are noted. The surprisingly long half life of RAD1901 in humans after PO dosing make this option particularly viable. Accordingly, the drug may be administered as 200 mg bid (400 mg total daily), 250 mg bid (500 mg total daily), 300 mg bid (600 mg total daily), 400 mg bid (800 mg daily) or 500 mg bid (1,000 mg total daily). Preferably the dosing is oral.

[0094] In certain embodiments, the cancers or tumors are resistant ER-driven cancers or tumors (e.g. having mutant ER binding domains (e.g. ERα comprising one or more mutations including, but not limited to, $Y537X_1$ wherein X_1 is S, N, or C, D538G, $L536X_2$ wherein X_2 is R or Q, P535H, V534E, S463P, V392I, E380Q and combinations thereof), overexpressors of the ERs or tumor and/or cancer proliferation becomes ligand independent, or tumors and/or cancers that progress with treatment of SERD (e.g., fulvestrant, TAS-108 (SR16234), ZK191703, RU58668,

GDC-0810 (ARN-810), GW5638/DPC974, SRN-927, ICI182782 and AZD9496), Her2 inhibitors (e.g., trastuzumab, lapatinib, ado-trastuzumab emtansine, and/or pertuzumab), chemo therapy (e.g., abraxane, adriamycin, carboplatin, cytoxan, daunorubicin, doxil, ellence, fluorouracil, gemzar, helaven, lxempra, methotrexate, mitomycin, micoxantrone, navelbine, taxol, taxotere, thiotepa, vincristine, and xeloda), aromatase inhibitor (e.g., anastrozole, exemestane, and letrozole), selective estrogen receptor modulators (e.g., tamoxifen, raloxifene, lasofoxifene, and/or toremifene), angiogenesis inhibitor (e.g., bevacizumab), and/or rituximab.

[0095] RAD1901 or a solvate (e.g., hydrate) or salt thereof for use in the presently disclosed methods may be administered to a subject one time or multiple times. In those embodiments wherein the compounds are administered multiple times, they may be administered at a set interval, e.g., daily, every other day, weekly, or monthly. Alternatively, they can be administered at an irregular interval, for example on an as-needed basis based on symptoms, patient health, and the like.

[0096] RAD1901 or a solvate (e.g., hydrate) or salt thereof for use in the presently disclosed methods can be formulated into unit dosage forms, meaning physically discrete units suitable as unitary dosage for subjects undergoing treatment, with each unit containing a predetermined quantity of active material calculated to produce the desired therapeutic effect, optionally in association with a suitable pharmaceutical carrier. The unit dosage form can be for a single daily dose or one of multiple daily doses (e.g., about 1 to 4 or more times q.d.). When multiple daily doses are used, the unit dosage form can be the same or different for each dose. In certain embodiments, the compounds may be formulated for controlled release.

[0097] RAD1901 or a solvate (e.g., hydrate) or salt thereof for use in the presently disclosed methods can be formulated according to any available conventional method. Examples of preferred dosage forms include a tablet, a powder, a subtle granule, a granule, a coated tablet, a capsule, a syrup, a troche, an inhalant, a suppository, an injectable, an ointment, an ophthalmic ointment, an eye drop, a nasal drop, an ear drop, a cataplasm, a lotion and the like. In the formulation, generally used additives such as a diluent, a binder, an disintegrant, a lubricant, a colorant, a flavoring agent, and if necessary, a stabilizer, an emulsifier, an absorption enhancer, a surfactant, a pH adjuster, an antiseptic, an antioxidant and the like can be used. In addition, the formulation is also carried out by combining compositions that are generally used as a raw

material for pharmaceutical formulation, according to the conventional methods. Examples of these compositions include, for example, (1) an oil such as a soybean oil, a beef tallow and synthetic glyceride; (2) hydrocarbon such as liquid paraffin, squalane and solid paraffin; (3) ester oil such as octyldodecyl myristic acid and isopropyl myristic acid; (4) higher alcohol such as cetostearyl alcohol and behenyl alcohol; (5) a silicon resin; (6) a silicon oil; (7) a surfactant such as polyoxyethylene fatty acid ester, sorbitan fatty acid ester, glycerin fatty acid ester, polyoxyethylene sorbitan fatty acid ester, a solid polyoxyethylene castor oil and polyoxyethylene polyoxypropylene block co-polymer; (8) water soluble macromolecule such as hydroxyethyl cellulose, polyacrylic acid, carboxyvinyl polymer, polyethyleneglycol, polyvinylpyrrolidone and methylcellulose; (9) lower alcohol such as ethanol and isopropanol; (10) multivalent alcohol such as glycerin, propyleneglycol, dipropyleneglycol and sorbitol; (11) a sugar such as glucose and cane sugar; (12) an inorganic powder such as anhydrous silicic acid, aluminum magnesium silicicate and aluminum silicate; (13) purified water, and the like. Additives for use in the above formulations may include, for example, 1) lactose, corn starch, sucrose, glucose, mannitol, sorbitol, crystalline cellulose and silicon dioxide as the diluent; 2) polyvinyl alcohol, polyvinyl ether, methyl cellulose, ethyl cellulose, gum arabic, tragacanth, gelatine, shellac, hydroxypropyl cellulose, hydroxypropylmethyl cellulose, polyvinylpyrrolidone, polypropylene glycol-poly oxyethylene-block co-polymer, meglumine, calcium citrate, dextrin, pectin and the like as the binder; 3) starch, agar, gelatine powder, crystalline cellulose, calcium carbonate, sodium bicarbonate, calcium citrate, dextrin, pectic, carboxymethylcellulose/calcium and the like as the disintegrant; 4) magnesium stearate, talc, polyethyleneglycol, silica, condensed plant oil and the like as the lubricant; 5) any colorants whose addition is pharmaceutically acceptable is adequate as the colorant; 6) cocoa powder, menthol, aromatizer, peppermint oil, cinnamon powder as the flavoring agent; 7) antioxidants whose addition is pharmaceutically accepted such as ascorbic acid or alpha-tophenol.

[0098] RAD1901 or a solvate (e.g., hydrate) or salt thereof for use in the presently disclosed methods can be formulated into a pharmaceutical composition as any one or more of the active compounds described herein and a physiologically acceptable carrier (also referred to as a pharmaceutically acceptable carrier or solution or diluent). Such carriers and solutions include pharmaceutically acceptable salts and solvates of RAD1901 used in the methods of the instant invention, and mixtures comprising two or more of such compounds, pharmaceutically

acceptable salts of the compounds and pharmaceutically acceptable solvates of the compounds. Such compositions are prepared in accordance with acceptable pharmaceutical procedures such as described in Remington's Pharmaceutical Sciences, 17th edition, ed. Alfonso R. Gennaro, Mack Publishing Company, Eaton, Pa. (1985), which is incorporated herein by reference.

[0099] The term "pharmaceutically acceptable carrier" refers to a carrier that does not cause an allergic reaction or other untoward effect in patients to whom it is administered and are compatible with the other ingredients in the formulation. Pharmaceutically acceptable carriers include, for example, pharmaceutical diluents, excipients or carriers suitably selected with respect to the intended form of administration, and consistent with conventional pharmaceutical practices. For example, solid carriers/diluents include, but are not limited to, a gum, a starch (e.g., corn starch, pregelatinized starch), a sugar (e.g., lactose, mannitol, sucrose, dextrose), a cellulosic material (e.g., microcrystalline cellulose), an acrylate (e.g., polymethylacrylate), calcium carbonate, magnesium oxide, talc, or mixtures thereof. Pharmaceutically acceptable carriers may further comprise minor amounts of auxiliary substances such as wetting or emulsifying agents, preservatives or buffers, which enhance the shelf life or effectiveness of the therapeutic agent.

[00100] RAD1901 in a free form can be converted into a salt by conventional methods. The term "salt" used herein is not limited as long as the salt is formed with RAD1901 and is pharmacologically acceptable; preferred examples of salts include a hydrohalide salt (for instance, hydrochloride, hydrobromide, hydroiodide and the like), an inorganic acid salt (for instance, sulfate, nitrate, perchlorate, phosphate, carbonate, bicarbonate and the like), an organic carboxylate salt (for instance, acetate salt, maleate salt, tartrate salt, fumarate salt, citrate salt and the like), an organic sulfonate salt (for instance, methanesulfonate salt, ethanesulfonate salt, benzenesulfonate salt, toluenesulfonate salt, camphorsulfonate salt and the like), an amino acid salt (for instance, aspartate salt, glutamate salt and the like), a quaternary ammonium salt, an alkaline metal salt (for instance, sodium salt, potassium salt and the like), an alkaline earth metal salt (magnesium salt, calcium salt and the like) and the like. In addition, hydrochloride salt, sulfate salt, methanesulfonate salt, acetate salt and the like are preferred as "pharmacologically acceptable salt" of the compounds according to the present invention.

[00101] Isomers of RAD1901 (e.g., geometric isomers, optical isomers, rotamers, tautomers, and the like) can be purified using general separation means, including for example

recrystallization, optical resolution such as diastereomeric salt method, enzyme fractionation method, various chromatographies (for instance, thin layer chromatography, column chromatography, glass chromatography and the like) into a single isomer. The term "a single isomer" herein includes not only an isomer having a purity of 100%, but also an isomer containing an isomer other than the target, which exists even through the conventional purification operation. A crystal polymorph sometimes exists for RAD1901 or a salt thereof, and all crystal polymorphs thereof are included in the present invention. The crystal polymorph is sometimes single and sometimes a mixture, and both are included herein.

[00102] In certain embodiments, RAD1901 may be in a prodrug form, meaning that it must undergo some alteration (e.g., oxidation or hydrolysis) to achieve its active form. Alternative, RAD1901 may be a compound generated by alteration of a parental prodrug to its active form.

[00103] In certain embodiments, the methods of tumor growth inhibition provided herein further comprise gene profiling the subject, wherein the gene to be profiled is one or more genes selected from the group consisting of ABL1, AKT1, AKT2, ALK, APC, AR, ARID1A, ASXL1, ATM, AURKA, BAP, BAP1, BCL2L11, BCR, BRAF, BRCA1, BRCA2, CCND1, CCND2, CCND3, CCNE1, CDH1, CDK4, CDK6, CDK8, CDKN1A, CDKN1B, CDKN2A, CDKN2B, CEBPA, CTNNB1, DDR2, DNMT3A, E2F3, EGFR, EML4, EPHB2, ERBB2, ERBB3, ESR1, EWSR1, FBXW7, FGF4, FGFR1, FGFR2, FGFR3, FLT3, FRS2, HIF1A, HRAS, IDH1, IDH2, IGF1R, JAK2, KDM6A, KDR, KIF5B, KIT, KRAS, LRP1B, MAP2K1, MAP2K4, MCL1, MDM2, MDM4, MET, MGMT, MLL, MPL, MSH6, MTOR, MYC, NF1, NF2, NKX2-1, NOTCH1, NPM, NRAS, PDGFRA, PIK3CA, PIK3R1, PML, PTEN, PTPRD, RARA, RB1, RET, RICTOR, ROS1, RPTOR, RUNX1, SMAD4, SMARCA4, SOX2, STK11, TET2, TP53, TSC1, TSC2, and VHL.

[00104] In some embodiments, this invention provides a method of treating a subpopulation of breast cancer patients wherein said sub-population has increased expression of one or more of the following genes and treating said sub-population with an effective dose of RAD1901 (or combination) according to the dosing embodiments as described in this disclosure.

[00105]

[00106] In addition to establishing the ability of RAD1901 to inhibit tumor growth, the results provided herein show that RAD1901 inhibits estradiol binding to ER in the uterus and pituitary (Example III(A)). In these experiments, estradiol binding to ER in uterine and pituitary tissue

was evaluated by FES-PET imaging. After treatment with RAD1901, the observed level of ER binding was at or below background levels. These results establish that the antagonistic effect of RAD1901 on ER activity can be evaluated using real-time scanning. Based on these results, methods are provided herein for monitoring the efficacy of treatment with RAD1901 or a salt or solvate thereof by measuring estradiol-ER binding in one or more target tissues, wherein a decrease or disappearance in binding indicates efficacy.

[00107] Further provided are methods of adjusting the dosage of RAD1901 or a salt or solvate based on estradiol-ER binding. In certain embodiments of these methods, binding is measured at some point following one or more administrations of a first dosage of the compound. If estradiol-ER binding is not affected or exhibits a decrease below a predetermined threshold (e.g., a decrease in binding versus baseline of less than 5%, less than 10%, less than 20%, less than 30%, or less than 50%), the first dosage is deemed to be too low. In certain embodiments, these methods comprise an additional step of administering an increased second dosage of the compound. These steps can be repeated, with dosage repeatedly increased until the desired reduction in estradiol-ER binding is achieved. In certain embodiments, these steps can be incorporated into the methods of inhibiting tumor growth provided herein. In these methods, estradiol-ER binding can serve as a proxy for tumor growth inhibition, or a supplemental means of evaluating growth inhibition. In other embodiments, these methods can be used in conjunction with the administration of RAD1901 for purposes other than inhibition of tumor growth, including for example inhibition of cancer cell proliferation.

[00108] In certain embodiments, the methods provided herein for adjusting the dosage of RAD1901 or salt or solvate (e.g., hydrate) thereof comprise:

(1) administering a first dosage of RAD1901 or a solvate (e.g., hydrate) or salt thereof (e.g., about 350 to about 500 mg, or about 200 to about 600 mg/day) for 3, 4, 5, 6, or 7 days;

(2) detecting estradiol-ER binding activity, for example using FES-PET imaging as disclosed herein; wherein:

(i) if the ER binding activity is not detectable or is below a predetermined threshold level, continuing to administer the first dosage (i.e., maintain the dosage level); or

(ii) if the ER binding activity is detectable or is above a predetermined threshold level, administering a second dosage that is greater than the first dosage (e.g., the first dosage plus about 50 to about 200 mg) for 3, 4, 5, 6, or 7 days, then proceeding to step (3);

(3) detecting estradiol-ER binding activity, for example using FES-PET imaging as disclosed herein; wherein

(i) if the ER binding activity is not detectable or is below a predetermined threshold level, continuing to administer the second dosage (i.e., maintain the dosage level); or

(ii) if the ER binding activity is detectable or is above a predetermined threshold level, administering a third dosage that is greater than the second dosage (e.g., the second dosage plus about 50 to about 200 mg) for 3, 4, 5, 6, or 7 days, then proceeding to step (4);

(4) repeating the steps above through a fourth dosage, fifth dosage, etc., until no ER binding activity is detected.

[00109] In certain embodiments, the invention includes the use of PET imaging to detect and/or dose ER sensitive or ER resistant cancers.

[00110] Administration routes of RAD1901 or a solvate (e.g., hydrate) or salt thereof disclosed herein include but not limited to topical administration, oral administration, intradermal administration, intramuscular administration, intraperitoneal administration, intravenous administration, intravesical infusion, subcutaneous administration, transdermal administration, and transmucosal administration.

RAD1901-ERα interactions

(1) Mutant ERα in ER positive breast tumor samples from patients who received at least one line of endocrine treatment

[00111] In five studies reported in the past two years, a total of 187 metastatic ER positive breast tumor samples from patients who received at least one line of endocrine treatment were sequenced and ER LBD mutations were identified in 39 patients (21%) (Jeselsohn). Among the 39 patients, the six most frequent LBD mutations are shown in Scheme 1 adapted from Jeselsohn, shown as Fig. 42.

[00112] The frequency of all LBD mutations are summarized in Table 11.

[00113] Computer modeling showed that RAD1901-ERα interactions are not likely to be affected by mutants of LBD of ERα, e.g., Y537X mutant wherein X was S, N, or C; D538G; and S463P, which account for about 81.7% of LBD mutations found in a recent study of metastatic ER positive breast tumor samples from patients who received at least one line of endocrine treatment (Table 11, Example V).

[00114] Provided herein are complexes and crystals of RAD1901 bound to ERα and/or a mutant ERα, the mutant ERα comprises one or more mutations including, but not limited to, $Y537X_1$ wherein X_1 is S, N, or C, D538G, $L536X_2$ wherein X_2 is R or Q, P535H, V534E, S463P, V392I, E380Q and combinations thereof.

[00115] In certain embodiments of the methods provided herein, the LBD of ERα and a mutant ERα comprises AF-2. In other embodiments, the LBD comprises, consists of, or consists essentially of amino acids 299-554 of ERα. In certain embodiments, the LBD of the mutant ERα comprises one or more mutations including, but not limited to, $Y537X_1$ wherein X_1 is S, N, or C, D538G, $L536X_2$ wherein X_2 is R or Q, P535H, V534E, S463P, V392I, E380Q and combinations thereof. The term "and/or" as used herein includes both the "and" case and the "or" case.

[00116] The following examples are provided to better illustrate the claimed invention and are not to be interpreted as limiting the scope of the invention. To the extent that specific materials are mentioned, it is merely for purposes of illustration and is not intended to limit the invention. One skilled in the art may develop equivalent means or reactants without the exercise of inventive capacity and without departing from the scope of the invention. It will be understood that many variations can be made in the procedures herein described while still remaining within the bounds of the present invention. It is the intention of the inventors that such variations are included within the scope of the invention.

Examples

Materials and methods

Test compounds

[00117] RAD1901 used in the examples below was (6R)-6-(2-(N-(4-(2-(ethylamino)ethyl)benzyl)-N-ethylamino)-4-methoxyphenyl)-5,6,7,8-tetrahydronaphthalen-2-ol dihydrochloride, manufactured by IRIX Pharmaceuticals, Inc. (Florence, SC). RAD1901 was stored as a dry powder, formulated for use as a homogenous suspension in 0.5% (w/v)

methylcellulose in deionized water, and for animal models was administered p.o.. Tamoxifen, raloxifene and estradiol (E2) were obtained from Sigma-Aldrich (St. Louis, MO), and administered by subcutaneous injection. Fulvestrant was obtained from Tocris Biosciences (Minneapolis, MN) and administered by subcutaneous injection. Other laboratory reagents were purchased from Sigma-Aldrich unless otherwise noted.

Cell lines

[00118] MCF-7 cells (human mammary metastatic adenocarcinoma) were purchased from American Type Culture Collection (Rockville, MD) and were routinely maintained in phenol red-free minimal essential medium (MEM) containing 2 mM L-glutamine and Earle's BSS, 0.1 mM non-essential amino acids and 1 mM sodium pyruvate supplemented with 0.01 mg/ml bovine insulin and 10% fetal bovine serum (Invitrogen, Carlsbad, CA), at 5% CO_2.

[00119] T47D cells were cultured in 5% CO_2 incubator in 10 cm dishes to approximately 75% confluence in RPMI growth media supplemented with 10% FBS and 5 μg/mL human insulin.

***In vivo* Xenograft Models**

[00120] All mice were housed in pathogen-free housing in individually ventilated cages with sterilized and dust-free bedding cobs, access to sterilized food and water ad libitum, under a light dark cycle (12-14 hour circadian cycle of artificial light) and controlled room temperature and humidity. Tumors were measured twice weekly with Vernier calipers and volumes were calculated using the formula: $(L*W^2)*0.52$.

PDx models

[00121] Some examples of patient-derived xenograft models (PDx models) are shown in Fig. 1. PDx models with patient derived breast cancer tumor were established from viable human tumor tissue or fluid that had been serially passaged in animals (athymic nude mice (Nu (NCF)-Foxn1nu)) a limited number of times to maintain tumor heterogeneity. Pre-study tumor volumes were recorded for each experiment beginning approximately one week prior to its estimated start date. When tumors reached the appropriate Tumor Volume Initiation (TVI) range (150-250 mm^3), animals were randomized into treatment and control groups and dosing initiated (Day 0, 8-10 subjects in each group); animals in all studies followed individually throughout each experiment. Initial dosing began Day 0; animals in all groups were dosed by weight (0.01 mL per gram; 10 ml/kg). Each group was treated with vehicle (control, p.o./q.d. to the endpoint), tamoxifen (1 mg/subject, s.c./q.o.d. to the end point), fulvestrant (Faslodex®; 1 mg/subject or 3

mg/subject as needed, SC/weekly X 5 and extended if necessary), or RAD1901 (30, 60 or 120 mg/kg of the subject, p.o./q.d. to the endpoint) as specified from day 0. The treatment period lasted for 56-60 days depending on the models. The drinking water for these PDx models was supplemented with 17β-estradiol.

Agent Efficacy

[00122] For all studies, beginning Day 0, tumor dimensions were measured by digital caliper and data including individual and mean estimated tumor volumes (Mean TV ± SEM) recorded for each group; tumor volume was calculated using the formula (Yasui et al. Invasion Metastasis 17:259-269 (1997), which is incorporated herein by reference): $TV = width^2 \times length \times 0.52$. Each group or study was ended once the estimated group mean tumor volume reached the Tumor Volume (TV) endpoint (time endpoint was 60 days; and volume endpoint was group mean 2 cm^3); individual mice reaching a tumor volume of 2 cm^3 or more were removed from the study and the final measurement included in the group mean until the mean reached volume endpoint or the study reached time endpoint.

Efficacy Calculations and Statistical Analysis

[00123] %Tumor Growth Inhibition (%TGI) values were calculated at a single time point (when the control group reached tumor volume or time endpoint) and reported for each treatment group (T) versus control (C) using initial (i) and final (f) tumor measurements by the formula (Corbett TH et al. *In vivo* methods for screening and preclinical testing. In: Teicher B, ed., *Anticancer Drug Development Guide.* Totowa, NJ: Humana. 2004: 99-123.): $\%TGI = 1 - Tf-Ti / Cf-Ci$.

Statistics

[00124] TGI Studies- One way ANOVA + Dunnett's Multiple Comparisons Test (Corbett TH et al).

Sample Collection

[00125] At endpoint, tumors were removed. One fragment was flash frozen, while another fragment was placed in 10% NBF for at least 24 hours and formalin fixed paraffin embedded (FFPE). Flash frozen samples were stored at -80°C; FFPE blocks were stored at room temperature.

Western Blot

[00126] Cells were harvested and protein expression was analyzed using standard practice. Tumors were harvested at the indicated time points after the last day of dosing, homogenized in

RIPA buffer with protease and phosphatase inhibitors using a Tissuelyser (Qiagen). Equal amounts of protein were separated by MW, transferred to nitrocellulose membranes and blotted with the following antibodies using standard practice:

- Estrogen receptor (SantaCruz (HC-20); sc-543)
- Progesterone receptor (Cell Signaling Technologies; 3153)
- Vinculin (Sigma-Aldrich, v9131)

[00127] qPCR analyses were performed as follows: Cells were harvested, mRNA was extracted, and equal amounts used for cDNA synthesis and qPCR with primers specific for progesterone receptor, GREB1, and TFF1 (LifeTech). Bands were quantified using 1D Quant software (GE).

Immunohistochemistry

[00128] Tumors were harvested, formalin-fixed and embedded into paraffin. Embedded tumors were sectioned (6 μM) and stained with antibodies specific for ER, PR, and Her2. Quantitation was performed as follows: Five fields were counted for positive cells (0-100%) and intensity of staining (0-3+). H-scores (0-300) were calculated using the following formula: % positivity * intensity.

[00129] Example I. RAD1901 inhibited tumor growth in tumor and/or cancer expressing WT ER or mutant ER (e.g., Y537S), with different prior endocrine therapy.

[00130] I(A). Effectiveness of RAD1901 on animal xenografts models

[00131] *I(A)(i) RAD1901 inhibited tumor growth in PDx models (PDx-1 to PDx-12) regardless of ER status and prior endocrine therapy*

[00132] Fig. 1 demonstrates tumor growth inhibition effects in various PDx models for mice treated with RAD1901 alone. Twelve patient-derived xenograft models were screened to test RAD1901 response in a variety of genetic backgrounds with varied levels of ER, PR and Her2. Full efficacy study was carried out for PDx models marked with "*" (PDx-1 to PDx-4, and PDx-12), with n = 8-10. These PDx models were treated with vehicle (negative control) or RAD1901 at a dosage of 60 mg/kg for 60 days p.o., q.d. Screen study was carried out for other PDx models (PDx-5 to PDx-11), with n = 3 at treated with vehicle (negative control) or RAD1901 at a dosage of 90 mg/kg, for 60 days, p.o., q.d. As demonstrated in Fig. 1, PDx models in which the growth was driven by ER and an additional driver (e.g., PR+ and/or Her2+) benefited from the RAD1901 treatments. RAD1901 was efficacious in inhibiting tumor growth in models with ER

mutations and/or high level expression of Her2 (PDx), regardless of prior treatment, either treatment naïve (Rx-naïve), or treated with aromatase inhibitor, tamoxifen (tam), chemotherapy (chemo), Her2 inhibitors (Her2i, e.g., trastuzumab, lapatinib), bevacizumab, fulvestrant, and/or rituximab.

[00133] *I(A)(ii) RAD1901 drove regression in xenograft models expressing WT ER*

[00134] *I(A)(ii)(1) RAD1901 drove regression in MCF-7 xenografts that were responsive to fulvestrant treatments.*

MCF-7 Xenograft Model-I

[00135] The antitumor effects of RAD1901 were examined using a first MCF-7 xenograft model (MCF-7 Xenograft Model-I) in female athymic nude mice (Crl:NU(NCr)-*Foxn1nu*), with estradiol administration to stimulate tumor growth. Three days prior to tumor cell implantation, estrogen pellets (0.36 mg E2, 60-day release; Innovative Research of America, Sarasota, FL) were implanted subcutaneously between the scapulae of all test animals using a sterilized trochar. MCF-7 human breast adenocarcinoma cells were cultured to mid-log phase in RPMI-1640 medium containing 10% fetal bovine serum, 100 units/mL penicillin G, 100 µg/mL streptomycin sulfate, 2 mM glutamine, 10 mM HEPES, 0.075% sodium bicarbonate, and 25 µg/mL gentamicin. On the day of tumor cell implant, the MCF-7 cells were trypsinized, pelleted, and resuspended in phosphate buffered saline at a concentration of 5×10^7 cells/mL. Each test mouse received 1×10^7 MCF-7 cells implanted subcutaneously in the right flank, and tumor growth was monitored. When necessary, tumor weight was estimated based on the assumption that 1 mm^3 of tumor volume was equivalent to 1 mg tumor wet weight. Body weights were measured q.d. for five days after the MCF-7 cell implantation, then twice per week throughout the remainder of the study.

[00136] Fourteen days after tumor cell implantation (designated as day 1 of the study), mice were nine weeks of age with body weights ranging from 21.4 to 32.5 grams, individual tumor volumes ranging from 75 to 144 mm^3, and group mean tumor volume (MTV) of 108 mm^3. The mice were randomized into nine groups of 15 animals each and treated with vehicle p.o., tamoxifen (1 mg/animal s.c., q.o.d.), fulvestrant (0.5 mg/animal s.c., q.d.), or RAD1901 (0.3, 1, 3, 10, 30, 60, 90 and 120 mg/kg p.o., q.d.).

[00137] Tumor volumes were evaluated twice per week. The tumor endpoint was defined as a MTV of 1,500 mm^3 in the control group. Treatment tolerability was assessed through body

weight measurements and frequent observation for clinical signs of treatment-related adverse effects. Animals with weight loss exceeding 30% for one measurement, or exceeding 25% for three measurements, were humanely euthanized and classified as a treatment-related death. Acceptable toxicity was defined as a group-mean body weight loss of less than 20% during the study and not more than one treatment-related death per ten treated animals, or 10%. At the end of the study animals were euthanized by terminal cardiac puncture under isoflurane anesthesia.

[00138] Treatment outcome was evaluated based on percent tumor growth inhibition (TGI), defined as the percent difference between baseline (i.e., day 1) tumor volume and tumor volume at the end of the study (i.e., day 42). The data set for TGI analysis included all animals in each group, less any that died due to treatment-related or non-treatment-related causes. The threshold for potential therapeutic activity was defined as a treatment effect of $\geq$60% TGI. Results were analyzed using the Kruskal-Wallis or Mann-Whitney test, with a pre-specified alpha of 0.05.

[00139] Treatment with RAD1901 at dosages of 30 and 60 mg/kg resulted in significant TGI (66% TGI ($P<0.05$) and 88% TGI ($P<0.001$) at day 40, respectively). These results were similar to those obtained with tamoxifen (86% TGI at day 40) and fulvestrant (88% TGI at day 40) (Fig. 2A). In Fig. 2A, boxes represent the 25th through 75th percentile of observations, lines represent the median of observations, and whiskers represent the extreme observations.

[00140] To explore whether higher doses of RAD1901 induced a more robust effect in this model, dosages of RAD1901 up to 120 mg/kg were assessed (Figs. 2B-D). Consistent with the earlier results, RAD1901 induced significant tumor inhibition at a dosage 60 mg/kg (94% TGI at day 42 with 2/10 partial regressions). Higher dosages resulted in even greater TGI (97% TGI with 8/10 PRs at 90 mg/kg; 96% TGI with 7/10 PRs at 120 mg/kg). At all dosages tested, RAD1901 inhibited tumor growth to a greater degree than either tamoxifen or fulvestrant. Tamoxifen treatment yielded a TGI of 90% (with 2/10 PR), while fulvestrant treatment resulted in 87% TGI (with 1/10 PR). The RAD1901 inhibition in the 90 and 120 mg/kg group were significantly greater relative to both tamoxifen ($P<0.05$) and fulvestrant ($P<0.05$).

[00141] Overall, these results show that RAD1901 inhibits estrogen-induced tumor growth in a dose-dependent manner. End of treatment tumor volumes in mice treated with RAD1901 were equal to or lower than baseline, indicating that RAD1901 not only inhibits tumor growth but can also generate a regression in tumor size in a mouse xenograft model.

[00142] RAD1901 was well tolerated at all dosage levels, with no adverse effect on bodyweight (Fig. 2E).

[00143] The antitumor effects of RAD1901 were further examined using a second MCF-7 xenograft (MCF-7 Xenograft Model-II) prepared as described below.

MCF-7 Xenograft Model-II

[00144] Two days before cell implantation, Balb/C-Nude mice were inoculated with 0.18/90-day release 17β-estradiol pellets. MCF-7 cells (PR+, Her2-) were harvested and 1 x 10^7 cells were implanted subcutaneously in the right flank of Balb/C-Nude mice. When the tumors reached an average of 200 mm^3, the mice were randomized into treatment groups by tumor volume and treated with the test compounds. Each group was treated with vehicle (control, p.o., q.d. to the endpoint), fulvestrant (Faslodex®; 3 mg/subject, s.c., qwk, X 5 and extended if necessary), or RAD1901 (30 mg/kg or 60 mg/kg of the subject, p.o., q.d. to the endpoint) as specified from day 0. The treatment period lasted for 28 days.

[00145] Figs. 3A-B demonstrate that in MCF-7 Xenograft Model-II, RAD1901 (30 mg/kg and 60 mg/kg, p.o., q.d.) resulted in more significant tumor growth inhibition than fulvestrant (3 mg/subject, s.c., qwk). Unexpectedly, only one out of ten subjects in the fulvestrant treatment group showed slight tumor regression at the end of study, while five out of ten subjects in the 30 mg/kg RAD1901 treatment group and eight out of ten subjects in the 60 mg/kg RAD1901 treatment group showed various level of regression (Fig. 3B).

[00146] *I(A)(ii)(2) RAD1901 drove tumor regression in WT ER PDx models (e.g., PDx-4, PDx-2 and PDx-11) that were responsive to fulvestrant treatments.*

[00147] Although different WT ER PDx models (PDx-4, PR+, Her2-, and PDx-2 models, PR+, Her2+, both are treatment naïve; and PDx-11, PR+, Her2+, treated with AI, fulvestrant, and chemo) responded differently to fulvestrant (1 mg/dose, or 3 mg/dose, s.c., qwk), RAD1901 treatment at various doses (30 mg/kg, 60 mg/kg and/or 120 mg/kg, p.o., q.d.) caused more significant tumor growth inhibition in all PDx models than fulvestrant (Fig. 4A for PDx-4 models, Fig. 6 for PDx-2 models, and Fig. 7 for PDx-11 models). For example, in PDx-4 models that were responsive to fulvestrant treatment (1 mg/dose), RAD1901 unexpectedly stopped tumor growth or drove tumor regression in more subjects than fulvestrant (1 mg/subject) (Fig. 4B). Furthermore, in PDx-11 models that were responsive to fulvestrant treatment (3 mg/dose), RAD1901 unexpectedly stopped tumor growth and drove tumor regression in all subjects treated

while fulvestrant (3 mg/subject) only caused regression in two out of 10 subjects treated(Fig. 7B).

[00148] RAD1901 at 60 mg/kg p.o. alone achieved tumor growth inhibition similar to fulvestrant at 3 mg/dose s.c. alone in the PDx-2 model (Fig. 6). Furthermore, combination of RAD1901 and fulvestrant did not provide further benefit.

[00149] Finally, in PDx-4 model that were responsive to fulvestrant treatment (1 mg/dose, s.c., qwk), RAD1901-mediated tumor growth inhibition was maintained in the absence of treatment at least two months after RAD1901 treatment (30 mg/kg, p.o., q.d.) period ended, while estradiol treatment continued (Fig. 5).

[00150] *I(A)(ii)(3) RAD1901 drove regression in WT ER PDx models (e.g., PDx-12) that were hardly responsive to fulvestrant treatments.*

[00151] In WT ER PDx-12 (PR+, Her2+, treatment naïve) hardly responsive to fulvestrant (1 mg/dose, s.c., qwk), RAD1901 treatment at various doses (30 mg/kg, or 60 mg/kg, p.o., q.d.) unexpectedly caused tumor regression in PDx-12 models (Fig. 8).

[00152] *I(A)(iii) RAD1901 inhibited tumor growth and/or drove regression in xenograft models expressing mutant ER (ERα Y537S)*

[00153] *I(A)(iii)(1) RAD1901 inhibited tumor growth in PDx-5 models that were hardly responsive to fulvestrant treatments.*

[00154] PDx-5 models were prepared following similar protocol as described supra for PDx models. The tumor sizes of each dosing group were measured twice weekly with Vernier calipers, and volumes were calculated using the formula (L*W2)*0.52.

[00155] RAD1901 was more effective in tumor growth inhibition (60 mg/kg or 120 mg/kg, p.o., q.d.) than fulvestrant in PDx-5 models hardly responsive to fulvestrant treatment (3 mg/dose, s.c., qwk) (Figs. 9A-C). RAD1901 treatment with higher dose (120 mg/kg) was more effected than RAD1901 treatment with lower dose (60 mg/kg) (Figs. 9A-C). Tumor size of individual animals were measured at day 17 (Fig. 9B) and day 56 (Fig. 9C), respectively.

[00156] *I(A)(iii)(2) RAD1901 drove regression in PDx-6 model that were responsive to fulvestrant treatments.*

[00157] PDx models expressing mutant ER (e.g., Y537S) may be responsive to fulvestrant treatment (1 mg/dose, s.c., qwk) and tamoxifen (1 mg/dose, s.c., 3qwk) treatments, e.g., PDx-6 (PR+, Her2:1+, previously treated with tamoxifen, AI, and fulvestrant) (Figs. 10A-B).

RAD1901 (30 mg/kg, 60 mg/kg, and 120 mg/kg, p.o., q.d.) was more effective in tumor growth inhibition than fulvestrant and tamoxifen (Figs. 10A-B). For example, RAD1901 treatment of the PDx-6 models showed tumor regressions while fulvestrant treatment (1 mg/dose) did not (Fig. 10B, showing the change of the individual tumor size at the end of the study from baseline).

[00158] *I(A)(iv) Pharmacokinetic evaluation of fulvestrant treatments to non-tumor bearing mice.*

[00159] Various doses of fulvestrant were administered to mice and demonstrated significant dose exposure to the subjects (Fig. 11).

[00160] Fulvestrant was administered at 1, 3, or 5 mg/dose subcutaneously to nude mice on day 1 (D1 Rx) and day 8 (D8 Rx, n=4/dose level). Blood was collected at the indicated time points for up to 168 hours after the second dose, centrifuged, and plasma was analyzed by Liquid Chromatography-Mass Spectrometry.

[00161] *I(B) RAD1901 promoted survival in a mouse xenograft model of brain metastasis (MCF-7 intracranial models).*

[00162] The potential ability of RAD1901 to cross the blood-brain barrier and inhibit tumor growth was further evaluated using an MCF-7 intracranial tumor xenograft model.

[00163] Female athymic nude mice (Crl:NU(NCr)-*Foxn1nu)* were used for tumor xenograft studies. Three days prior to tumor cell implantation, estrogen pellets (0.36 mg E2, 60-day release, Innovative Research of America, Sarasota, FL) were implanted subcutaneously between the scapulae of all test animals using a sterilized trochar. MCF-7 human breast adenocarcinoma cells were cultured to mid-log phase in RPMI-1640 medium containing 10% fetal bovine serum, 100 units/mL penicillin G, 100 μg/mL streptomycin sulfate, 2 mM glutamine, 10 mM HEPES, 0.075% sodium bicarbonate and 25 g/mL gentamicin. On the day of tumor cell implant, the cells were trypsinized, pelleted, and resuspended in phosphate buffered saline at a concentration of 5x 10^7 cells/mL. Each test mouse received 1 x 10^6 MCF-7 cells implanted intracranially.

[00164] Five days after tumor cell implantation (designated as day 1 of the study), mice were randomized into three groups of 12 animals each and treated with vehicle, fulvestrant (0.5 mg/animal q.d.), or RAD1901 (120 mg/kg q.d.), as described above.

[00165] The endpoint was defined as a mortality or 3X survival of the control group, whichever comes first. Treatment tolerability was assessed by body weight measurements and frequent observation for clinical signs of treatment-related adverse effects. Animals with weight loss

exceeding 30% for one measurement, or exceeding 25% for three measurements, were humanely euthanized and classified as a treatment-related death. Acceptable toxicity was defined as a group-mean body weight loss of less than 20% during the study and not more than one treatment-related death among ten treated animals, or 10%. At the end of study animals were euthanized by terminal cardiac puncture under isoflurane anesthesia. RAD1901 and fulvestrant concentration in plasma and tumor were determined using LC-MS/MS.

[00166] Kaplan Meier survival analysis demonstrated that RAD1901 significantly prolonged survival compared to fulvestrant ($P<0.0001$; Fig. 12). No animals in the control or fulvestrant group survived beyond day 20 and day 34 respectively, whereas 41% (5/12) of the RAD1901 treated animals survived until the end of the study on day 54.

[00167] Concentration of RAD1901 in the plasma was 738 ± 471 ng/mL and in the intracranial tumor was 462 ± 105 ng/g supporting the hypothesis that RAD1901 is able to effectively cross the blood-brain barrier. In contrast, concentrations of fulvestrant were substantially lower in the plasma (21 ± 10 ng/mL) and in the intracranial tumor (8.3 ± 0.8 ng/g).

[00168] *I(C). Phase 1 study of RAD1901 treatment for ER+ advanced breast cancer.*

[00169] In the phase 1 study, safety, tolerability and pharmacokinetics were evaluated in 44 healthy post-menopausal females. No dose limiting toxicites were observed, maximum tolerated dose (MTD) was not established. Plasma exposure increased more than dose proportionally over the dose range tested.

Subjects

[00170] 8 post-menopausal females with advanced adenocarcinoma of the breast (ER+ tumor with no less than 1% staining by IHC, HER2-negative tumor with ECOG performance status of 0 or 1) were enrolled as subjects for this phase 1 study. The subjects must have received the following prior treatments:

- no greater than 2 prior chemotherapy regimens in the advanced/metastatic setting
- 6 months prior endocrine therapy and had progressed on prior endocrine therapy
- Subjects with untreated or symptomatic CNS metastases or prior anticancer treatment within the following windows were excluded:
- Tamoxifen < 14 days before _first dose study treatment
- Fulvestrant < 90 days before _first dose study treatment
- Chemotherapy < 28 days before _first dose study treatment

- LHRH analogue < 12 months before _first dose study treatment

DLT Criteria

- Any Grade no less than 3 non-hematologic toxicity (excluding alopecia and nausea, vomiting or diarrhea that has not been treated with optimal medication)
- Any Grade no less than 3 hematologic toxicity
- Any grade toxicity that leads to study drug interruption for > 7 days
- Dose limiting toxicity observation period is day 1-28 of Cycle 1

Dosing and tumor evaluation

[00171] The subjects were treated with one dose at 200 mg or 400 mg p.o., q.d., and evaluated q8w until disease progression (Fig. 13). The key baseline demographics of the 8 post-menopausal females with advanced breast adenocarcinoma enrolled in the phase 1 study are summarized in Table 1.

[00172] The prior cancer treatment of the subjects are shown in Fig. 14A; and the RAD1901 treatment received is shown in Fig. 14B, Subject Nos. 1-3 were treated with 200 mg RAD1901 p.o., q.d., and Subject Nos. 4-7 were treated with 400 mg RAD1901 p.o., q.d. The arrows show ongoing studies, and the bar shows discontinued treatments. In Fig. 14A, "AC" is doxorubicin/cyclophosphamide; and "FAC" is 5-fluorouracil/doxorubicin /cyclophosphamide.

Treatment emergent adverse events (TEAEs)

[00173] TEAEs were recorded throughout the study. Preliminary data are summarized in Table 2. "n" is number of subjects with at least one treatment-related AE in a given category, AEs graded as per the Common Terminology Criteria for Adverse Events (CTCAE) v4.0, and any patient with multiple scenarios of a same preferred term was counted only once to the most severe grade. No death or dose limiting toxicities were observed, maximum tolerated dose (MTD) was not established. Most AEs were grade 1 or 2. Most common treatment-related AEs were dyspepsia (5/8 patients) and nausea (3/8 patients). Two serious AEs (SAEs) were observed, one a grade 3 treatment-related constipation, and the other shortness of breath (pleural effusion) not related to the treatment.

[00174] The heavily pretreated subjects of this phase 1 study included subjects previously treated with multiple endocrine and targeted agents, e.g., CDK4/6, PI3K and mTOR inhibitors. No dose limiting toxicities were observed after RAD1901 treatment at 200 mg dose p.o., q.d. up to 6 months, and at 400 mg dose p.o., q.d. up to two months. Thus, RAD1901 showed potential

for treating ER+ advanced breast cancer, especially in subjects previously treated with endocrine and/or targeted agents such as CDK4/6, PI3K and mTOR inhibitors.

[00175] Example II. RAD1901 preferably accumulated in tumor and could be delivered to brain.

[00176] MCF-7 xenografts as described in Example I(A)(i) were further evaluated for RAD1901 concentration in plasma and tumor using LC-MS/MS. At the end of study, the concentration of RAD1901 in plasma was 344 ± 117 ng/mL and in tumor in 11,118 ± 3,801 ng/mL for the 60 mg/kg dose level. A similar tumor to plasma ratio was also observed at lower dose levels where tumor concentrations were approximately 20-30 fold higher than in plasma. RAD1901 levels in plasma, tumor, and brain for mice treated for 40 days are summarized in Table 3. A significant amount of RAD1901 was delivered to the brain of the treated mice (e.g., see the B/P ratio (RAD1901 concentration in brain/the RAD1901 concentration in plasma)), indicating that RAD1901 was able to cross the blood-brain barrier (BBB). Unexpectedly, RAD1901 preferably accumulated in the tumor. See, e.g., the T/P (RAD1901 concentration in tumor/RAD1901 concentration in plasma) ratio shown in Table 3.

[00177] Example III. RAD1901 inhibited ER pathway and degraded ER.

[00178] *III(A). RAD1901 decreased ER-engagements in uterus and pituitary in healthy post-menopausal female human subjects.*

[00179] The subjects had an amenorrhea duration of at least 12 months and serum FSH consistent with menopause. The subjects were 40-75 years old with BMI of 18.0-30 kg/m^2. Subjects had intact uterus. Subjects having evidence of clinically relevant pathology, increased risk of stroke or of history venous thromboembolic events, or use of concomitant medication less than 14 days prior to admission to clinical research center (paracetamol allowed up to 3 days prior) were excluded.

[00180] FES-PET was performed at baseline and after 6 days of exposure to RAD1901 to evaluate ER engagement in the uterus. RAD1901 occupied 83% and 92% of ER in the uterus at the 200 mg (7 subjects) and 500 mg (6 subjects) dose levels, respectively.

[00181] FES-PET imaging showed significant reduction in binding of labelled-estradiol to both the uterus and pituitary after RAD1901 treatment with 200 mg or 500 mg (p.o., q.d., 6 days).

[00182] Due to the high ER expression, the uterus showed a strong FES-PET signal at baseline before RAD1901 treatment (Fig. 15A, baseline transversal view for uterus FES-PET scan of

Subject 3 treated with 200 mg dose level; Fig. 15B, baseline sagittal view and transversal view for uterus FES-PET scan respectively of Subject 7 treated with 500 mg dose level). However, when scanned four hours post dosing on day 6 in the study, the uterus was hardly visible (at or close to background FES-PET signal (Fig. 15A, Day 6 transversal view for uterus scan of Subject 3; and Fig. 15B, Day 6 sagittal view and transversal view for uterus scan respectively of Subject 7). Such data were consistent with ER degradation and/or competition for the binding to the receptor. Figs 15A and 15B also include CT scan of the uterus scanned by FES-PET showing the existence of the uterus before and after RAD1901 treatment.

[00183] The FES-PET uterus scan results were further quantified to show the change of post-dose ER-binding from baseline for 7 subjects (Fig. 15C), showing Subjects 1-3 and Subjects 4-7 as examples of the 200 mg dose group and 500 mg dose group, respectively. RAD1901 showed robust ER engagement at the lower dose level (200 mg).

[00184] Fig. 16 showed a representative image of FES-PET scan of the uterus (A) and pituitary (B) before (Baseline) and after (Post-treatment) RAD1901 treatment at 500 mg p.o., q.d., after six days. Fig. 16A showed the FES-PET scan of the uterus by (a) Lateral cross-section; (b) longitude cross-section; and (c) longitude cross-section.

[00185] The subject's post-dose FES-PET scan of uterus and pituitary showed no noticeable signal of ER binding at uterus (Fig. 16A, Post-treatment) and at pituitary (Fig. 16B, Post-treatment), respectively.

[00186] Thus, the results showed that RAD1901 effectively engaged ER in human at a dosage of 200 and 500 mg p.o., q.d., after six days.

[00187] Standard uptake value (SUV) for uterus, muscle and bone were calculated and summarized for RAD1901 treatments at 200 mg and 500 mg p.o., q.d. in Tables 4 and 5, respectively. Post-dose uterine signals were a tor close to levels from "non-target tissues," suggesting a complete attenuation of FES-PET uptake post RAD1901 treatment. Almost no change was observed in pre- versus post-treatment PET scans in tissues that did not significant express estrogen receptor.

[00188] Thus, RAD1901 or salt or solvate (e.g., hydrate) thereof may be used in treating cancer and/or tumor cells having overexpression of ER (e.g., breast cancer, uterus cancer, and ovary cancer), without negative effects to other organs (e.g. bones, muscles). RAD1901 or salt or solvate (e.g., hydrate) thereof may be especially useful in treating metastatic cancers and/or

tumors having overexpression of ER in other organs, e.g., the original breast cancer, uterus cancer, and/or ovary cancer migrated to other organs (e.g., bones, muscles), to treat breast cancer, uterus cancer, and/or ovary cancer lesions in other organs (e.g., bones, muscles), without negative effect to said organs.

[00189] *III(B). RAD1901 decreased ER expression and inhibited ER pathway.*

[00190] *III(B)(i)(1) Comparison of RAD1901 and fulvestrant in MCF-7 and T47D cell lines.*

[00191] The effects of RAD1901 and fulvestrant were compared using MCF-7 and T47D cell lines, both are human breast cancer cell lines, at various concentrations, 0.01 μM, 0.1 μM and 1 μM (Fig. 17A for MCF-7 cell line assays; and Fig. 17B for T47D cell lines). Three ER target genes, progesterone receptor (*PgR*), growth regulation by estrogen in breast cancer 1 (*GREB1*) and trefoil factor 1 (*TFF1*), were used as markers. RAD1901 caused ER degradation and inhibited ER signaling (Figs. 17A-B). Unexpectedly, RAD1901 was comparable or more effective than fulvestrant in inhibiting tumor growth, and driving tumor regression as disclosed supra in Examples I(A) and I(B).

[00192] *III(B)(i)(2) RAD1901 treatment resulted in ER degradation and abrogation of ER signaling in MCF-7 Xenograft Model-II described supra in Example I(A)(ii)(1).*

[00193] RAD1901 treatment resulted in ER degradation *in vivo* (Figs. 18A-B, student's t-test: *p-value <0.05, **p-value <0.01) and inhibited of ER signaling *in vivo* (Figs. 19A and 19C, student's t-test: *p-value <0.05, **p-value <0.01).

[00194] Tumor harvested from MCF-7 xenograft 2 hours after the final dose of RAD1901 (30 mg/kg, 60 mg/kg, p.o., q.d.) or fulvestrant (3mg/dose, s.c., qwk) showed significantly decreased ER and PR expression (Figs. 18A-B). Tumor harvested from MCF-7 xenograft 8 hours after the final dose of fulvestrant treatment showed varied PR and ER expression. However, tumor harvested from MCF-7 xenograft 8 hours after the final dose of RAD1901 treatment showed reduced PR and ER expression (Figs. 18A and 18C).

[00195] Tumor harvested from MCF-7 xenograft 8 hours or 12 hours after the single dose of RAD1901 (30 mg/kg, 60 mg/kg, or 90 mg/kg, p.o., q.d.) showed rapidly decreased PR expression (Fig. 19A). Tumor harvested from MCF-7 xenograft 4 hours or 24 hours after the 7th dose of RAD1901 (30 mg/kg, 60 mg/kg, or 90 mg/kg, p.o., q.d.) showed consistent and stable inhibition of ER signaling (Fig. 19B). Quantification of western blot analyses of tumor

harvested from MCF-7 xenograft at various time points during the treatment of RAD1901 (30 mg/kg, 60 mg/kg, or 90 mg/kg, p.o., q.d.) showed a dose-dependent decrease in PR (Fig. 19C).

[00196] RAD1901 treatment caused a rapid decrease in proliferation in MCF-7 xenograft models. For example, tumor harvested from MCF-7 xenograft models 8 hours after the single dose of RAD1901 (90 mg/kg, p.o., q.d.) and 24 hours after the 4th dose of RAD1901 (90 mg/kg, p.o., q.d.) were sectioned and stained to show a rapid decrease of the proliferation marker Ki67 (Figs. 20A and 20B).

[00197] These results suggest that RAD1901 treatment results in ER degradation and inhibition of ER signaling in WT ER xenografts *in vivo*.

[00198] *III(B)(i)(3) RAD1901 treatment resulted in ER degradation and abrogation of ER signaling in PDx-4 models described supra in Example I(A)(ii).*

[00199] RAD1901 treatment caused a rapid decrease in proliferation in the PDx-4 models. For example, four hours after the final dose on the last day of a 56 day efficacy study, tumor harvested from PDx-4 models treated with RAD1901 (30, 60, or 120 mg/kg, p.o., q.d.) or fulvestrant (1 mg/animal, qwk) were sectioned and showed a rapid decrease of the proliferation marker Ki67 compared to PDx-4 models treated with fulvestrant (Fig. 21).

[00200] These results suggest that RAD1901 treatment results in ER degradation and inhibition of ER signaling in WT ER xenografts *in vivo*.

[00201] *III(B)(ii) RAD1901 treatment resulted in decreased ER signaling in a Mutant ER xenograft models (PDx-5) described supra in Example I(A)(iii)(1).*

[00202] Tumors were harvested at the indicated time points after the last day of dosing (unless otherwise specified), homogenized in RIPA buffer with protease and phosphatase inhibitors using a Tissuelyser (Qiagen). Equal amounts of protein were separated by MW, transferred to nitrocellulose membranes and blotted with the following antibody as described in the Materials and methods section: progesterone receptor (PR, Cell Signaling Technologies; 3153).

[00203] Bands were quantified using 1D Quant software (GE), and PR (Allred scores) obtained from the PDx-5 models as described in Example I(A)(iii)(1) are shown in Fig. 22. Fulvestrant exerted little influence to PR expression, while RAD1901 showed efficacy at dosages of both 60 mg/kg and 120 mg/kg (p.o., q.d., Fig. 22).

[00204] These results indicate that for tumors expressing certain ERα mutations (e.g., Y537S), RAD1901 was more effective than fulvestrant at inhibiting the tumor growth, regardless whether

the tumor was responsive to fulvestrant/tamoxifen treatments (Fig. 9 for PDx-5 and Fig. 10 for PDx-6), and was especially effective in inhibiting the growth of tumors which were hardly responsive to fulvestrant treatment (e.g., at a dosage of 3 mg/dose, s.c., qwk, Fig. 9 for PDx-5). Furthermore, for the tumors which did not respond well to fulvestrant treatment (e.g., PDx-5), RAD1901 was effective in reducing PR expression *in vivo*, while fulvestrant was not (Fig. 23).

[00205] Example IV Impact of RAD1901 treatment to uterine tissue and/or BMD

[00206] *IV(A(1)): RAD1901 antagonized estradiol stimulation of uterine tissue.*

[00207] The uterotropic effects of RAD1901 were investigated by assessing changes in uterine weight, histology, and C3 gene expression in immature rats. Results from a representative study are shown in Fig. 23.

Assessment of uterotropic activity

[00208] Sprague-Dawley rat pups were weaned at 19 days of age, randomized into groups (n = 4), and administered vehicle (aqueous methylcellulose), E2 (0.01 mg/kg), raloxifene (3 mg/kg), tamoxifen (1 mg/kg), RAD1901 alone (0.3 to 100 mg/kg), or RAD1901 (0.01 to 10 mg/kg) in combination with E2 (0.01 mg/kg), either s.c. or p.o. as appropriate (see reagents, above) q.d. for 3 consecutive days. Twenty-four hours after the final dose, all animals were euthanized by carbon dioxide inhalation. Body weights and wet uterine weights were recorded for each animal. Similar assays were also conducted with RAD1901 (0.03 to 100 mg/kg) in rats and mice (Charles River Laboratories, Montreal, QC).

[00209] Fresh uterine tissue from each rat was fixed in 4% paraformaldehyde, dehydrated with ethanol, and embedded into JB4 plastic resin. Sections were cut at 8 μm and stained with 0.1% Toluidine Blue O. Thickness of the endometrial epithelium was measured using a Zeiss Axioskop 40 microscope using the Spot Advanced program; the mean of 9 measurements per specimen was calculated.

Uterine complement component 3 (C3) gene expression

[00210] To determine relative expression levels of C3 in the treated uterine tissue, RNA was extracted from the remaining tissue using the Micro to Midi Total RNA Purification Kit (Invitrogen, Carlsbad, CA) according to the manufacturer's instructions. RNA was quantified, and equal amounts were reverse-transcribed using the High Capacity cDNA Archive Kit (Applied Biosystems, Foster City, CA).

[00211] Quantitative PCR was performed using the ABI Prism 7300 System (Applied Biosystems). PCR was done using the Taqman Universal Master Mix with probe sets for C3 and for the 18S ribosomal RNA as a reference gene. Thermal cycling conditions comprised an initial denaturation step at 95° C for 10 min, followed by 40 cycles at 95° C for 15 second and 60° C for 1 minute.

[00212] Relative gene expression was determined by normalizing each sample to the endogenous control (18S) and comparing with a calibrator (vehicle). Relative gene expression was determined using the following equation: $2^{-\Delta\Delta Ct}$ (where Ct = cycle threshold or the cycle number at which PCR product was first detected, ΔCt = normalized sample value, and $\Delta\Delta Ct$ = normalized difference between dosed subjects and the vehicle). Five replicate gene expression determinations were conducted for each dose, within each study.

[00213] Treatment with E2 (0.01 mg/kg), raloxifene (RAL, 3 mg/kg) or tamoxifen (TAM, 1 mg/kg) resulted in significant increases in uterine wet weight compared to vehicle alone, whereas RAD1901 treatment at a range of doses between 0.3 and 100 mg/kg did not significantly affect uterine wet weight (Fig. 23A). Data shown (Fig. 23A) are means (± SEM); n=4 rats per group; P vs. vehicle: * < 0.05; vs. E2: ‡ < 0.05. Further, when administered in combination with E2 (0.01 mg/kg), RAD1901 antagonized E2-mediated uterine stimulation in a dose-dependent manner, exhibiting significant inhibition of uterotropic activity at doses of 0.1 mg/kg and greater and complete inhibition at 3 mg/kg. The EC_{50} for RAD1901 was approximately 0.3 mg/kg. Similar results were obtained in mice where RAD1901 doses 0.03 to 100 mg/kg also had no effect on uterine wet weight or epithelial thickness (data not shown).

[00214] Treatment-dependent changes in uterine tissue were further investigated by quantitative microscopic histology. There was a statistically significant increase in endometrial epithelial thickness after treatment with E2 at both 0.01 and 0.3 mg/kg (Fig. 23B). A significant increase in epithelial thickness was also observed after treatment with tamoxifen (1 mg/kg) or raloxifene (3 mg/kg). In contrast, RAD1901 treatment did not increase endometrial epithelial thickness up to the highest evaluated dose of 100 mg/kg. Representative images of the endometrial epithelium are shown in Fig. 23C.

[00215] Consistent with the changes in both uterine weight and endometrial epithelial thickness, E2, tamoxifen, and raloxifene all significantly increased the expression of the estrogen-regulated complement gene, C3 (Fig. 23D). In contrast, RAD1901 did not increase C3 gene expression at

any of the doses tested (0.3 to 100 mg/kg). Furthermore, RAD1901 at 1, 3 and 10 mg/kg significantly suppressed E2-stimulated C3 gene expression.

RAD1901 did not stimulate the uterus of immature female rats

[00216] Immature female rats were administered p.o., q.d., for 3 consecutive days with vehicle (VEH), estradiol (E2), raloxifene (RAL), tamoxifen (TAM), RAD1901 or RAD1901+E2. Wet uterine weights were measured. Data shown (Fig. 23A) are means (± SEM); n=4 rats per group; P vs. vehicle: * < 0.05; vs. E2: ‡ < 0.05.

Example II(A)(2). Treatment with RAD1901 protected against bone loss in ovariectomized rats

[00217] The bone-specific effects of RAD1901 was examined in ovariectomized rats.

[00218] As a model of post-menopausal bone loss, ovariectomy was performed on anesthetized adult female Sprague-Dawley rats, with sham surgery as a control. Following surgery, ovariectomized rats were treated q.d. for 4 weeks with vehicle, E2 (0.01 mg/kg), or RAD1901 (0.1, 0.3, 1, 3 mg/kg), administered as described above, with 20 animals per group. Animals in the sham surgery group were vehicle treated. All animals were euthanized by carbon dioxide inhalation 24 hours after the final dose. Bone mineral density was assessed at baseline and again after 4 weeks of treatment using PIXImus dual emission x-ray absorptiometry.

[00219] At necropsy, the left femur of each animal was removed, dissected free of soft tissue and stored in 70% ethanol before analysis. A detailed qualitative and quantitative 3-D evaluation was performed using a micro-CT40 system (Scanco Systems, Wayne, PA). For each specimen, 250 image slices of the distal femur metaphysis were acquired. Morphometric parameters were determined using a direct 3-D approach in pre-selected analysis regions. Parameters determined in the trabecular bone included bone volume density, bone surface density, trabecular number, trabecular thickness, trabecular spacing, connectivity density, and apparent bone density.

[00220] Following ovariectomy, untreated (vehicle control) rats experienced a decrease in bone mineral density both in the whole full femur and in the lumbar spine compared to baseline (Table 6). Treatment with E2 was associated with prevention of bone loss in both the femur and spine. Treatment with RAD1901 resulted in a dose-dependent and statistically significant suppression of ovariectomy-induced bone loss (data shown for the 3 mg/kg treatment group). At doses of 0.1 mg/kg to 3 mg/kg, bone mineral density in RAD1901-treated rats was complete, with no statistically significant difference from the E2-treated group.

[00221] Micro-CT analysis of the distal femur (Table 7) demonstrated that ovariectomy induced significant changes in a number of key micro-architectural parameters when compared to sham surgery animals. These changes were consistent with a decrease in bone mass and include decreased bone volume, reduced trabecular number, thickness and density, and increased trabecular separation. Consistent with the preservation of bone mineral density observed after treatment with RAD1901, significant preservation of trabecular architecture was observed in key micro-structural parameters (Table 7)

[00222] *Example IV(B): Phase 1 dose escalation study of RAD101 in healthy post-menopausal women*

[00223] In the phase 1 study, safety, tolerability and pharmacokinetics were evaluated in 44 healthy post-menopausal females. No dose limiting toxicites (DLT) were observed, maximum tolerated dose (MTD) was not established. Plasma exposure increased more than dose proportionally over the dose range tested.

Subjects

[00224] 44 healthy post-menopausal females were enrolled as subjects for this phase 1 study. The subjects had an amenorrhea duration of at least 12 months and serum FSH consistent with menopause. The subjects were 40-75 years old with BMI of 18.0-30 kg/m^2. Subjects having evidence of clinically relevant pathology, increased risk of stroke or of history venous thromboembolic events, or use of concomitant medication less than 14 days prior to admission to clinical research center (paracetamol allowed up to 3 days prior) were excluded.

Dosing

[00225] The subjects were treated with placebo or at least one dose p.o., q.d. after a light breakfast for 7 days at dose levels of 200 mg, 500 mg, 750 mg and 1000 mg, respectively. The key baseline demographics of the 44 healthy post-menopausal females enrolled in the phase 1 study are summarized in Table 8.

Treatment emergent adverse events (TEAEs)

[00226] TEAEs were recorded, and the most frequent (>10% of patients in the total active group who had any related TEAEs) adverse events (AEs) are summarized in Table 9, "n" is number of subjects with at least one treatment-related AE in a given category, AEs graded as per the Common Terminology Criteria for Adverse Events (CTCAE) v4.0, and any patient with multiple

scenarios of a same preferred term was counted only once to the most severe grade. No dose limiting toxicites were observed, maximum tolerated dose (MTD) was not established.

Pharmacokinetic Evaluations

[00227] A series of blood samples were taken during the study for the analysis of RAD1901 in plasma. Blood samples of 5 mL each were taken via an indwelling IV catheter or by direct venipuncture into tubes containing K_3-EDTA as anticoagulant. Steady state was achieved by day 5 of treatment. Geometric Mean (Geo-Mean) plasma concentration-time profiles of RAD1901 were evaluated. Plasma pharmacokinetic results of the groups treated with RAD1901 (200, 500, 750 or 1,000 mg) on Day 7 (N=35) in the study are provided in Table 10 and Fig. 24, as an example. The median $t_{1/2}$ was between 37.5−42.3 hours (Table 10). After multiple dose administration of RAD1901, median t_{max} ranged between 3-4 hours post-dose.

[00228] Example V(A)-1. Modeling of RAD1901-ERα binding using select published ER structures.

[00229] Unless specified otherwise, when structures are shown by their stick model, each end of a bond is colored with the same color as the atom to which it is attached, wherein grey is carbon, red is oxygen, blue is nitrogen and white is hydrogen.

[00230] Fourteen published structures (i.e., models) of ERα ligand-binding domain (LBD) complexed with various ER ligands were selected from 96 published models by careful evaluation. One of these fourteen models was 3ERT (human ERα LBD bound to 4-hydroxytamoxifen (OHT)). OHT is the active metabolite of tamoxifen and a first generation SERM that functions as an antagonist in breast tissue.

[00231] In 3ERT (Figs. 25 and 26), the ERα binding site adopts a three layer "helical sandwich" forming a hydrophobic pocket which includes Helix 3 (H3), Helix 5 (H5), and Helix 11 (H11) (Fig. 25). The dotted box in Fig. 26 represents the binding site and residues within the binding site that are important or are effected by OHT binding. OHT functions as an antagonist by displacing H12 into the site where LXXLL coactivator(s) binds. OHT occupies the space normally filled by L540 and modifies the conformation of four residues on the C-terminal of Helix 11 (G521, H524, L525, and M528). OHT also forms a salt bridge with D351, resulting in charge neutralization.

[00232] The other thirteen ERα LBD-ER ligand models were compared to 3ERT. Differences in their residue poses are summarized in Table 12. Superimposition of the ERα structures of the

fourteen models (Fig. 27) shows that these structures differed significantly at residues E380, M421, G521, M522, H524, Y526, S527, M528, P535, Y537, L540, and various combinations thereof.

[00233] Root-mean-square deviation (RMSD) calculations of any pair of the fourteen models are summarized in Table 13. Structures were considered to be overlapping when their RMSD was <2Å. Table 13 shows that all fourteen models had a RMSD <1.5 Å. Using conditional formatting analysis suggested that 1R5K and 3UUC were the least similar to the other models (analysis not shown). Therefore, 1R5K and 3UUC were considered a unique, separate structural cluster to be examined.

[00234] ERα residues bound by ligand in the fourteen models are summarized in Table 14. Table 14 also shows the EC_{50} in the ERα LBD-antagonist complexes. Out of the fourteen models, thirteen showed H-bond interactions between the ligand and E353; twelve showed pi interactions between the ligand and F404; five showed H-bond interactions between the ligand and D351; six showed H-bond interactions between the ligand and H524; four showed H-bond interactions between the ligand and R394; and one (3UUC) showed interactions between the ligand and T347.

[00235] Each of the fourteen models was used to dock a random library of 1,000 compounds plus the ligand the model was published with (the known antagonist) to determine whether the model could identify and prioritize the known antagonist. If the model could identify the known antagonist, the model was determined to be able to predict the pose of its own published ligand. EF_{50} was then calculated to quantify the model's strength to see how much better it was than a random selection. RAD1901 was docked in the selected models (e.g., Figs. 28-32). Docking scores of the published ligand and RAD1901 in the models were determined. EC_{50} was also determined. Visual inspection of RAD1901 showed that it "obeyed" the interactions shown with the published ligands in 1R5K, 1SJ0, 2JFA, 2BJ4, and 2OUZ. No spatial clashes were noticed. In certain embodiments, e.g., in 1R5k and 2BJ4, RAD1901 had a higher docking score than the published ligand.

[00236] The evaluation results of nine models (1ERR, 3ERT, 3UCC, 2IOK, 1R5K, 1SJ0, 2JFA, 2BJ4, and 2OUZ) are summarized in Table 15.

[00237] 1ERR and 3ERT could not predict the correct pose of their crystallized ligand. RAD1901 did not dock in 3UCC. The tetrahydronaphtaalen in 2IOK-RAD1901 bound in a non-traditional manner.

[00238] The major differences between the models 1R5K, 1SJ0, 2JFA, 2BJ4, and 2OUZ were the residues in the C-term of Helix 11 (G521-M528).

[00239] Figs. 28A-B shows the modeling of RAD1901-1R5K (A) and GW5-1R5K (B). RAD1901 bound with H-bond interactions to E353, R394, and L536; and with p-interaction with F404.

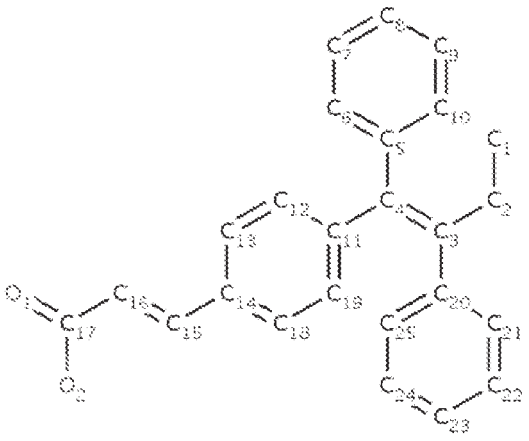
[00240] Figs. 29A-B shows the modeling of RAD1901-1SJ0 (A) and E4D-1SJ0 (B). RAD1901 bound with H-bond interactions to E353, and D351; and with p-interaction with F404.

[00241] Figs. 30A-B shows the modeling of RAD1901-2JFA (A) and RAL-2JFA (B). RAD1901 bound with p-interaction with F404.

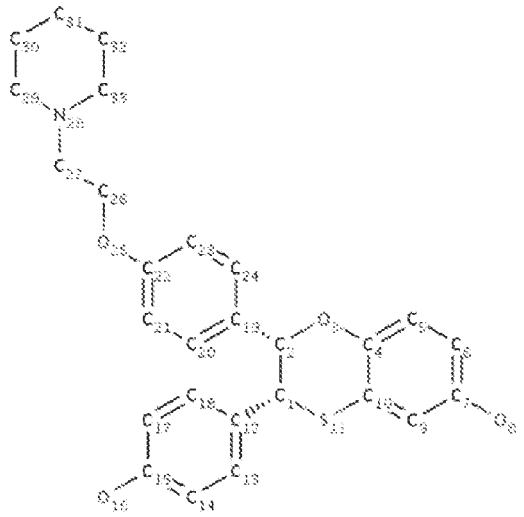
[00242] Figs. 31A-B shows the modeling of RAD1901-2BJ4 (A) and OHT-2BJ4 (B). RAD1901 bound with H-bond interactions with E353 and R394; and p-interaction with F404.

[00243] Figs. 32A-B shows the modeling of RAD1901-2IOK (A) and IOK-2IOK (B). RAD1901 bound with H-bond interactions with E353, R394, and D351; and p-interaction with F404.

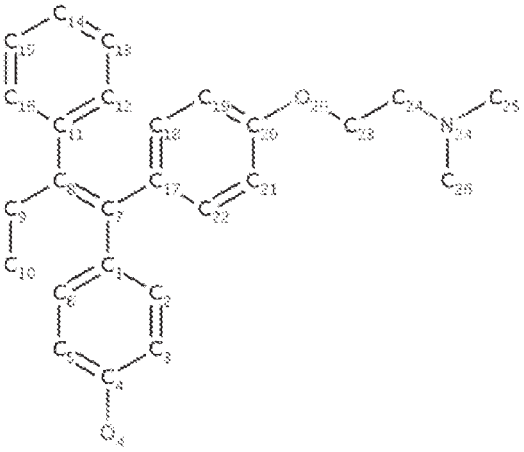
[00244] The published ligands in the models have the following structures:



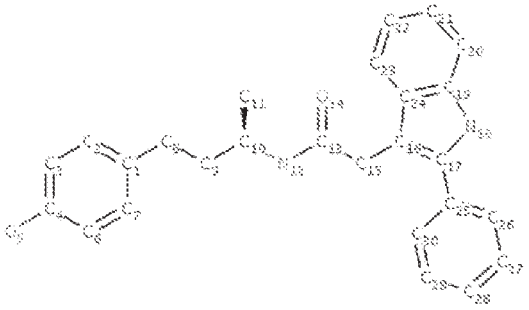
GW5, (2E)-3-{4-[(1E)-1,2-DIPHENYLBUT-1-ENYL]PHENYL}ACRYLIC ACID



E4D, (2S,3R)-2-(4-(2-(PIPERIDIN-1-YL)ETHOXY)PHENYL)-2,3-DIHYDRO-3-(4-HYDROXYPHENYL)BENZO[B][1,4]OXATHIIN-6-OL



OHT, 4-HYDROXYTAMOXIFEN



IOK, N-[(1R)-3-(4-HYDROXYPHENYL)-1-METHYLPROPYL]- 2-(2-PHENYL-1H-INDOL-3-YL)ACETAMIDE

[00245] Example V(A)-2. Induced fit docking (IFD) of ERα with RAD1901 and fulvestrant

[00246] Binding conformation of RAD1901 in ERα was further optimized by IFD analysis of the five ERα crystal structures 1R5K, 1SJ0, 2JFA, 2BJ4, and 2OUZ. IFD analysis accounted for the receptor flexibility (upon ligand binding) to accommodate its correct binding conformation.

[00247] A library of different conformations for each ligand (e.g., RAD1901 and fulvestrant) was generated by looking for a local minima as a function of rotations about rotatable bonds. The library for RAD1901 had 25 different conformations.

[00248] The five ERα crystal structures were prepared and minimized. The corresponding ligand in the published X-ray structures were used to define the ERα binding pocket.

[00249] RAD1901 conformations were docked into the prepared ERα structures wherein they were allowed to induce side-chain or back-bone movements to residues located in the binding pocket. Those movements allowed ERα to alter its binding site so that it was more closely conformed to the shape and binding mode of the RAD1901 conformation. In some examples, small backbone relaxations in the receptor structure and significant side-chain conformation changes were allowed in the IFD analysis.

[00250] An empirical scoring function was used to approximate the ligand binding free energy to provide a docking score or Gscore. Gscore is also known as GlideScore, which may be used interchangeably with docking score in this example. The docking score was an estimate of the

binding affinity. Therefore, the lower the value of the docking score, the "better" a ligand bound to its receptor. A docking score of -13 to -14 corresponded to a very good binding interaction.

[00251] The RAD1901 conformations resulted from the IFD analysis with 1R5K, 1SJ0, 2JFA, 2BJ4, and 2OUZ respectively were superimposed to show their differences (Figs. 33-35, shown in stick model). All bonds in each RAD1901 conformation were shown in the same color in Figs. 33, 34 and 35A.

[00252] The RAD1901 conformations resulted from the IFD analysis with1R5K (blue) and 2OUZ (yellow) had N-benzyl-N-ethylaniline group of RAD1901 on the front (Fig. 33). The RAD1901 conformations resulted from the IFD analysis with 2BJ4 (green) and 2JFA (pink) had N-benzyl-N-ethylaniline group of RAD1901 on the back (Fig. 34). The RAD1901 conformations resulted from the IFD analysis with 2BJ4 (green), 2JFA (pink) and 1SJ0 (brown) were quite similar as shown by their superimpositions (Figs. 34A and 34B). The RAD1901 IFD docking scores are summarized in Table 16.

[00253] The IFD of RAD1901 with 2BJ4 showed hydrogen bond interactions with E353 and D351 and pi-interactions with F404 (Figs. 36A-36C). Fig. 36A showed regions within the binding site suitable for H-bond acceptor group (red), H-bond donor group (blue) and hydrophobic group (yellow). In Fig. 36A-36B, light blue was for carbon for RAD1901. Figs. 37A-37C show a protein-surface interactions of the IFD of RAD1901 with 2BJ4. Figs. 37A and 37B are the front view, and Fig. 37C is the side view. The molecular surface of RAD1901 was blue in Fig. 37A, and green in Fig. 37C. Figs. 37B and 37C are electrostatic representation of the solvent accessible surface of ERα, wherein red represented electronegative and blue represented electropositive.

[00254] Similar IFD analysis was carried out for fulvestrant with 2BJ4 as described supra. The fulvestrant-2BJ4 IFD resulted in a Gscore of -14.945 and showed hydrogen bond interactions with E353, Y526, and H524 and pi-interactions with F404 (Figs. 38A-38C). Fig. 38A showed regions within the binding site suitable for H-bond acceptor group (red), H-bond donor group (blue) and hydrophobic group (yellow). In Fig. 38A, light blue was for carbon for RAD1901.

[00255] Figs. 39A and 39B showed RAD1901 and fulvestrant docked in 2BJ4 by IFD both had pi-interactions with F404 and hydrogen bond interactions with E353. Furthermore, RAD1901 had hydrogen bond interaction with D351 (blue representing RAD1901 molecular surface, Fig. 39B), while fulvestrant had hydrogen bond interactions with Y526, and H524 (green

representing fulvestrant molecular surface, Fig. 39C). Superimpositions of 2BJ4 docked with RAD1901 and fulvestrant are shown in Figs. 40A and 40B. In Fig. 40A, green represents fulvestrant molecular surface and blue represents RAD1901 molecular surface. In Fig. 40B, the brown structure is fulvestrant and the blue structure is RAD1901.

[00256] Example V(A)-3. Modeling evaluation of select ERα mutations.

[00257] Effects of various ERα mutations on the C-terminal ligand-binding domain were evaluated. Specific ERα mutations evaluated were Y537X mutant wherein X was S, N, or C; D538G; and S463P.

[00258] Y537 resides in Helix 12. It may regulate ligand binding, homodimerization, and DNA binding once it is phosphorylated, and may allow ERα to escape phosphorylation-mediated controls and provide a cell with a potential selective tumorigenic advantage. In addition, it may cause conformational changes that makes the receptor constitutively active.

[00259] The Y537S mutation favors the transcriptionally active closed pocket conformation, whether occupied by ligand or not. The closed but unoccupied pocket may account for ERα's constitutive activity (Carlson et al. Biochemistry 36:14897-14905 (1997)). Ser537 establishes a hydrogen-bonding interaction with Asp351 resulting in an altered conformation of the helix 11–12 loop and burial of Leu536 in a solvent-inaccessible position. This may contribute to constitutive activity of the Y537S mutant protein. The Y537S surface mutation has no impact on the structure of the LBD pocket.

[00260] Y537N is common in ERα -negative metastatic breast cancer. A mutation at this site may allow ERα to escape phosphorylation-mediated controls and provide a cell with a potential selective tumorigenic advantage. Specifically, Y537N substitution induces conformational changes in the ERα that might mimic hormone binding, not affecting the ability of the receptor to dimerize, but conferring a constitutive transactivation function to the receptor (Zhang et al. Cancer Res 57:1244-1249 (1997)).

[00261] Y537C has a similar effect to Y537N.

[00262] D538G may shift the entire energy landscape by stabilizing both the active and inactive conformations, although more preferably the active. This may lead to constitutive activity of this mutant in the absence of hormones as observed in hormone-resistant breast cancer (Huang et al., "A newfound cancer activating mutation reshapes the energy landscape of estrogen-binding domain," *J.Chem. Theory Comput.* 10:2897-2900 (2014)).

[00263] None of these mutations are expected to impact the ligand binding domain nor specifically hinder RAD1901 binding. Y537 and D538 may cause conformational changes that leads to constitutive receptor activation independent of ligand binding.

[00264] Example V(B). *In vitro* binding assay of ERα constructs of wildtype and LBD mutant with RAD1901 and other compounds

[00265] *In vitro* binding assay of ERα constructs of wildtype (WT) and LBD mutant with RAD1901 showed that RAD1901 bound to mutant ERα with a similar affinity as to WT ERα.

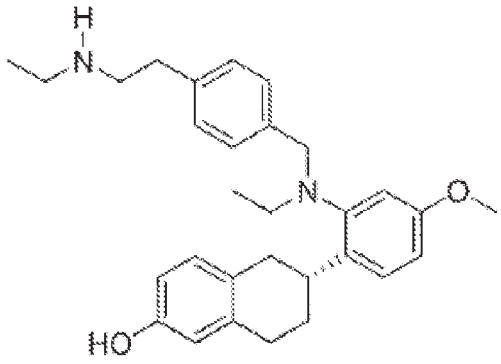
[00266] ERα constructs of WT and LBD mutant were prepared by expressing and purifying the corresponding LBD residues 302-552 with N-terminal thioredoxin and 6xHis tags which were cleaved by TEV protease.

[00267] Fluorescence polarization (FP) was used to determine binding of test compounds (RAD1901, fulvestrant, bazedoxifene, raloxifene, tamoxifene, and AZD9496) to ERα as per manufacturer's instructions (Polar Screen, Invitrogen) with 2 nM fluoromone, 100 nM ERα construct of WT or LBD mutant. Each set was carried out in duplicate and tested one test compound to determine the IC_{50} for different ERα constructs (Fig. 41 for RAD1901 binding essay).

[00268] As stated above, the foregoing is merely intended to illustrate various embodiments of the present invention. The specific modifications discussed above are not to be construed as limitations on the scope of the invention. It will be apparent to one skilled in the art that various equivalents, changes, and modifications may be made without departing from the scope of the invention, and it is understood that such equivalent embodiments are to be included herein. All references cited herein are incorporated by reference as if fully set forth herein.

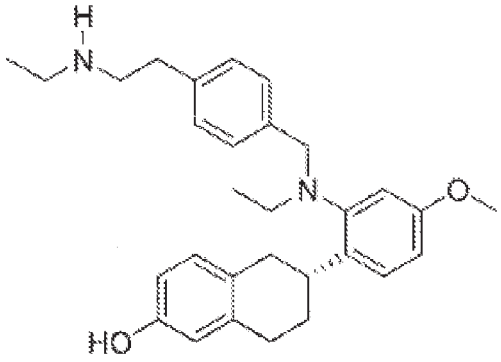
What is claimed is:

1. A method of inhibiting tumor growth or producing tumor regression in a subject having a drug-resistant estrogen receptor alpha positive cancer comprising administering to said subject a therapeutically effective amount of RAD1901 having the structure:



or a salt or solvate thereof.

2. A method of inhibiting tumor growth or producing tumor regression in a subject having a mutant estrogen receptor alpha positive cancer comprising administering to said subject a therapeutically effective amount of RAD1901 having the structure:



or a salt or solvate thereof.

3. The method of claim 1 or 2, wherein the cancer is selected from the group consisting of breast cancer, uterine cancer, ovarian cancer, and pituitary cancer.

4. The method of claim 1 or 2, wherein the cancer is a metastatic cancer.

5. The method of claim 1 or 2, wherein said cancer is positive for the mutant estrogen receptor alpha comprising one or more mutations selected from the group consisting of $Y537X_1$, $L536X_2$, P535H, V534E, S463P, V392I, E380Q and combinations thereof, wherein:

X_1 is S, N, or C, D538G; and X_2 is R or Q,

6. The method of claim 5, wherein the mutation is Y537S.

7. The method of claim 1 or 2, wherein the ratio of the concentration of RAD1901 or a salt or solvate thereof in the tumor to the concentration of RAD1901 or a salt or solvate thereof in plasma (T/P) following administration is at least about 15.

8. The method of claim 1 or 2, wherein subject has osteoporosis or a high risk of osteoporosis.

9. The method of claim 1 or 2, wherein the subject is a pre-menopausal woman.

10. The method of claim 1 or 2, wherein the subject is a post-menopausal woman who had relapsed or progressed after previous treatment with SERMs and/or AIs.

11. The method of claim 1 or 2, wherein the therapeutically effective amount is about 150 to about 1,500 mg q.d.

12. The method of claim 1 or 2, wherein the salt thereof is RAD1901 dihydrochloride.

13. The method of claim 1 or 2, wherein the tumor is resistant to a drug selected from the group consisting of anti-estrogens, aromatase inhibitors, and combinations thereof.

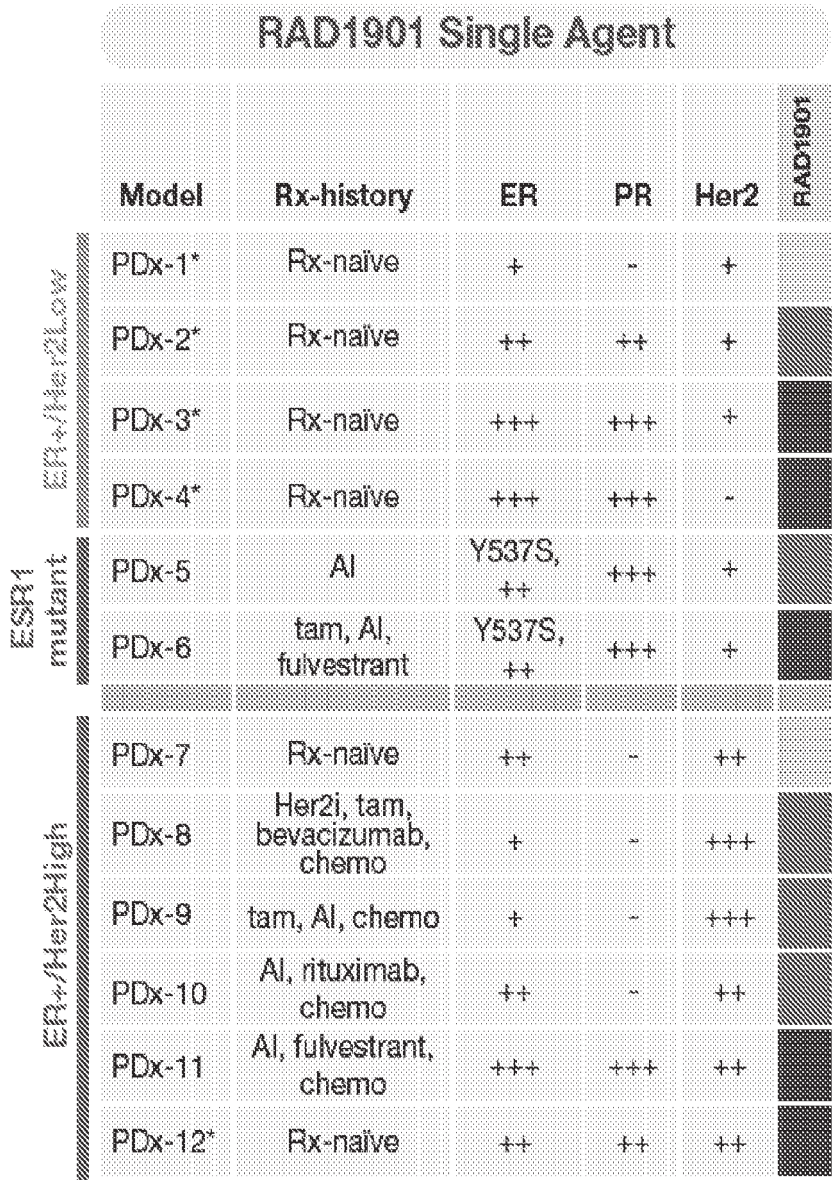
14. The method of claim 13, wherein the anti-estrogen is tamoxifen or fulvestrant.

15. The method of claim 13, wherein the aromatase inhibitor is aromasin.

16. The method of claim 1 or 2, wherein the therapeutically effective amount is 150 mg to 2,000 mg.

17. The method of claim 16, wherein the therapeutically effective amount is 200 mg, 400 mg, or 500 mg.

Fig. 1



AI: aromatase inhibitor;
tam: tamoxifen;
chemo: chemotherapy;
Her2i: trastuzumab, lapatinib;
Rx-naive: Treatment naive

RAD1901, po, qd
palbociclib, po, qd
Screen: n=3
*Full efficacy study n=6-10

IHC-scores (H-score)
- = 0-100
-+ = 101-200
-++ = 201-300

<25% TGI
26-64% TGI
65-100% TGI

Tumor growth inhibition (TGI) = (1-[Mean tumor volume of RAD1901 group/Mean tumor volume of control group])*100

Fig. 2A

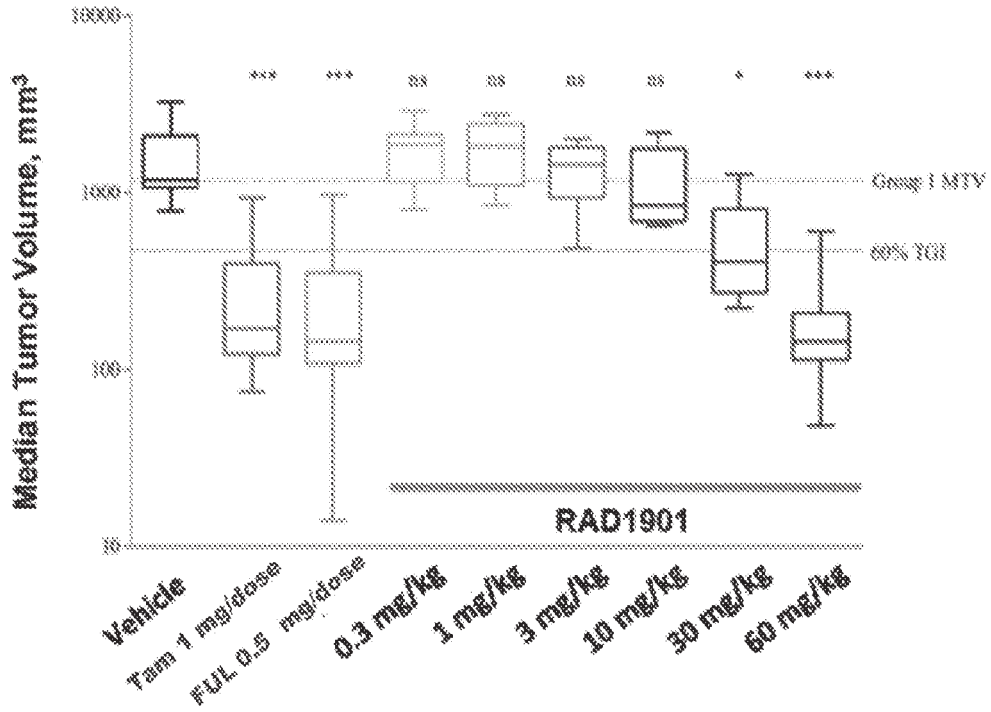

Median Tumor Volume, mm³
1000
100
10
Group 1 MTV
60% TGI
RAD1901
Vehicle
Tam 1 mg/dose
FUL 0.5 mg/dose
0.3 mg/kg
1 mg/kg
3 mg/kg
10 mg/kg
30 mg/kg
60 mg/kg

Fig. 2B

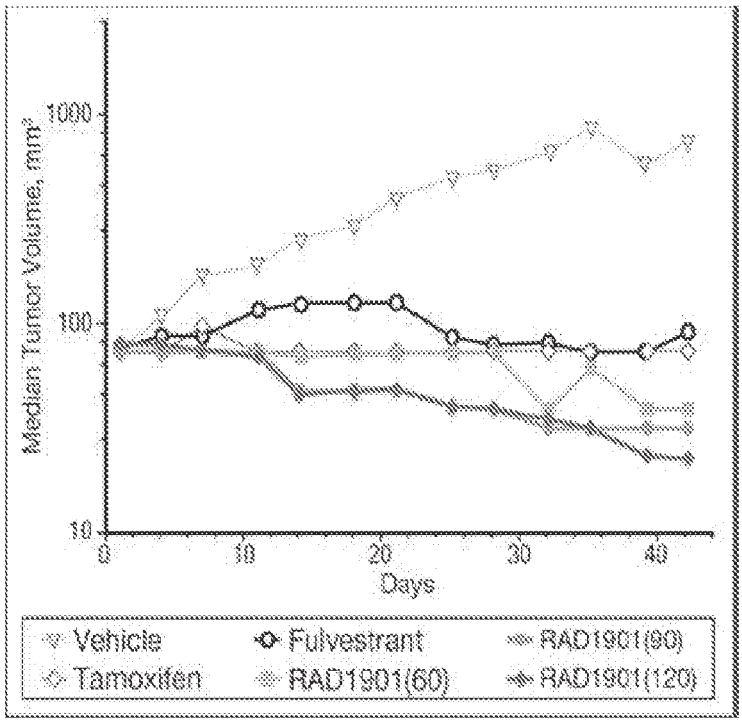

Median Tumor Volume, mm³
1000
100
10
0
10
20
30
40
Days
Vehicle
Tamoxifen
Fulvestrant
RAD1901(60)
RAD1901(90)
RAD1901(120)

Fig. 2C

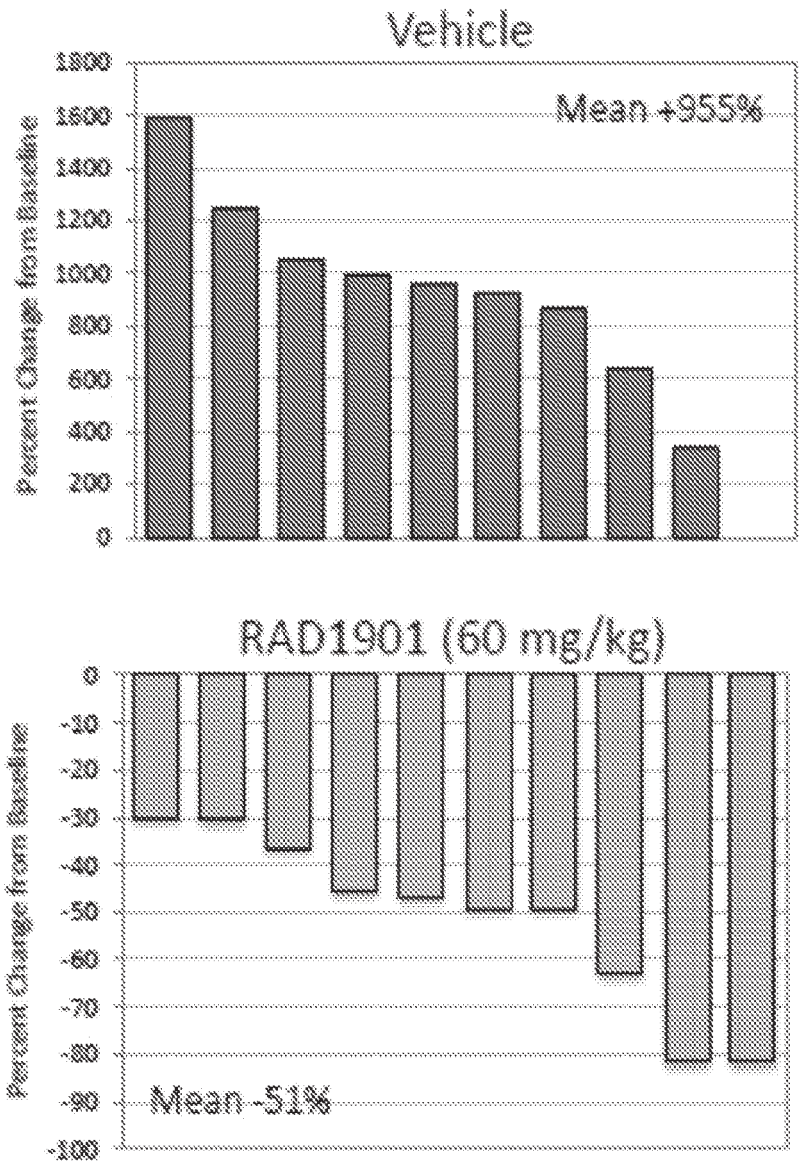

Vehicle
Mean +955%
Percent Change from Baseline
1800
1600
1400
1200
1000
800
600
400
200
0
RAD1901 (60 mg/kg)
Mean -51%
0
-10
-20
-30
-40
-50
-60
-70
-80
-90
-100

Fig. 2C (continued)

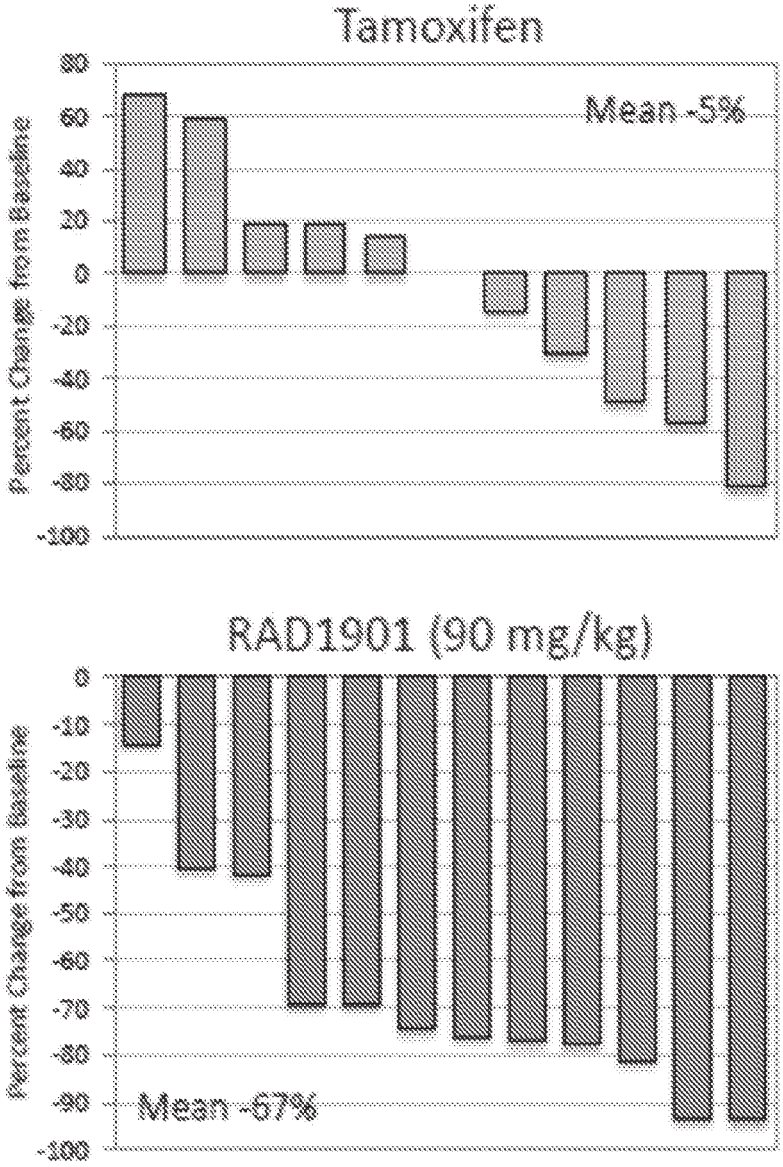


Fig. 2C (continued)

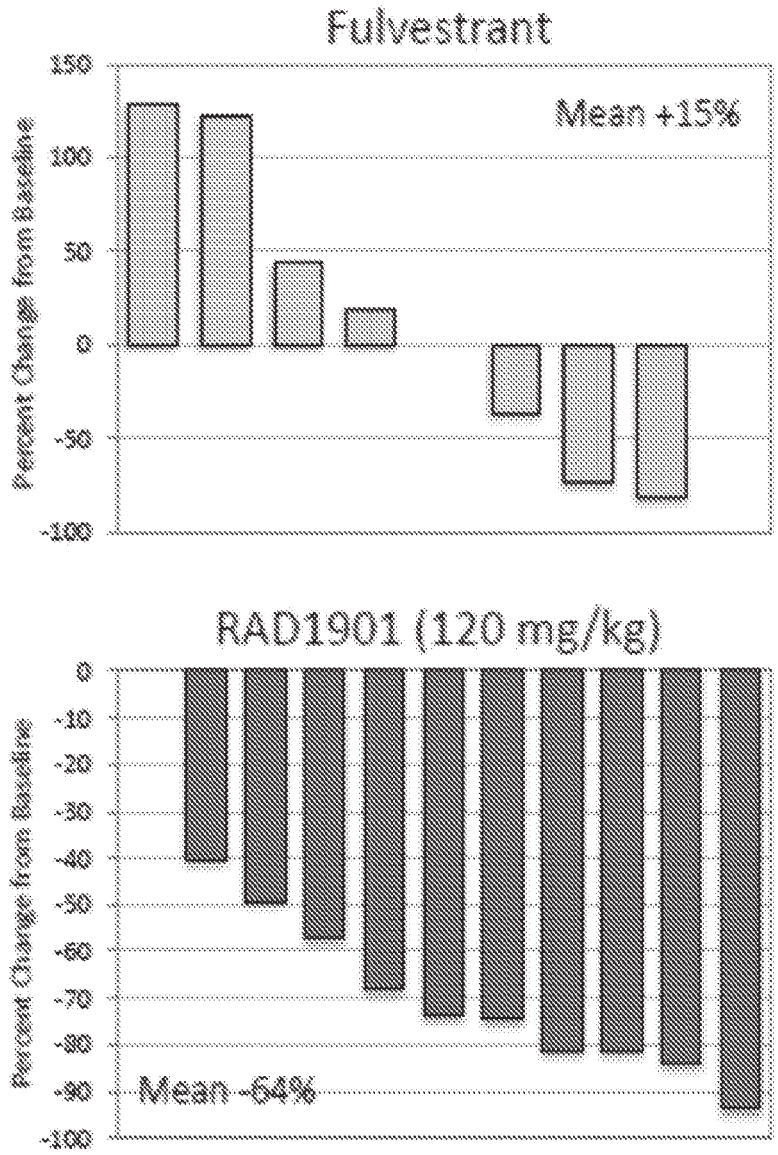


Fig. 2D

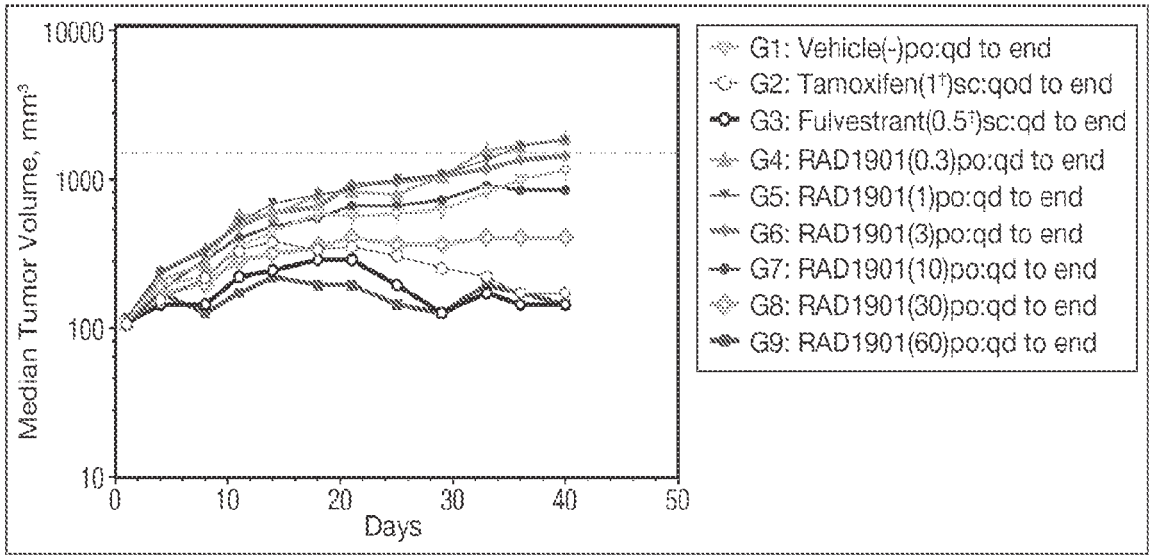

Median Tumor Volume, mm³
10000
1000
100
10
0
10
20
30
40
50
Days
G1: Vehicle(-)po:qd to end
G2: Tamoxifen(1)sc:qod to end
G3: Fulvestrant(0.5)sc:qd to end
G4: RAD1901(0.3)po:qd to end
G5: RAD1901(1)po:qd to end
G6: RAD1901(3)po:qd to end
G7: RAD1901(10)po:qd to end
G8: RAD1901(30)po:qd to end
G9: RAD1901(60)po:qd to end

Fig. 2E

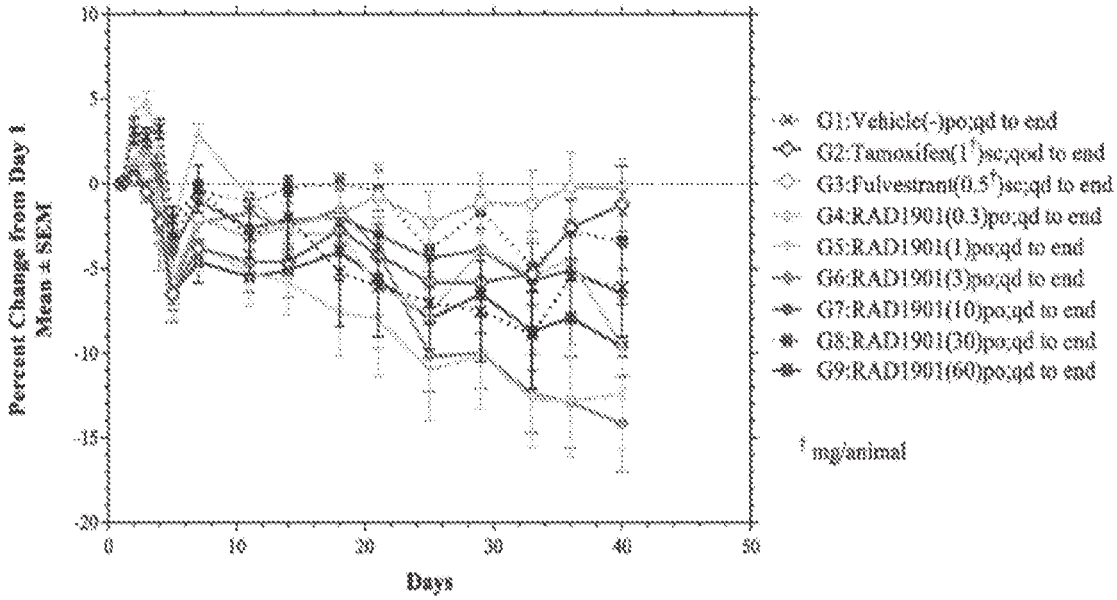

Percent Change from Day 1
Mean ± SEM
10
5
0
-5
-10
-15
-20
0
10
20
30
40
50
Days
G1:Vehicle(-)po;qd to end
G2:Tamoxifen(1[1])sc;qod to end
G3:Fulvestrant(0.5[1])sc;qd to end
G4:RAD1901(0.3)po;qd to end
G5:RAD1901(1)po;qd to end
G6:RAD1901(3)po;qd to end
G7:RAD1901(10)po;qd to end
G8:RAD1901(30)po;qd to end
G9:RAD1901(60)po;qd to end
[1] mg/animal

Fig. 3A

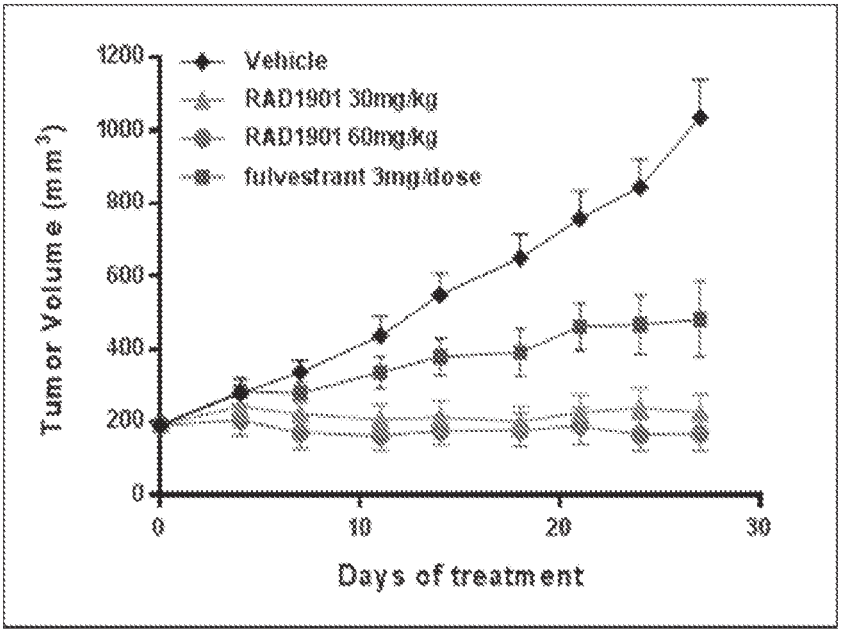

Vehicle
RAD1901 30mg/kg
RAD1901 60mg/kg
fulvestrant 3mg/dose
Tumor Volume (mm3)
1200
1000
800
600
400
200
0
0
10
20
30
Days of treatment

Fig. 3B

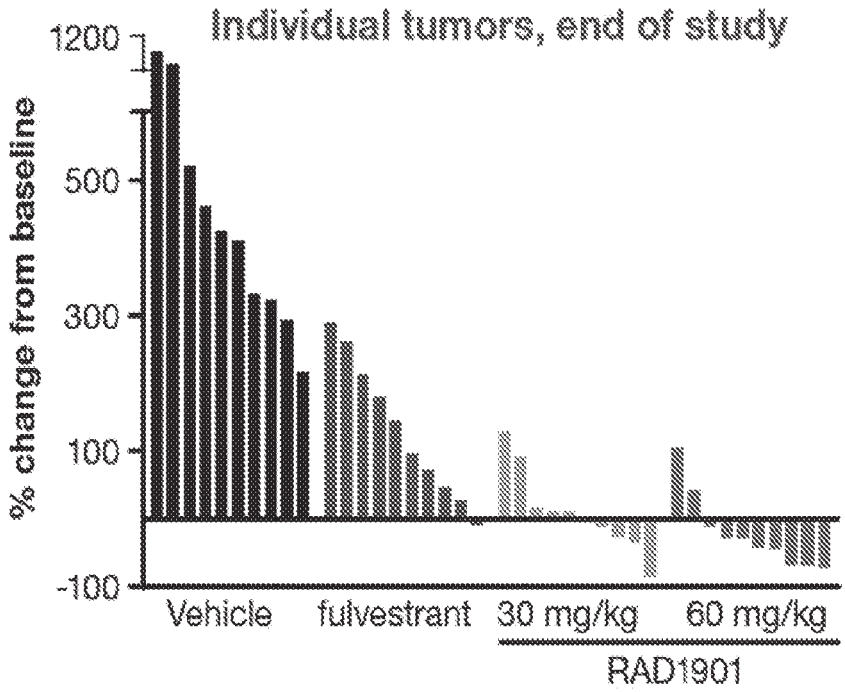

Individual tumors, end of study
% change from baseline
1200
500
300
100
-100
Vehicle
fulvestrant
30 mg/kg
60 mg/kg
RAD1901

Fig. 4A

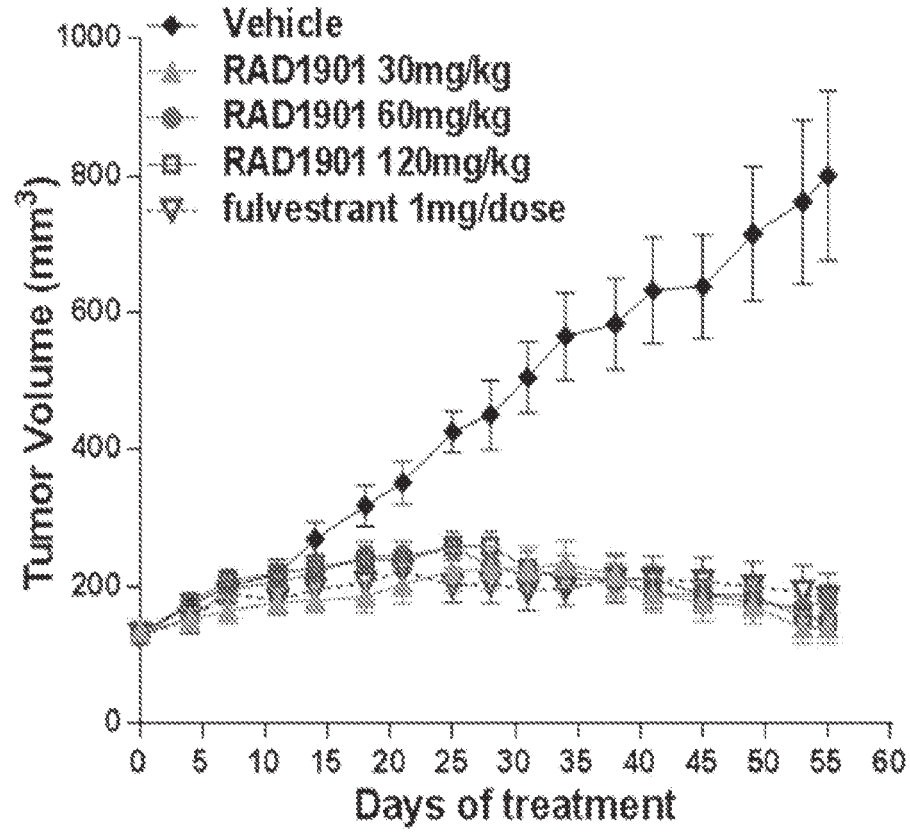

Vehicle
RAD1901 30mg/kg
RAD1901 60mg/kg
RAD1901 120mg/kg
fulvestrant 1mg/dose
Tumor Volume (mm3)
1000
800
600
400
200
0
0 5 10 15 20 25 30 35 40 45 50 55 60
Days of treatment

Fig. 4B

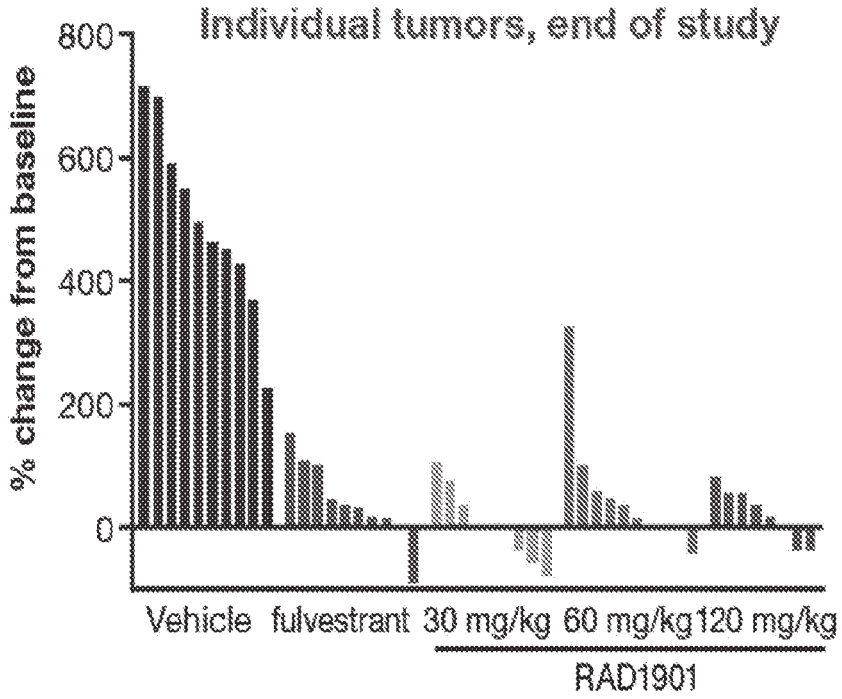

Individual tumors, end of study
% change from baseline
800
600
400
200
0
Vehicle
fulvestrant
30 mg/kg
60 mg/kg
120 mg/kg
RAD1901

Fig. 5

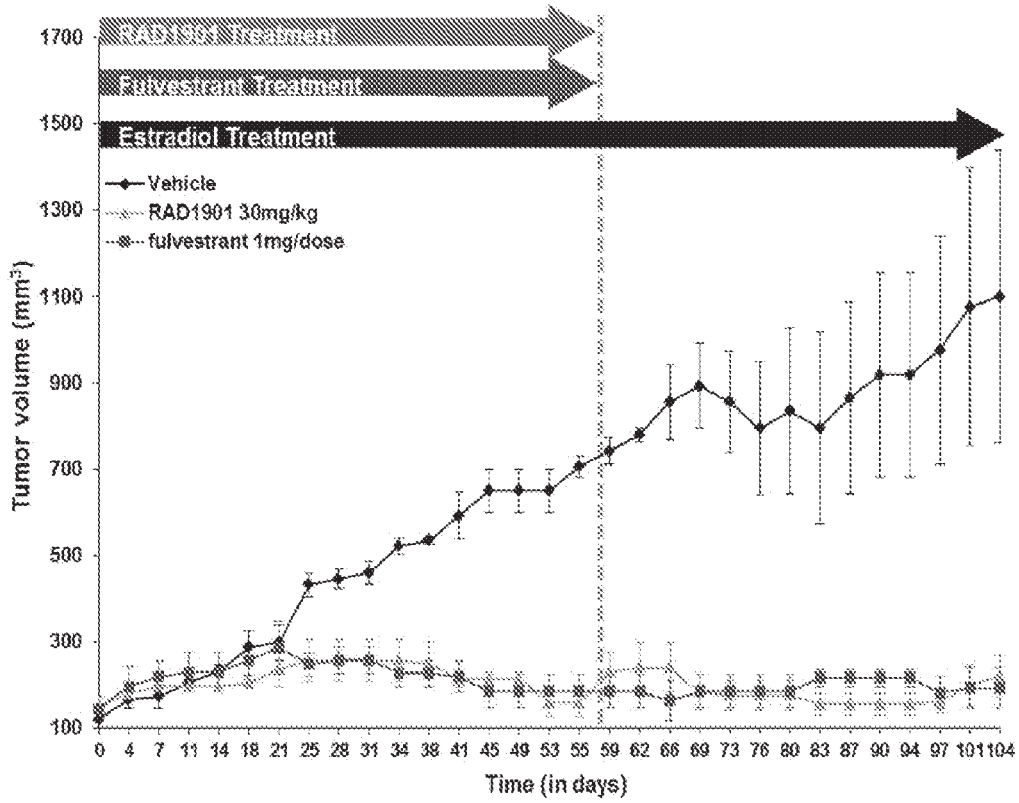

RAD1901 Treatment
Fulvestrant Treatment
Estradiol Treatment
Vehicle
RAD1901 30mg/kg
fulvestrant 1mg/dose
Tumor volume (mm3)
1700
1500
1300
1100
900
700
500
300
100
0 4 7 11 14 18 21 25 28 31 34 38 41 45 49 53 55 59 62 66 69 73 76 80 83 87 90 94 97 101 104
Time (in days)

Fig. 6

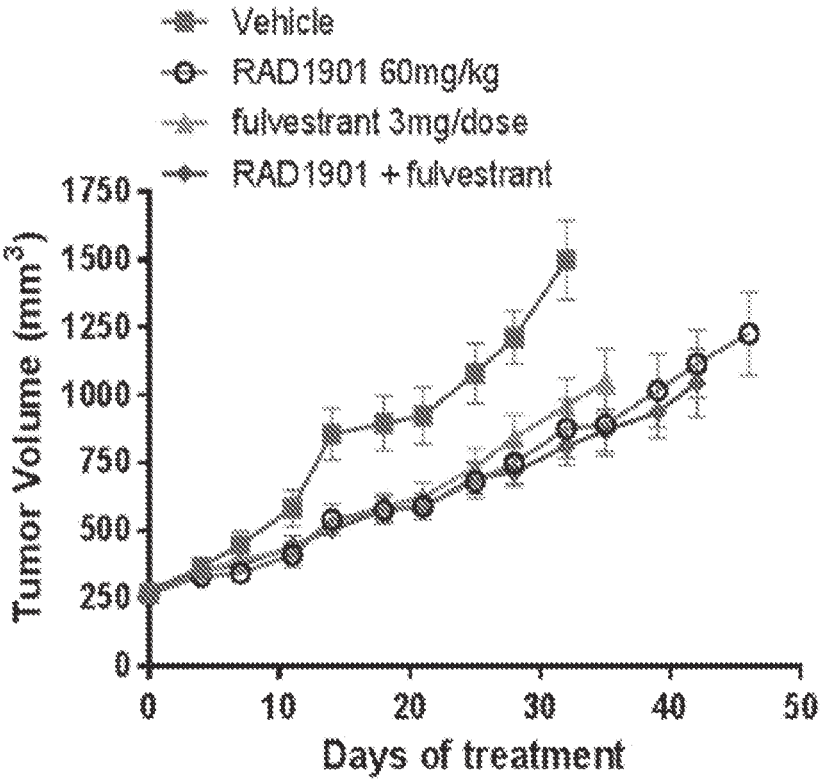

Vehicle
RAD1901 60mg/kg
fulvestrant 3mg/dose
RAD1901 + fulvestrant
Tumor Volume (mm3)
1750
1500
1250
1000
750
500
250
0
0
10
20
30
40
50
Days of treatment

Fig. 7A

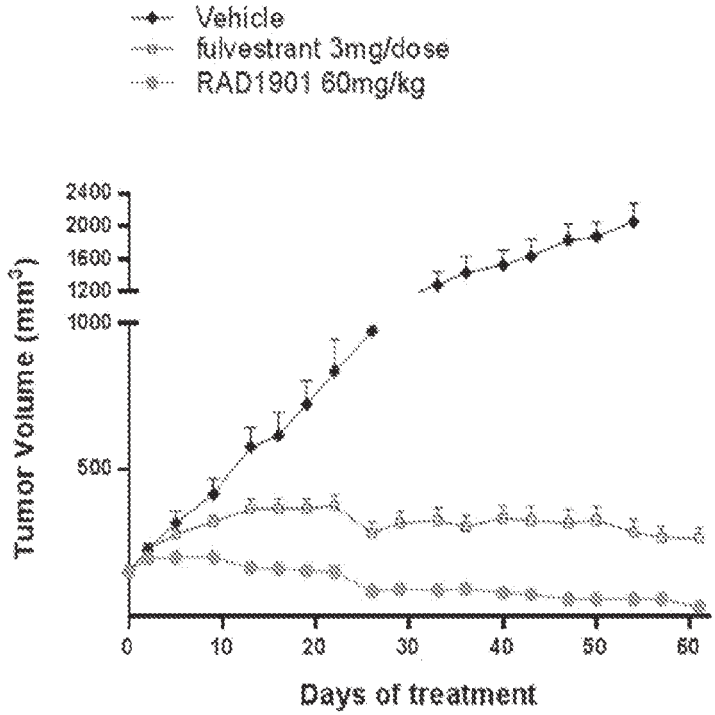

Vehicle
fulvestrant 3mg/dose
RAD1901 60mg/kg
Tumor Volume (mm3)
2400
2000
1600
1200
1000
500
0
10
20
30
40
50
60
Days of treatment

Fig. 7B

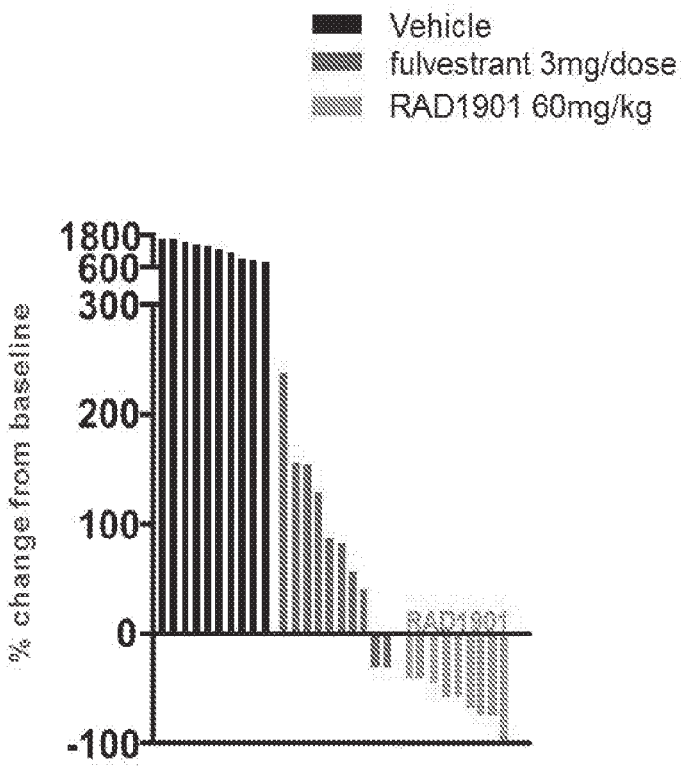

Vehicle
fulvestrant 3mg/dose
RAD1901 60mg/kg
% change from baseline
1800
600
300
200
100
0
-100
RAD1901

Fig. 8

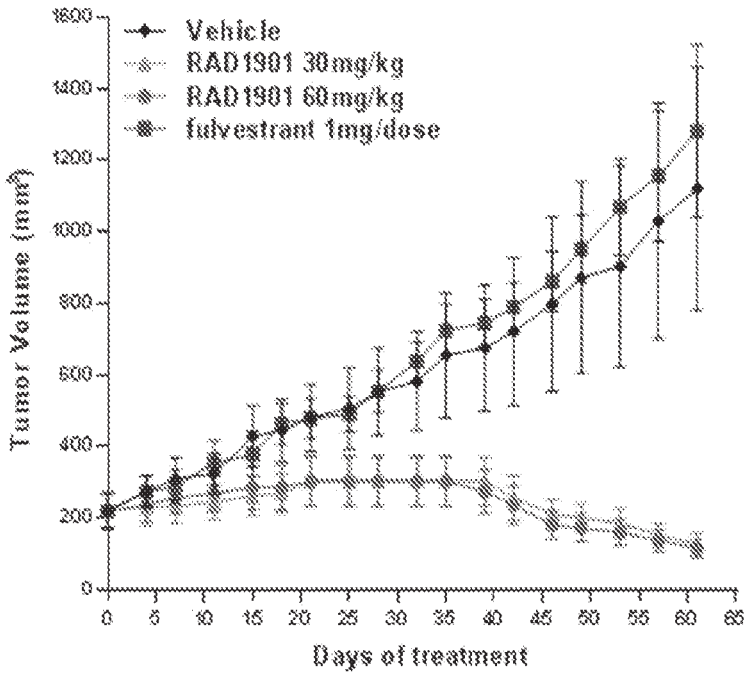

Vehicle
RAD1901 30mg/kg
RAD1901 60mg/kg
fulvestrant 1mg/dose
Tumor Volume (mm³)
Days of treatment
0
200
400
600
800
1000
1200
1400
1600
0
5
10
15
20
25
30
35
40
45
50
55
60
65

Fig. 9A

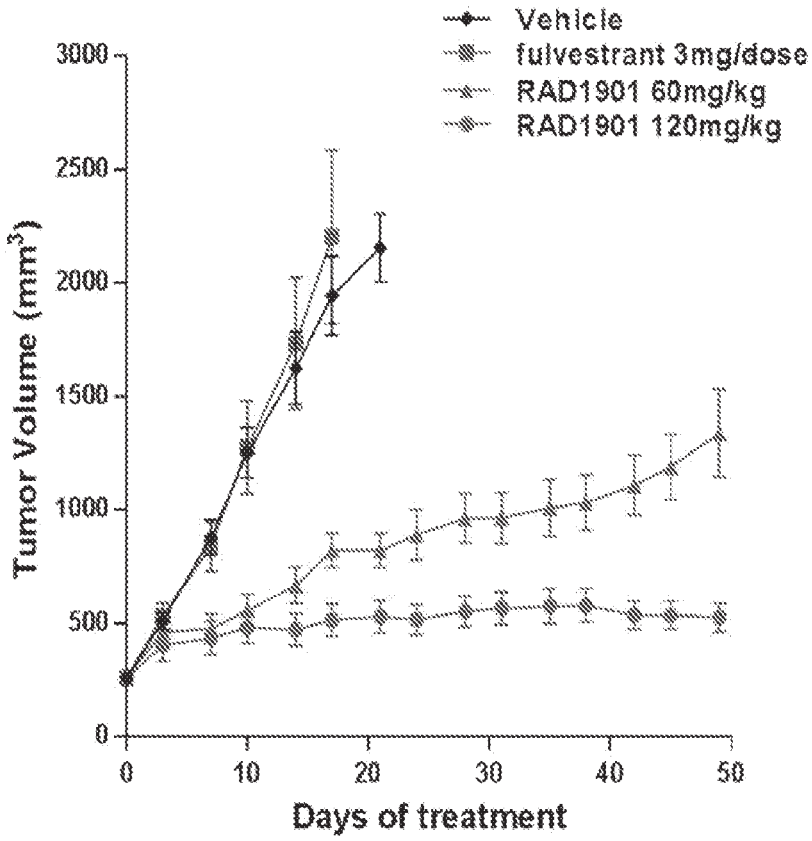

Vehicle
fulvestrant 3mg/dose
RAD1901 60mg/kg
RAD1901 120mg/kg
Tumor Volume (mm3)
3000
2500
2000
1500
1000
500
0
0
10
20
30
40
50
Days of treatment

Fig. 9B

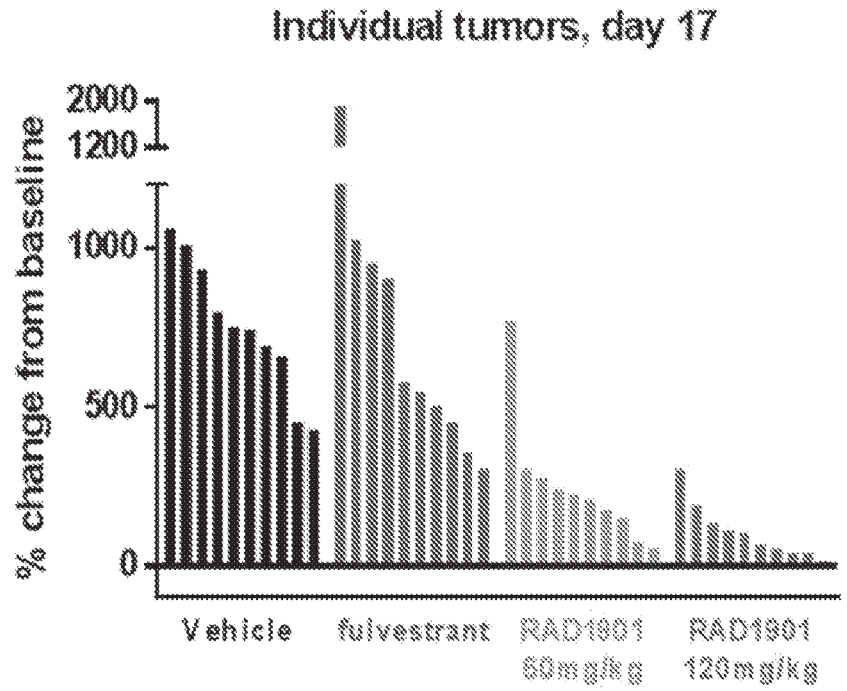

Individual tumors, day 17
% change from baseline
2000
1200
1000
500
0
Vehicle
fulvestrant
RAD1901 60mg/kg
RAD1901 120mg/kg

Fig. 9C

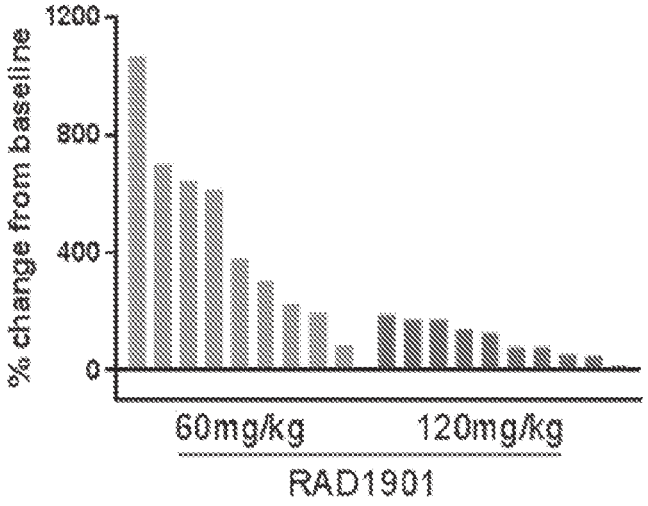

% change from baseline
1200
800
400
0
60mg/kg
120mg/kg
RAD1901

Fig. 10A

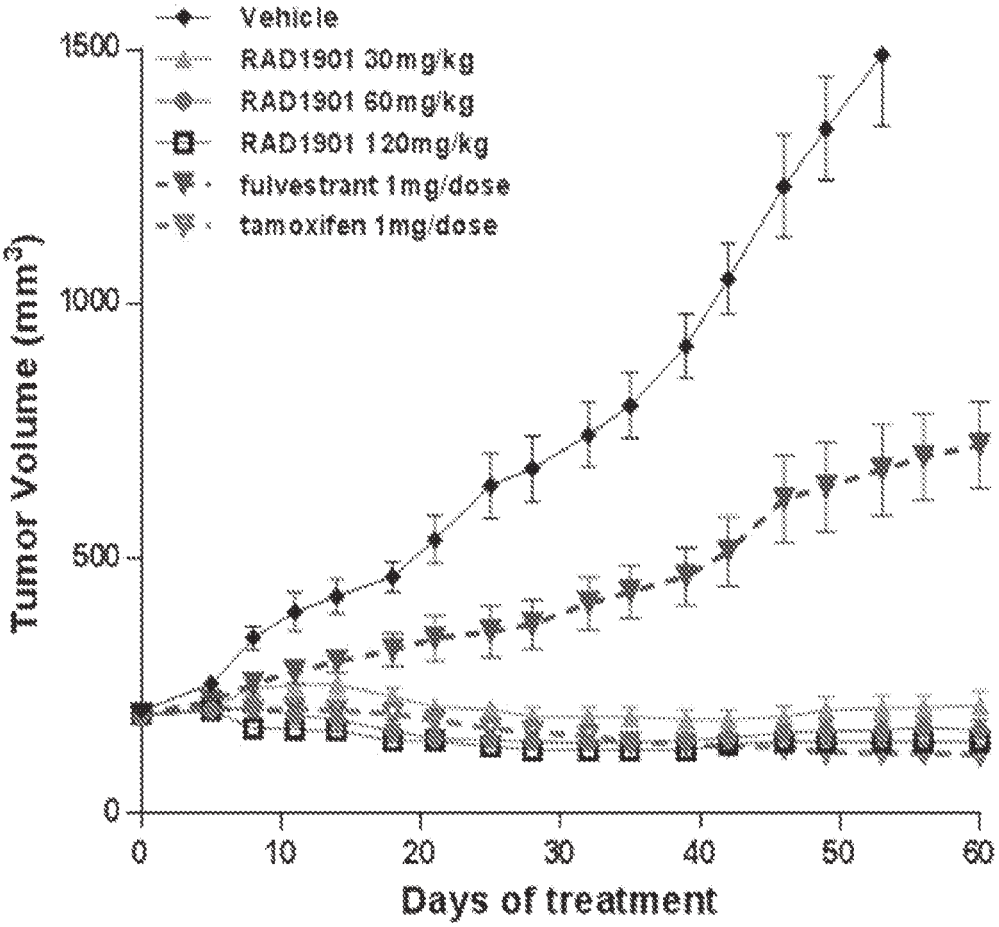


Fig. 10B

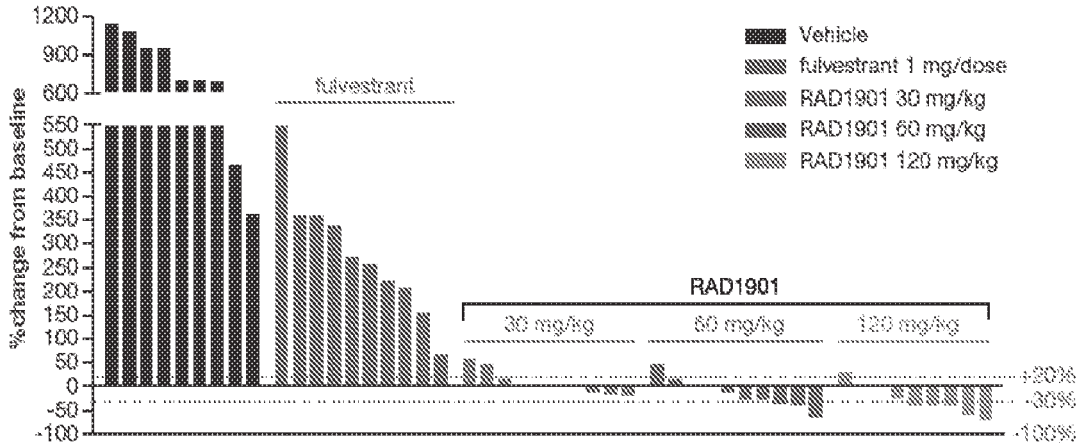


Fig. 11

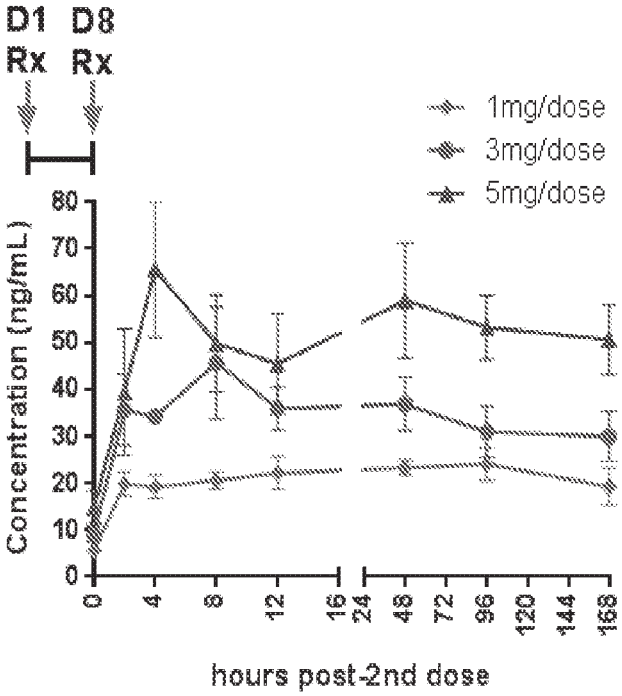

D1
Rx
D8
Rx
1mg/dose
3mg/dose
5mg/dose
Concentration (ng/mL)
0
10
20
30
40
50
60
70
80
0
4
8
12
16
24
48
72
96
120
144
168
hours post-2nd dose

Fig. 12

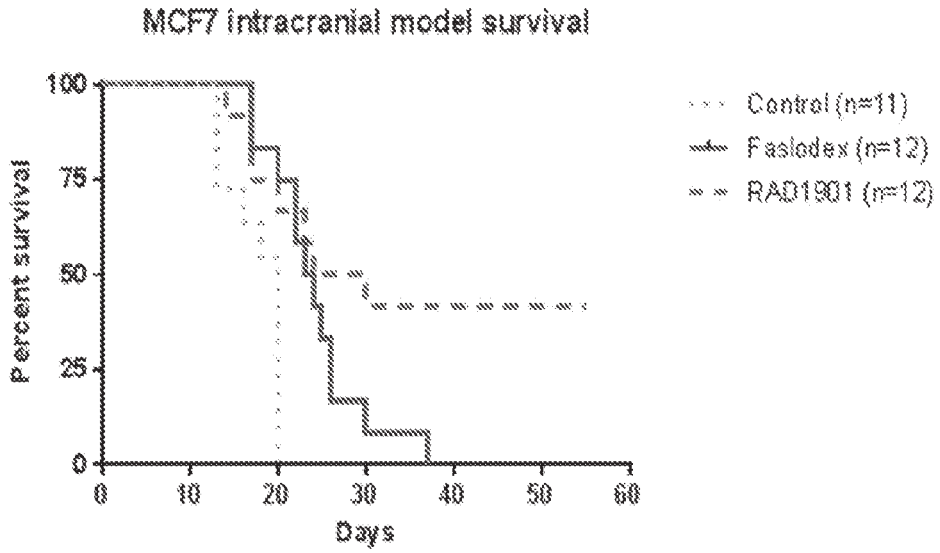

MCF7 intracranial model survival
Percent survival
100
75
50
25
0
0
10
20
30
40
50
60
Days
Control (n=11)
Faslodex (n=12)
RAD1901 (n=12)

Fig. 13

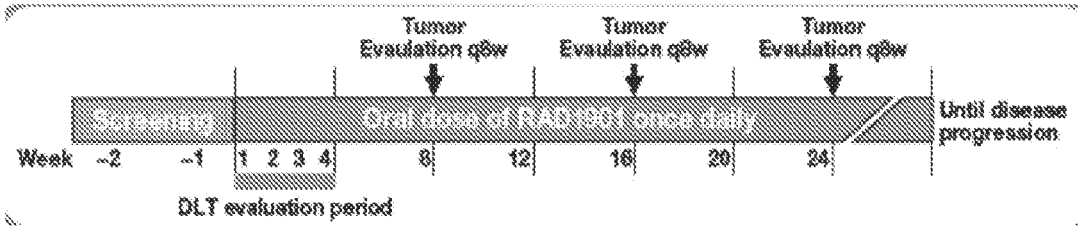

Tumor Evaluation qow
Tumor Evaluation qow
Tumor Evaluation qow
Screening
Oral dose of RAD1901 once daily
Until disease progression
Week -2 -1 1 2 3 4 8 12 16 20 24
DLT evaluation period

Fig. 14A

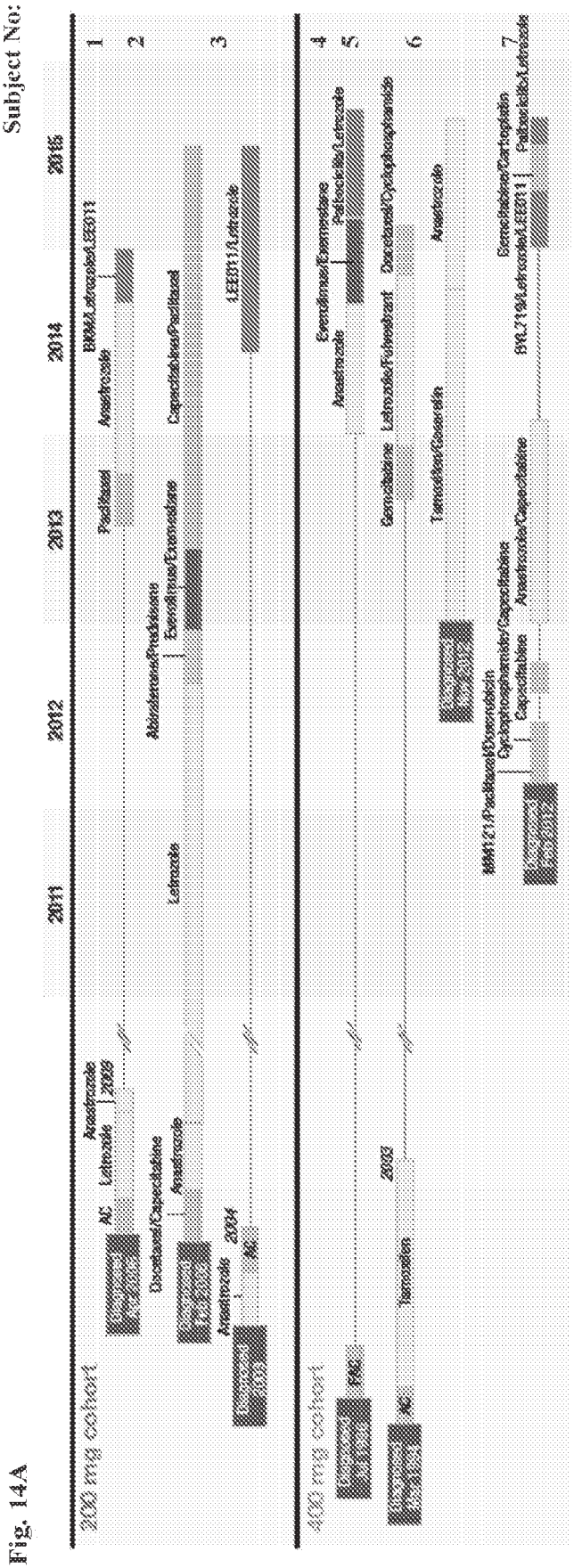

Subject No:
2011
2012
2013
2014
2015
200 mg cohort
400 mg cohort
Anastrozole
AC
Letrozole
Docetaxel/Capecitabine
Exemestane/Everolimus
Capecitabine/Paclitaxel
Paclitaxel
Cyclophosphamide/Capecitabine
Cyclophosphamide
Docetaxel/Cyclophosphamide
Fulvestrant
Tamoxifen/Goserelin
Palbociclib/Letrozole
Abbreviations: AC, doxorubicin/cyclophosphamide; FAC, 5-fluorouracil/doxorubicin/cyclophosphamide

Fig. 14B

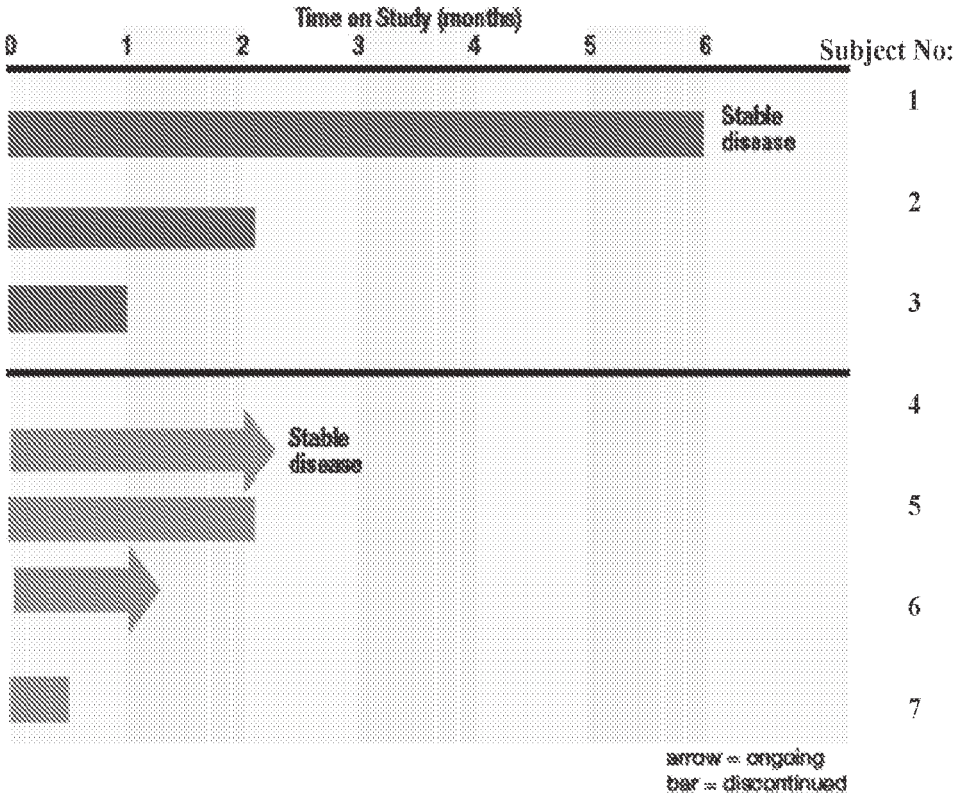

Time on Study (months)
0
1
2
3
4
5
6
Subject No:
1
2
3
4
5
6
7
Stable disease
Stable disease
arrow = ongoing
bar = discontinued

Fig. 15A

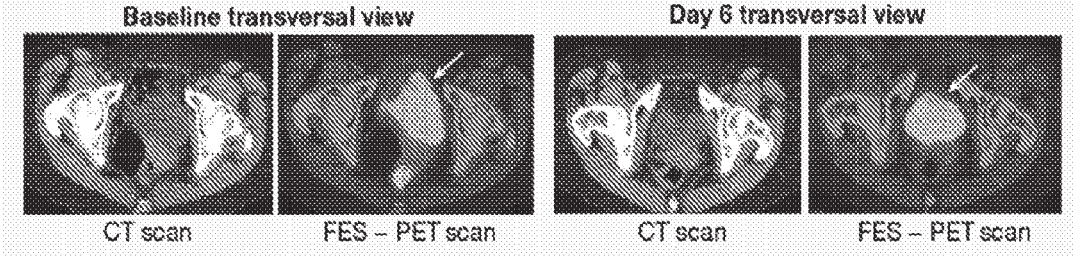


Fig. 15B

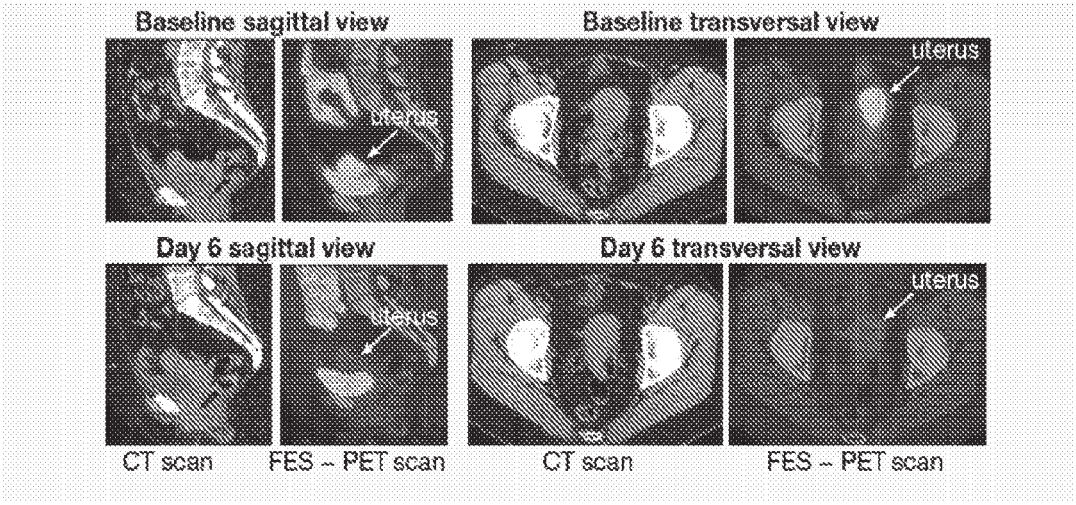


Fig. 15C

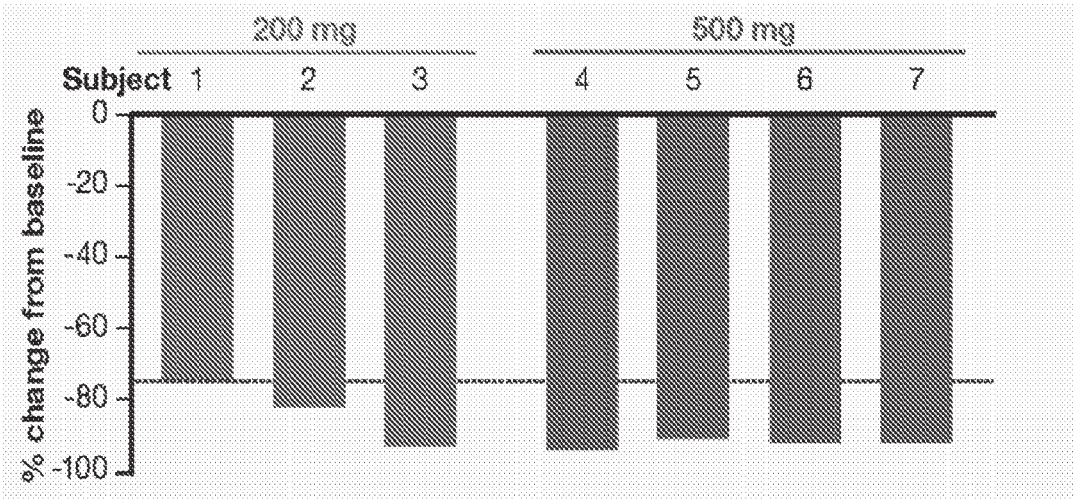

200 mg
500 mg
Subject 1 2 3 4 5 6 7
0
-20
-40
-60
-80
-100
% change from baseline

Fig. 16A

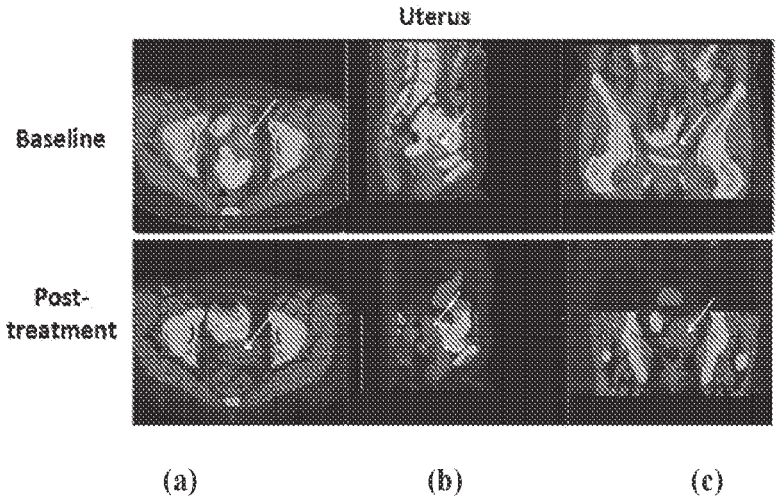


Fig. 16B

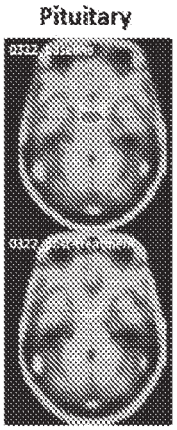


Fig. 17A

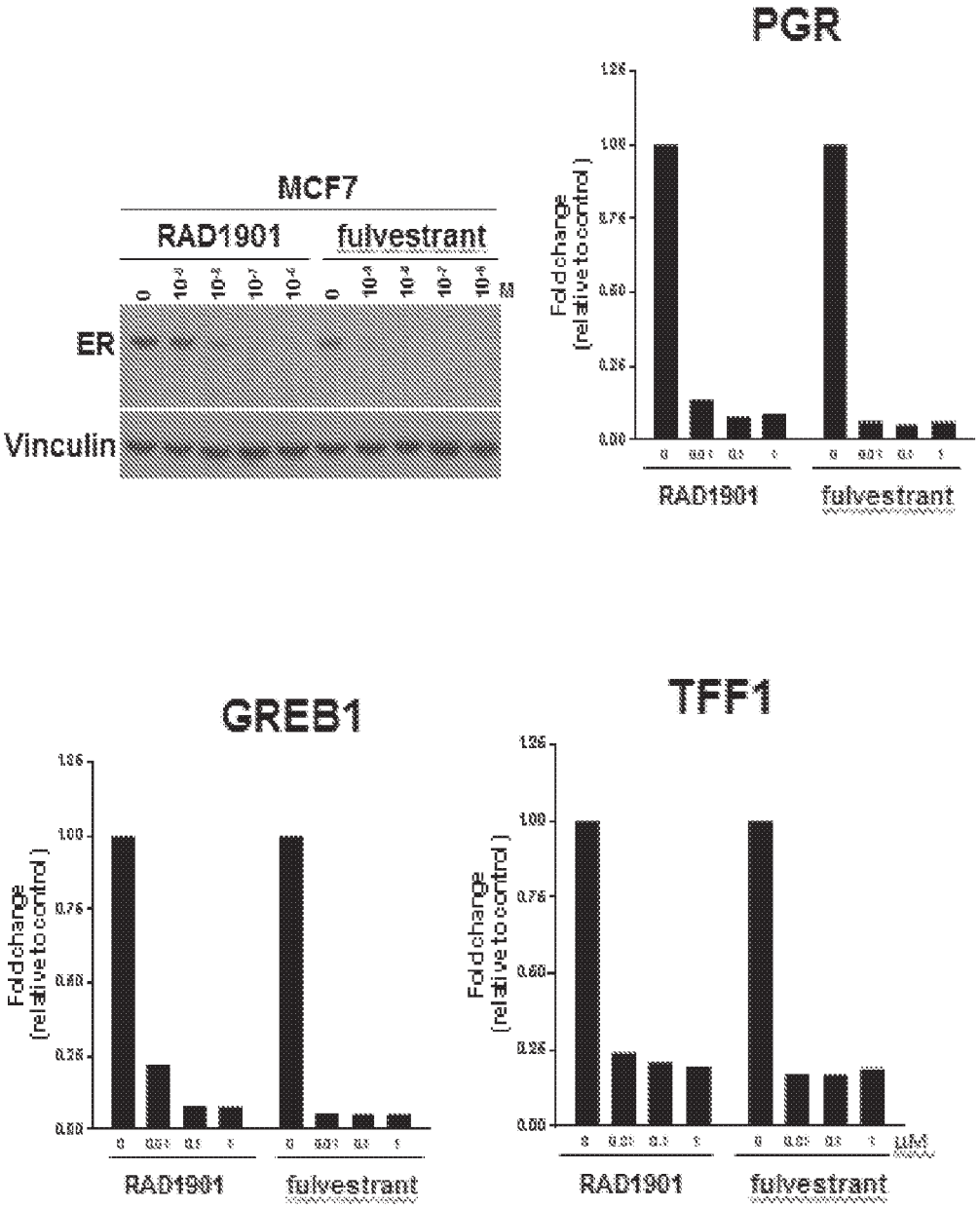

MCF7
RAD1901
fulvestrant
ER
Vinculin
PGR
GREB1
TFF1
Fold change (relative to control)
RAD1901
fulvestrant

Fig. 17B

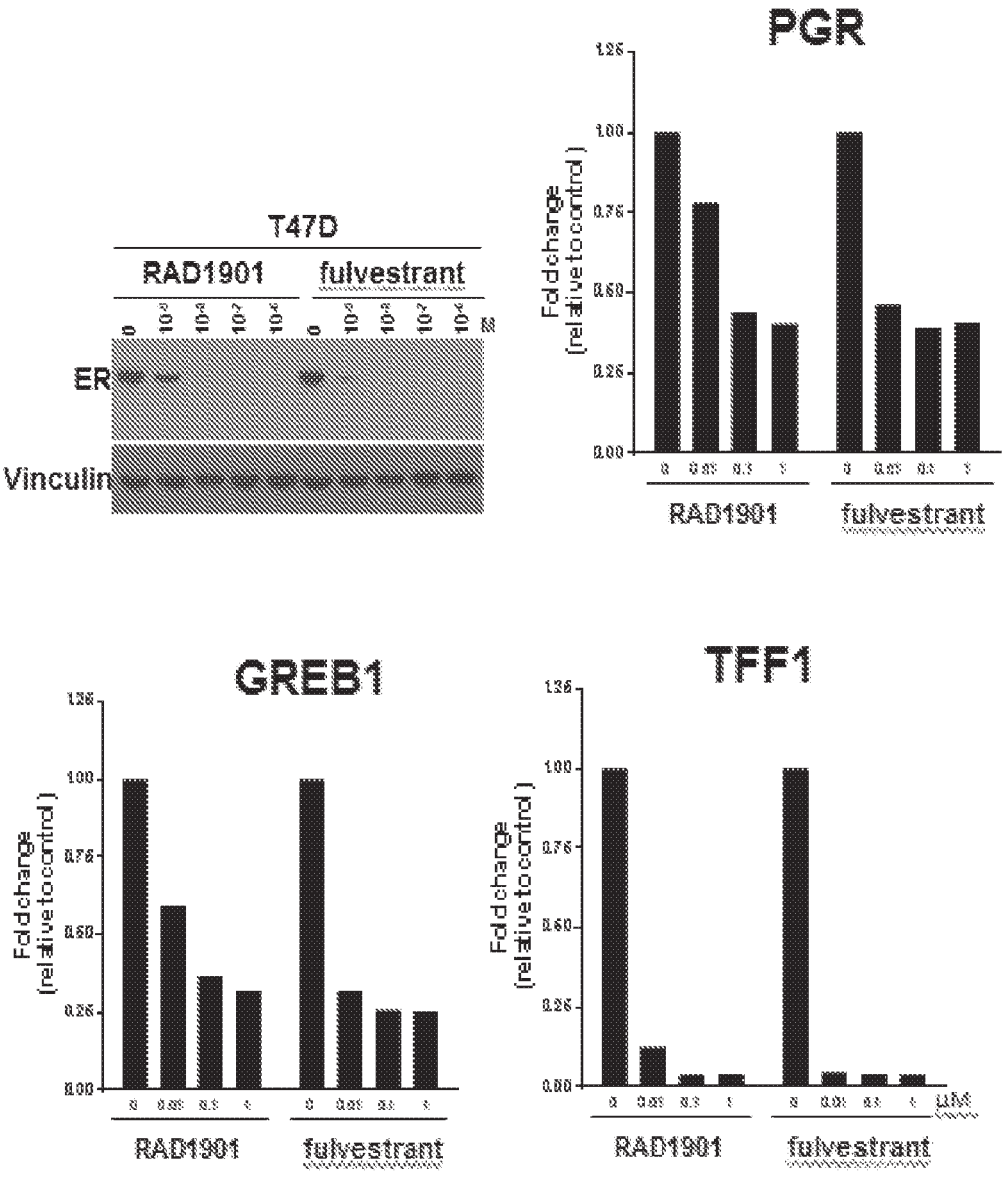

T47D
RAD1901
fulvestrant
0
10-5
10-4
10-3
10-2
10-1
M
ER
Vinculin
PGR
Fold change (relative to control)
RAD1901
fulvestrant
GREB1
TFF1
μM

Fig. 18A

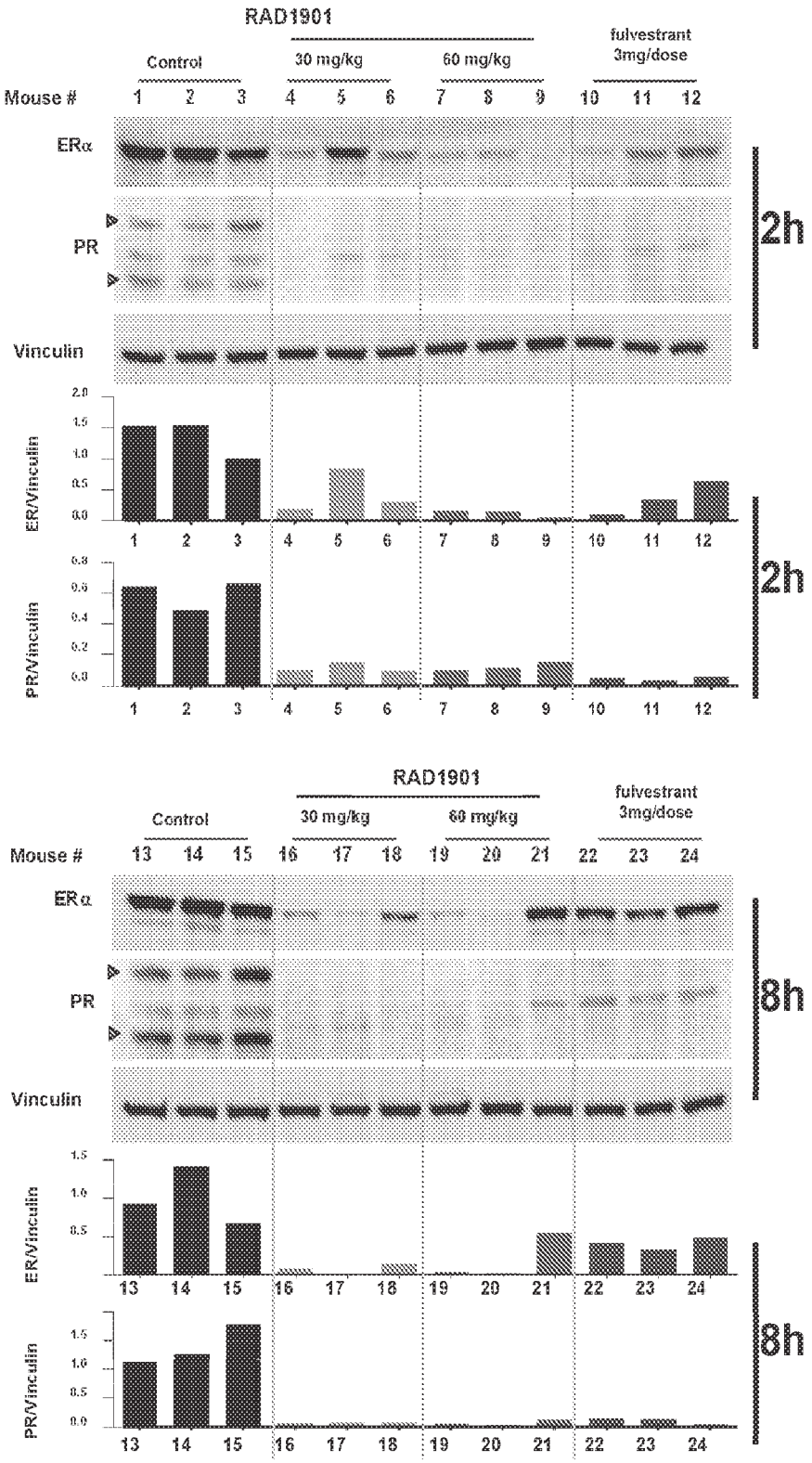

RAD1901
Control
30 mg/kg
60 mg/kg
fulvestrant 3mg/dose
Mouse #
1 2 3 4 5 6 7 8 9 10 11 12
ERα
PR
Vinculin
2h
ER/Vinculin
PR/Vinculin
2h
RAD1901
Control
30 mg/kg
60 mg/kg
fulvestrant 3mg/dose
Mouse #
13 14 15 16 17 18 19 20 21 22 23 24
ERα
PR
Vinculin
8h
ER/Vinculin
PR/Vinculin
8h

Fig. 18B

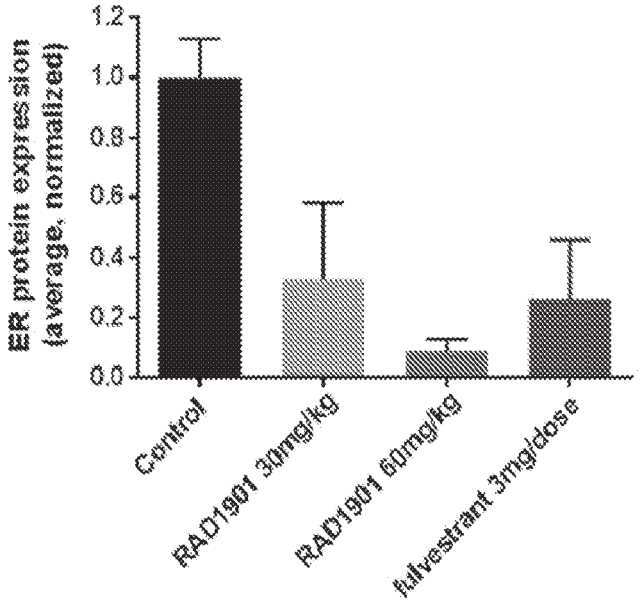


Fig. 18C

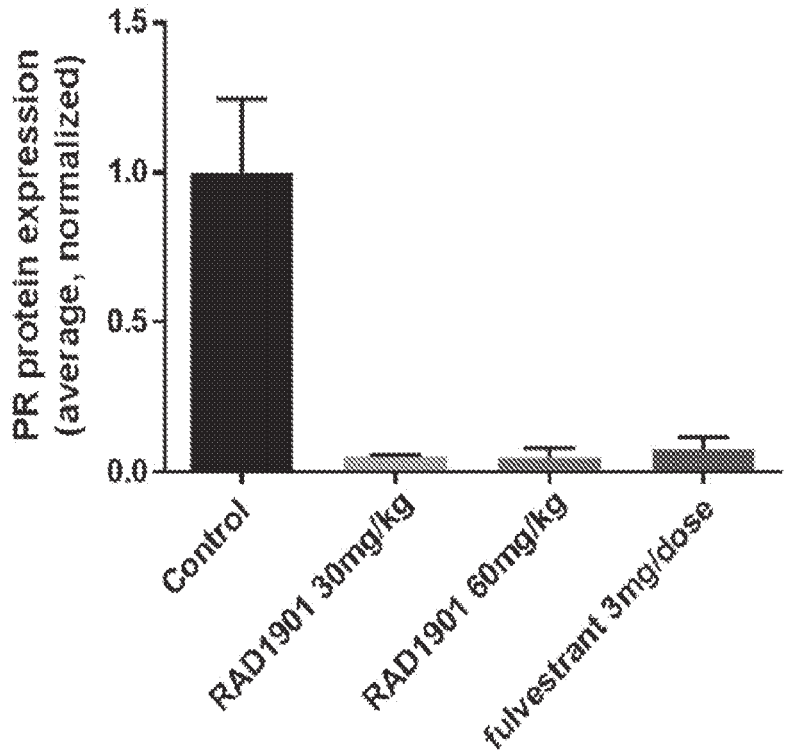


Fig. 19A

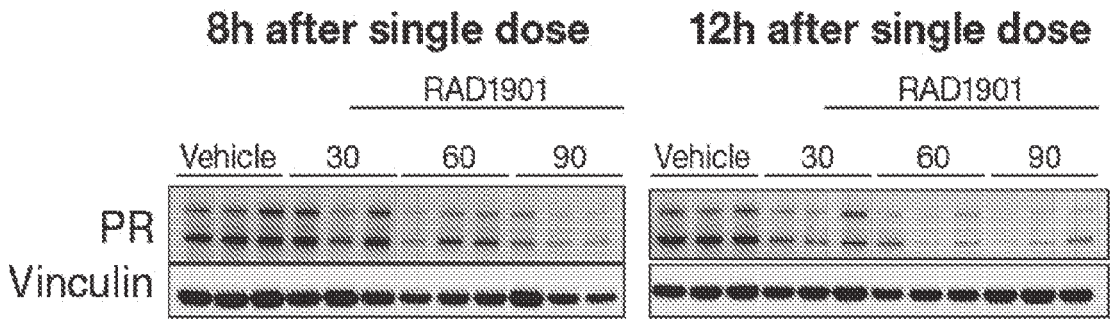


Fig. 19B

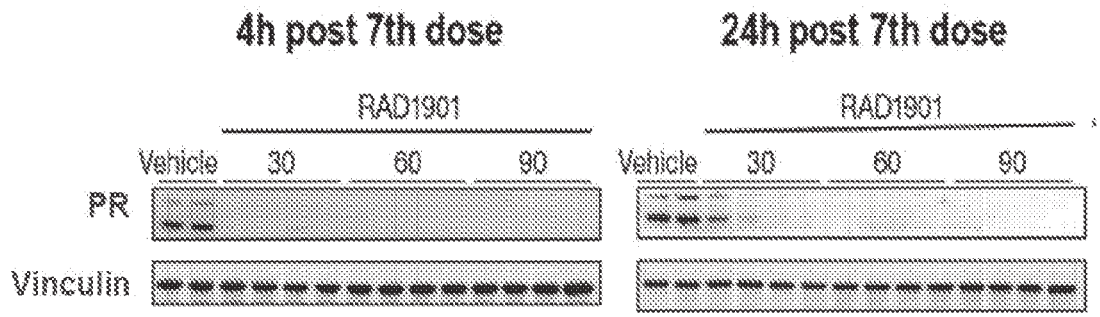


Fig. 19C

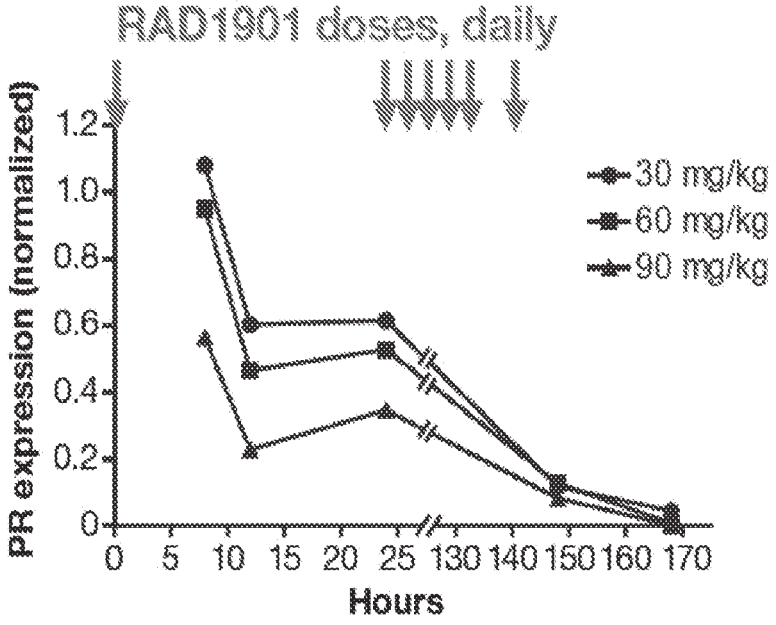


Fig. 20A

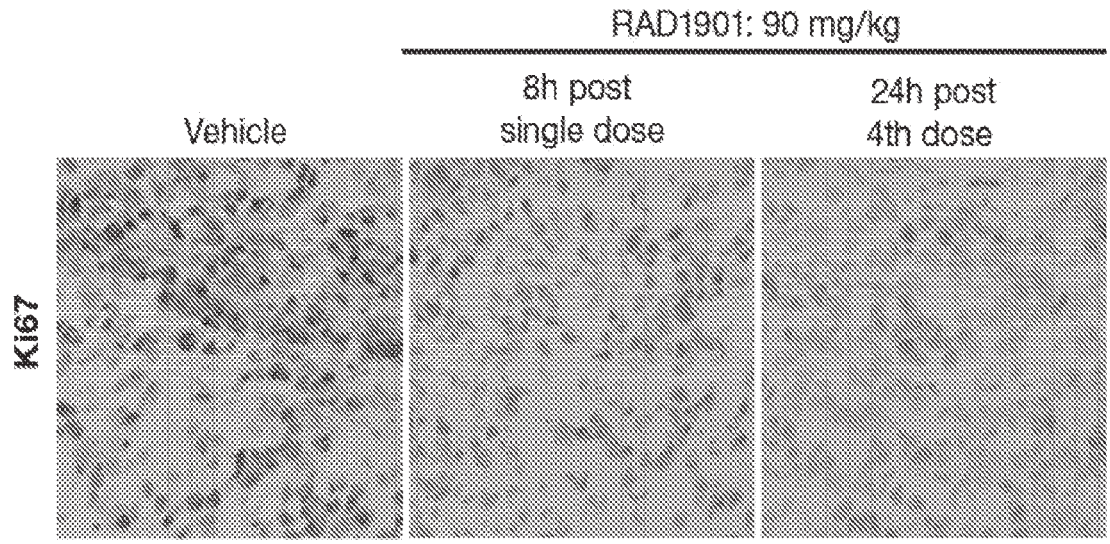


Fig.. 20B

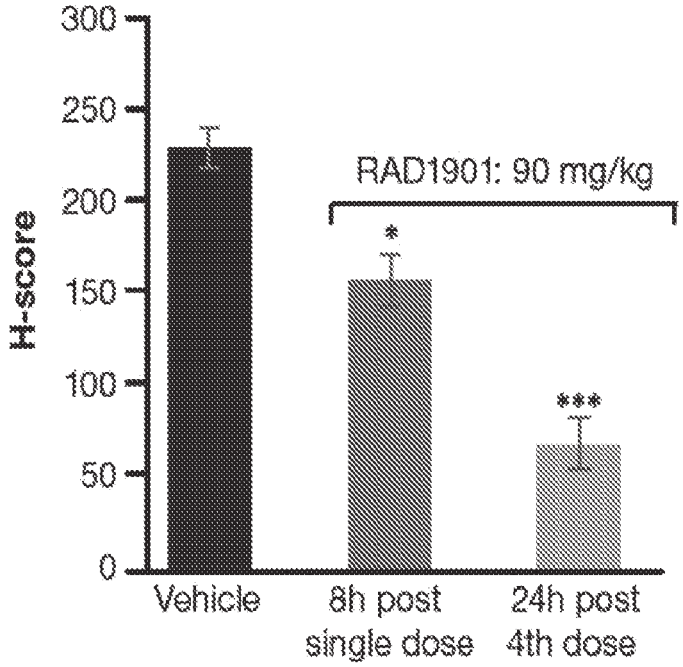


Fig. 21

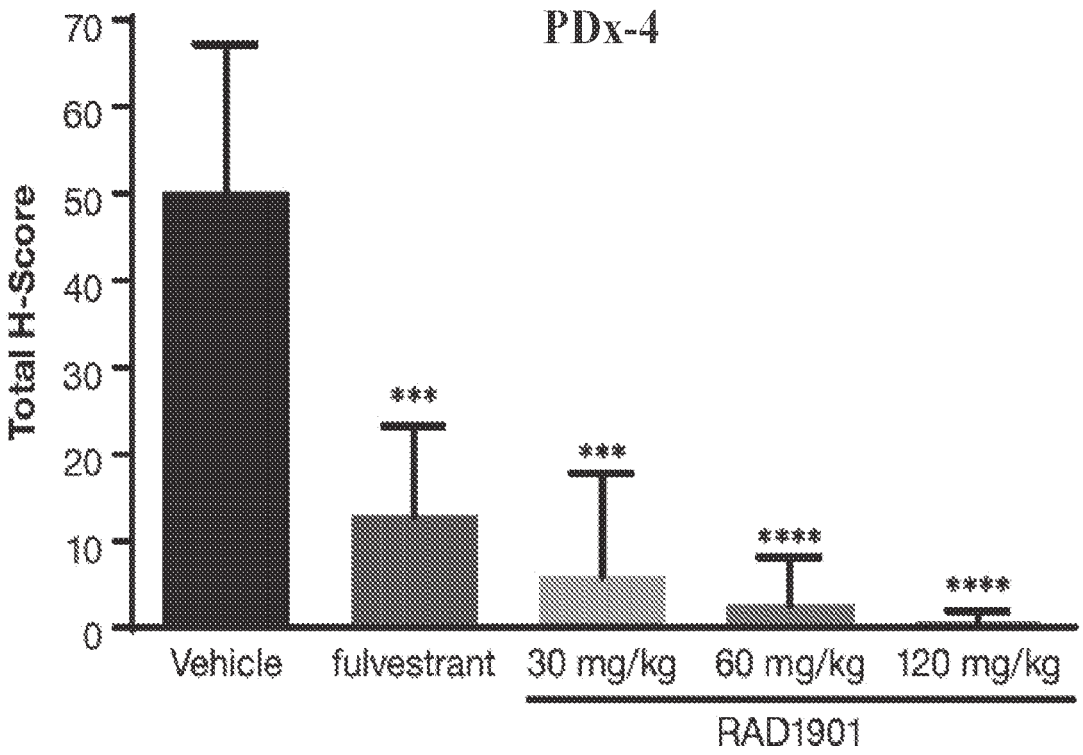
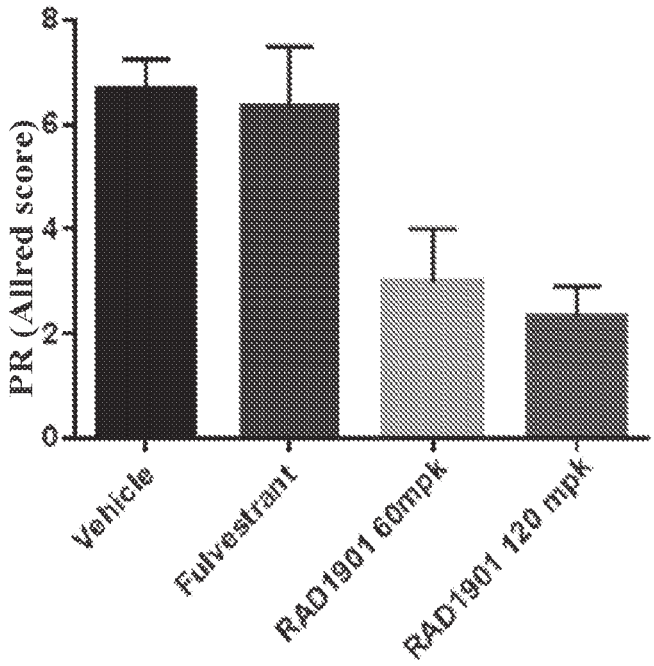

PDx-4
Total H-Score
70
60
50
40
30
20
10
0
***
***
****
****
Vehicle
fulvestrant
30 mg/kg
60 mg/kg
120 mg/kg
RAD1901

Fig. 22


PR (Allred score)
0
2
4
6
8
Vehicle
Fulvestrant
RAD1901 60mpk
RAD1901 120 mpk

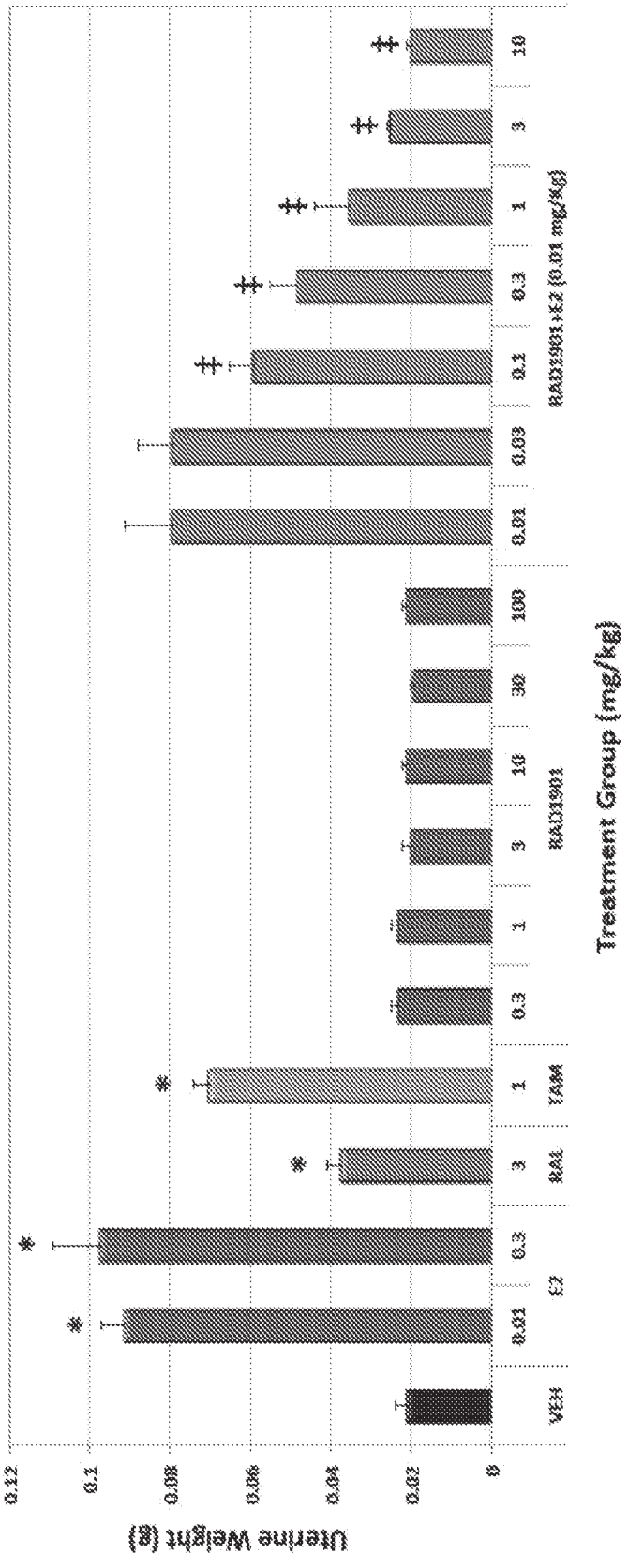

Uterine Weight (g)
0.12
0.1
0.08
0.06
0.04
0.02
0
VEH
0.01
E2
0.3
3
RAL
1
TAM
0.3
1
3
10
RAD1901
30
100
0.01
0.03
0.1
0.3
1
3
10
RAD1901+E2 (0.01 mg/kg)
Treatment Group (mg/kg)

Fig. 23A

Fig. 23B

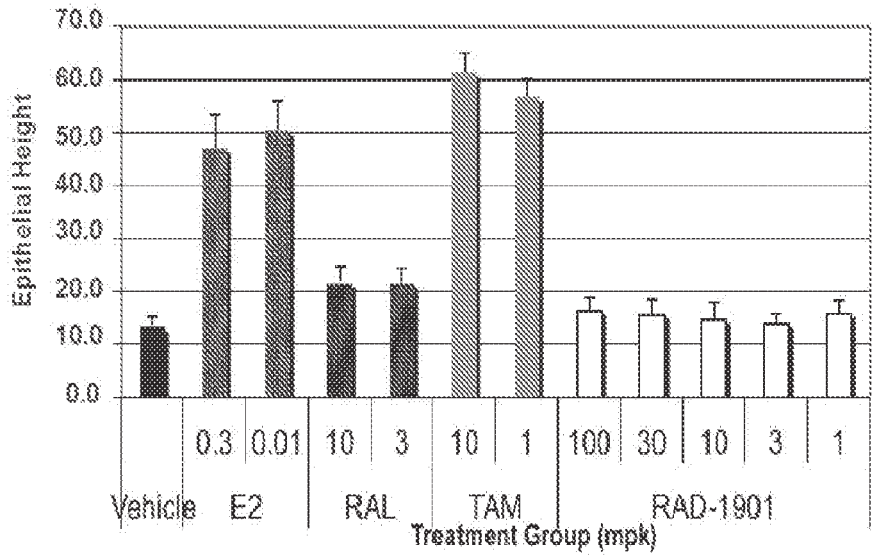


Fig. 23C

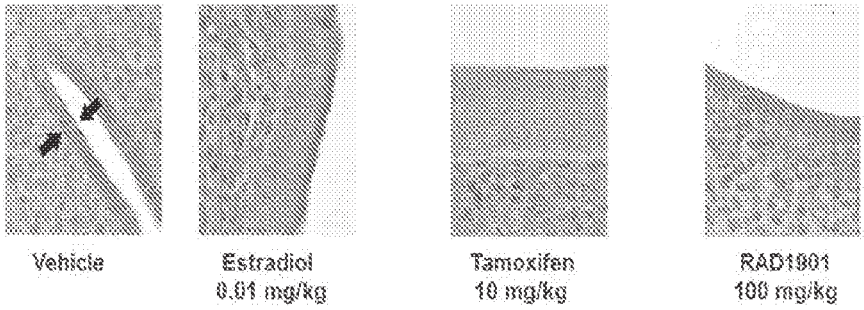


Fig. 23D

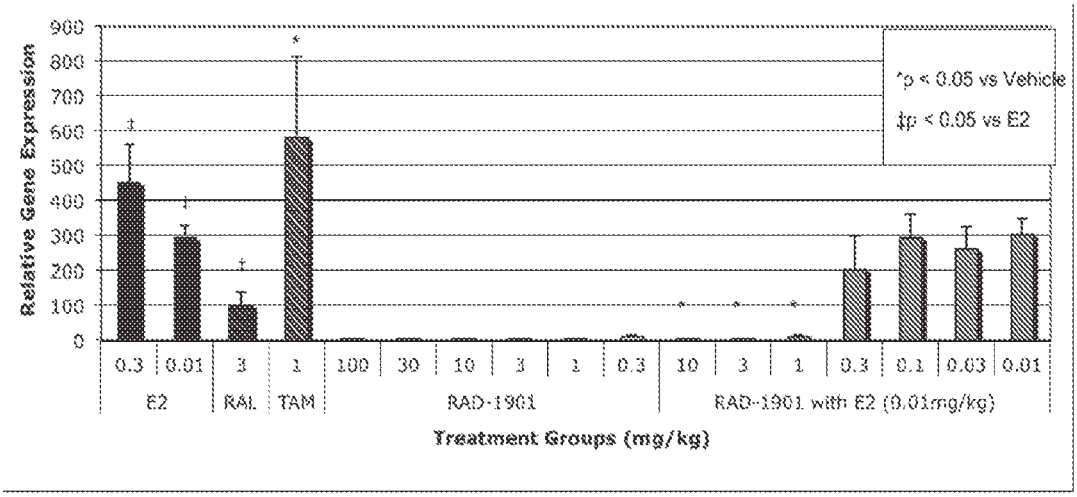

Relative Gene Expression
900
800
700
600
500
400
300
200
100
0
*p < 0.05 vs Vehicle
‡p < 0.05 vs E2
0.3
0.01
3
1
100
30
10
3
1
0.3
10
3
1
0.3
0.1
0.03
0.01
E2
RAL
TAM
RAD-1901
RAD-1901 with E2 (0.01mg/kg)
Treatment Groups (mg/kg)

Fig. 24

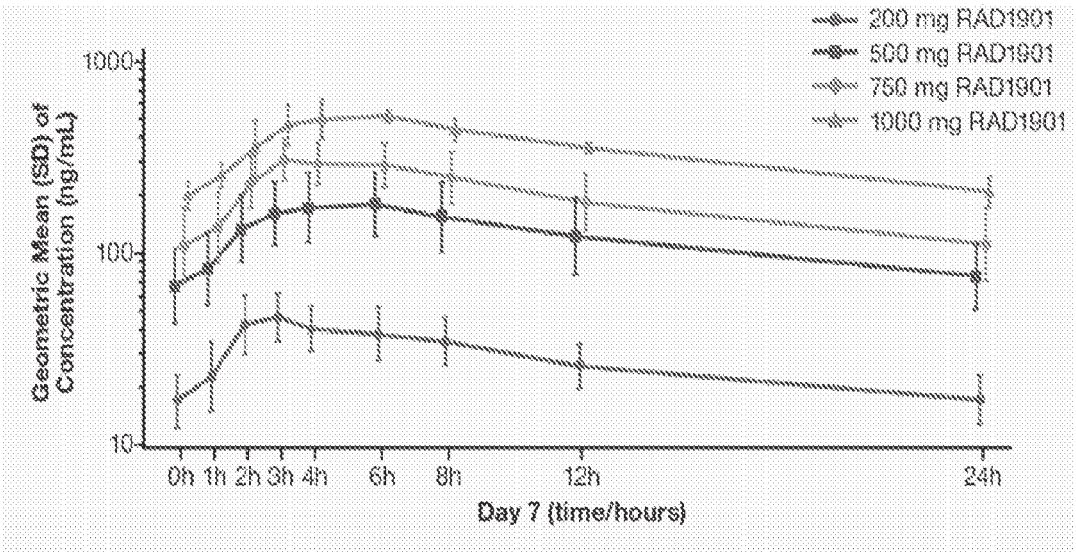

200 mg RAD1901
500 mg RAD1901
750 mg RAD1901
1000 mg RAD1901
Geometric Mean (SD) of Concentration (ng/mL)
1000
100
10
0h 1h 2h 3h 4h 6h 8h 12h 24h
Day 7 (time/hours)

Fig. 25

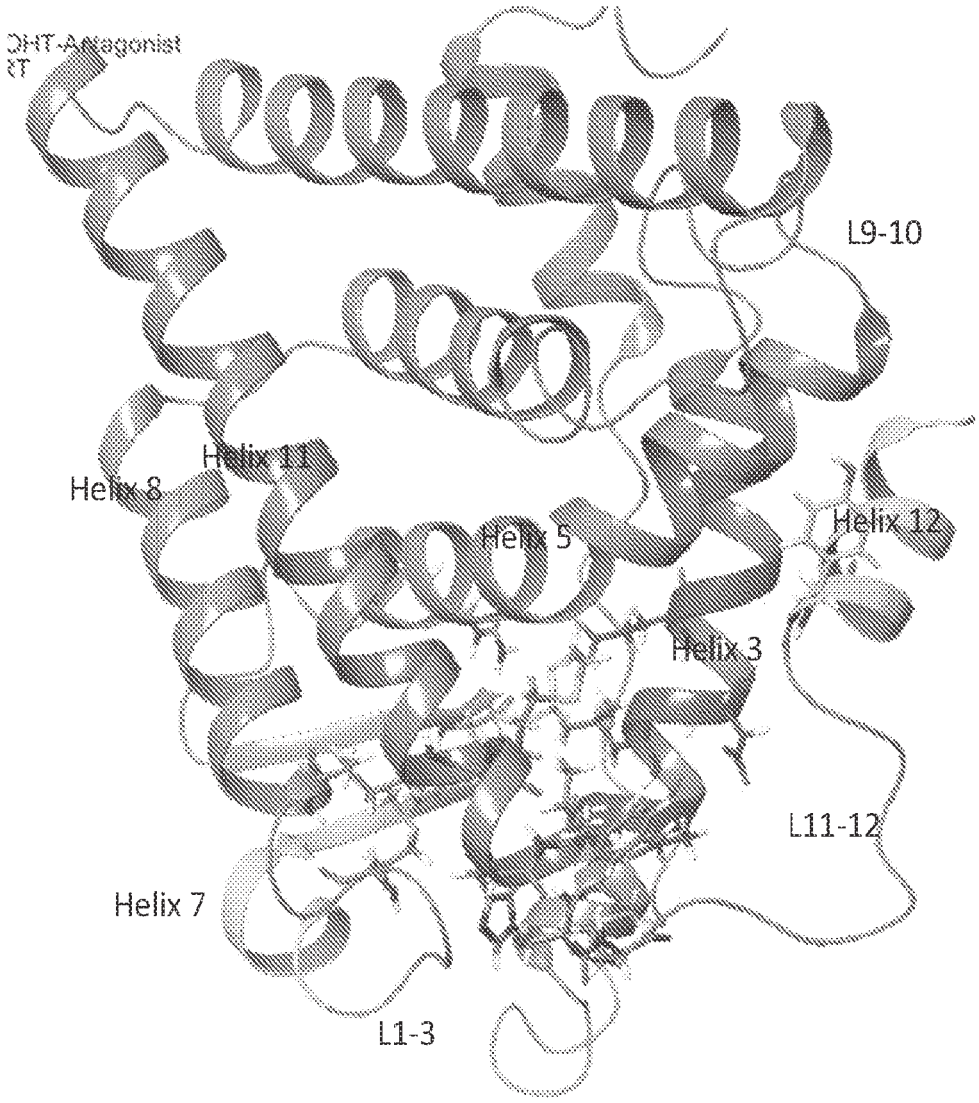

DHT-Antagonist
RT
L9-10
Helix 11
Helix 8
Helix 5
Helix 12
Helix 3
L11-12
Helix 7
L1-3

Fig. 26

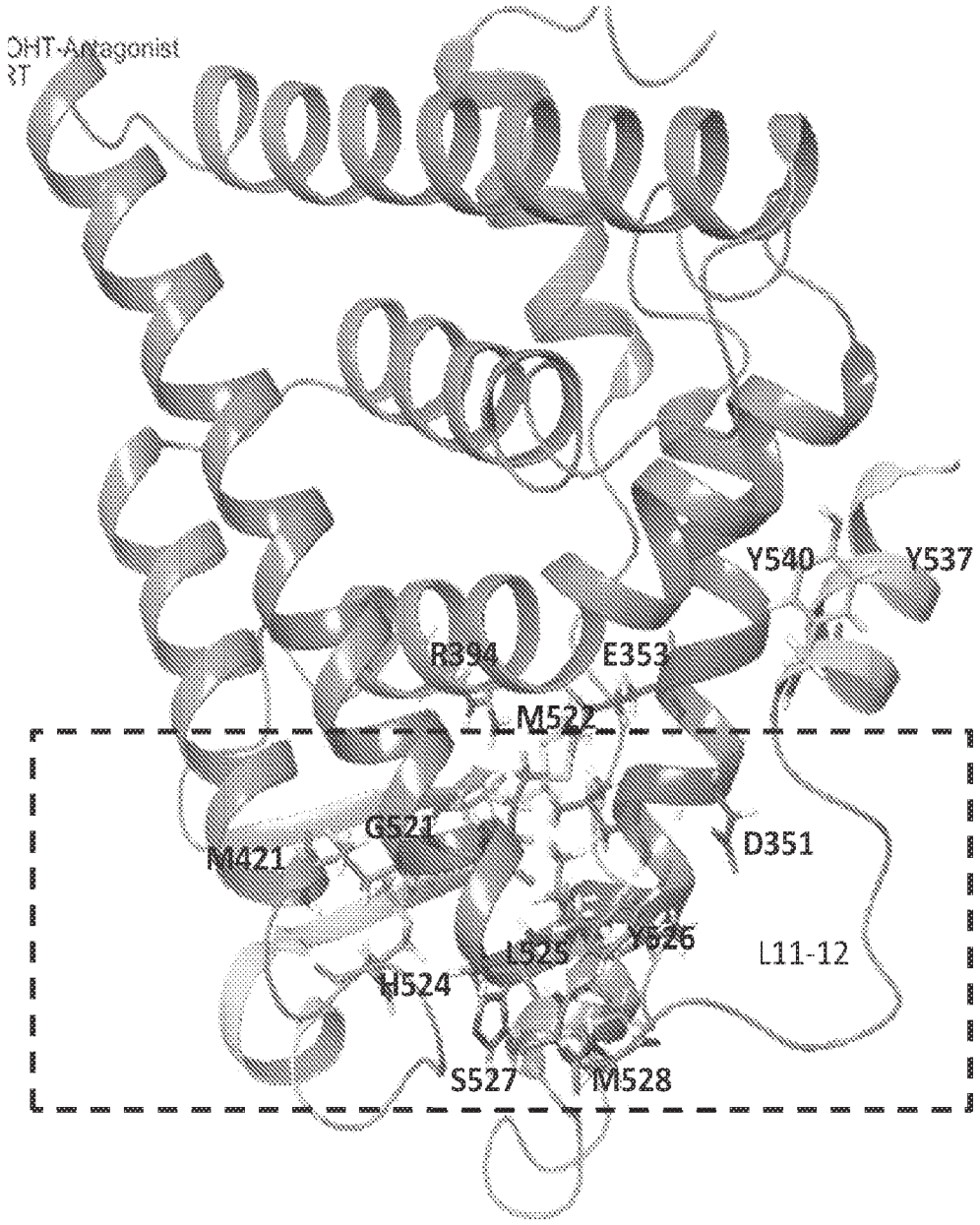

OHT-Antagonist
RT
Y540
Y537
R394
E353
M522
G521
M421
D351
Y526
L525
L11-12
H524
S527
M528

Fig. 27

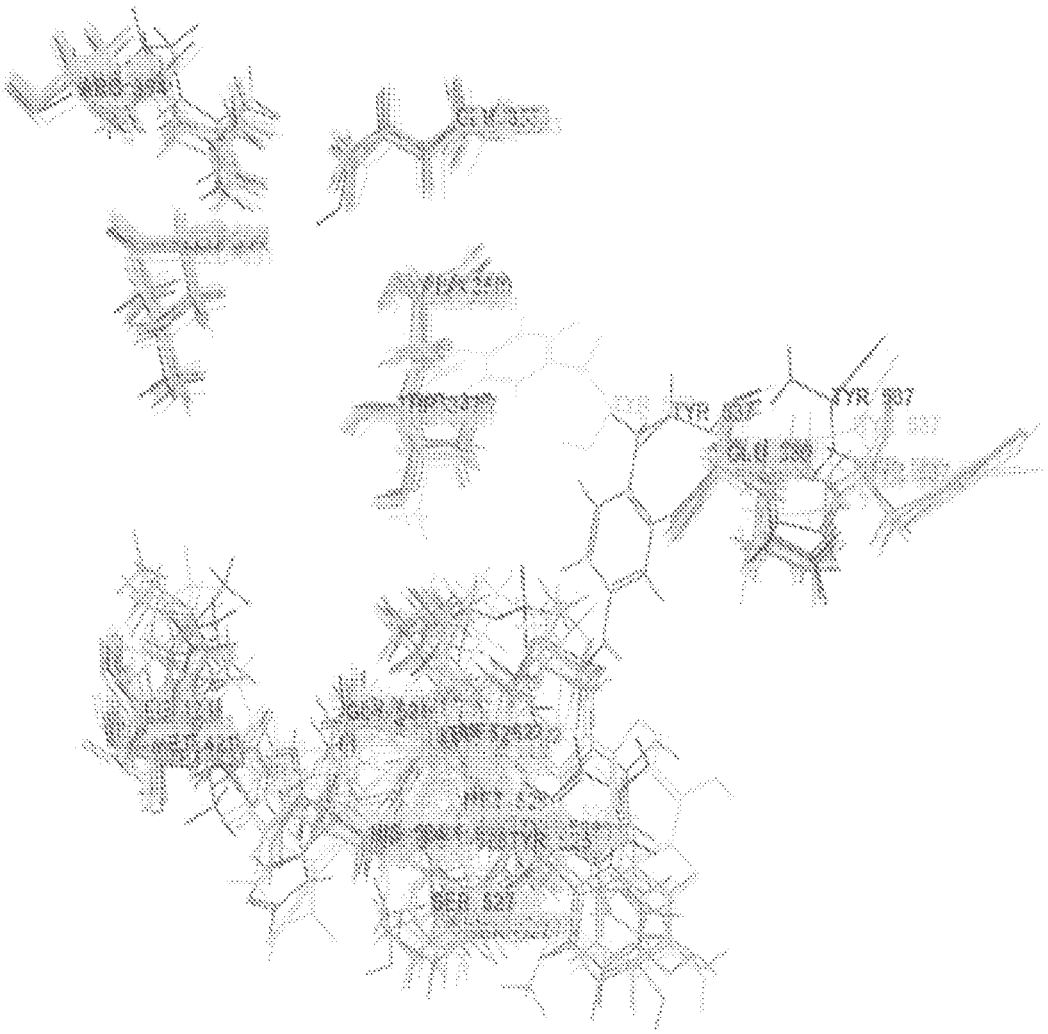


Fig. 28A

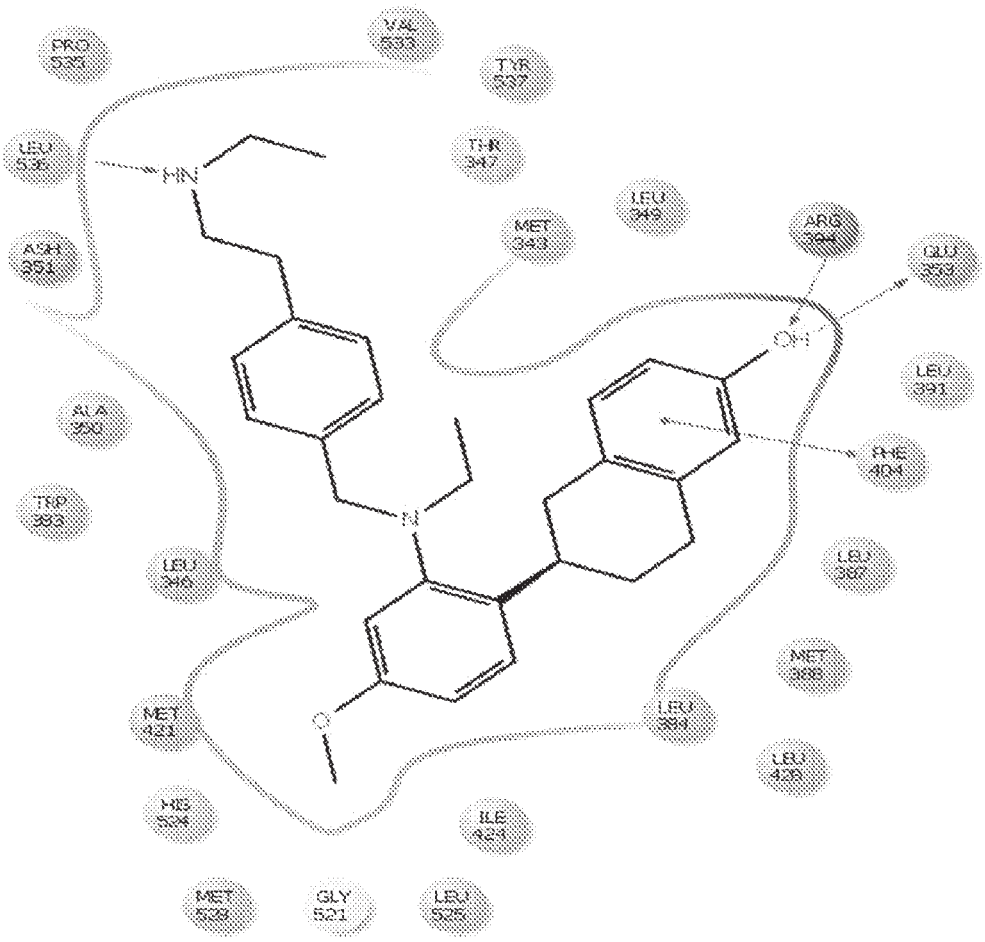

PRO
VAL
TYR
LEU
THR
HN
LEU
MET
ARG
GLU
ASH
OH
LEU
ALA
PHE
TRP
N
LEU
LEU
MET
MET
LEU
LEU
HIS
ILE
MET
GLY
LEU
O

Fig. 28B

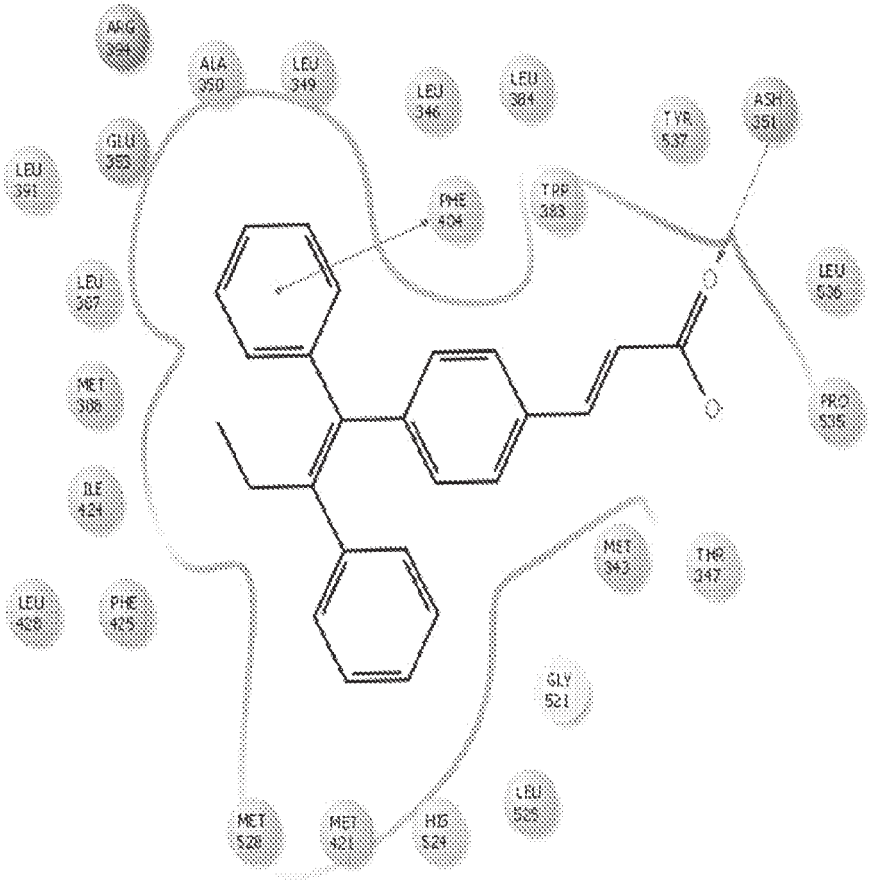

ARG 394
ALA 350
LEU 349
LEU 346
LEU 384
TYR 537
ASN 391
GLU 350
LEU 391
PHE 404
TRP 393
LEU 357
LEU 536
MET 306
PRO 535
ILE 424
MET 342
THR 347
LEU 425
PHE 425
GLY 521
LEU 525
MET 520
MET 421
HIS 524

Fig. 29A

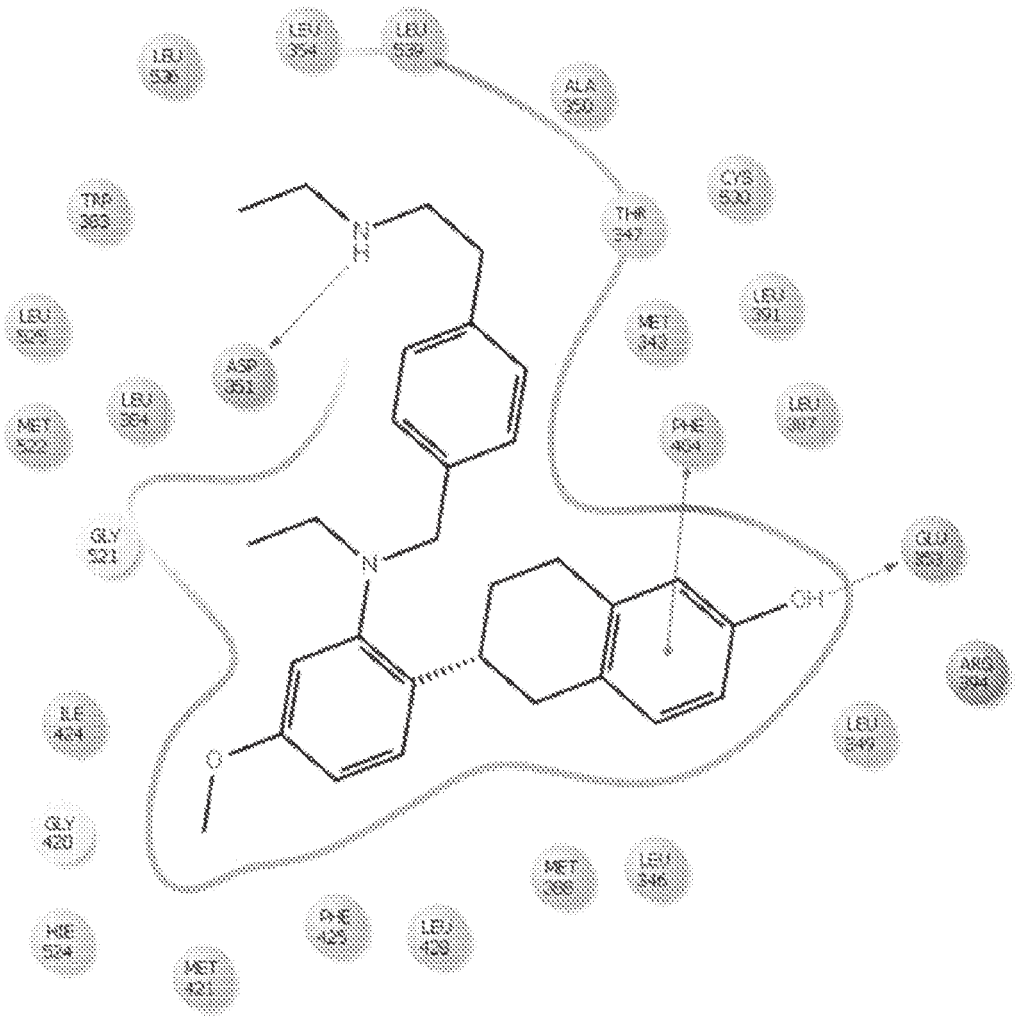

LEU 204
LEU 203
ALA 232
LEU 201
THR 347
CYS 342
THR 203
LEU 201
MET 343
LEU 204
ASP 293
LEU 294
MET 296
PHE 404
LEU 407
GLY 291
GLU 402
OH
ASN 405
ILE 404
LEU 344
GLY 420
MET 420
LEU 346
PHE 404
LEU 420
MET 421

Fig. 29B

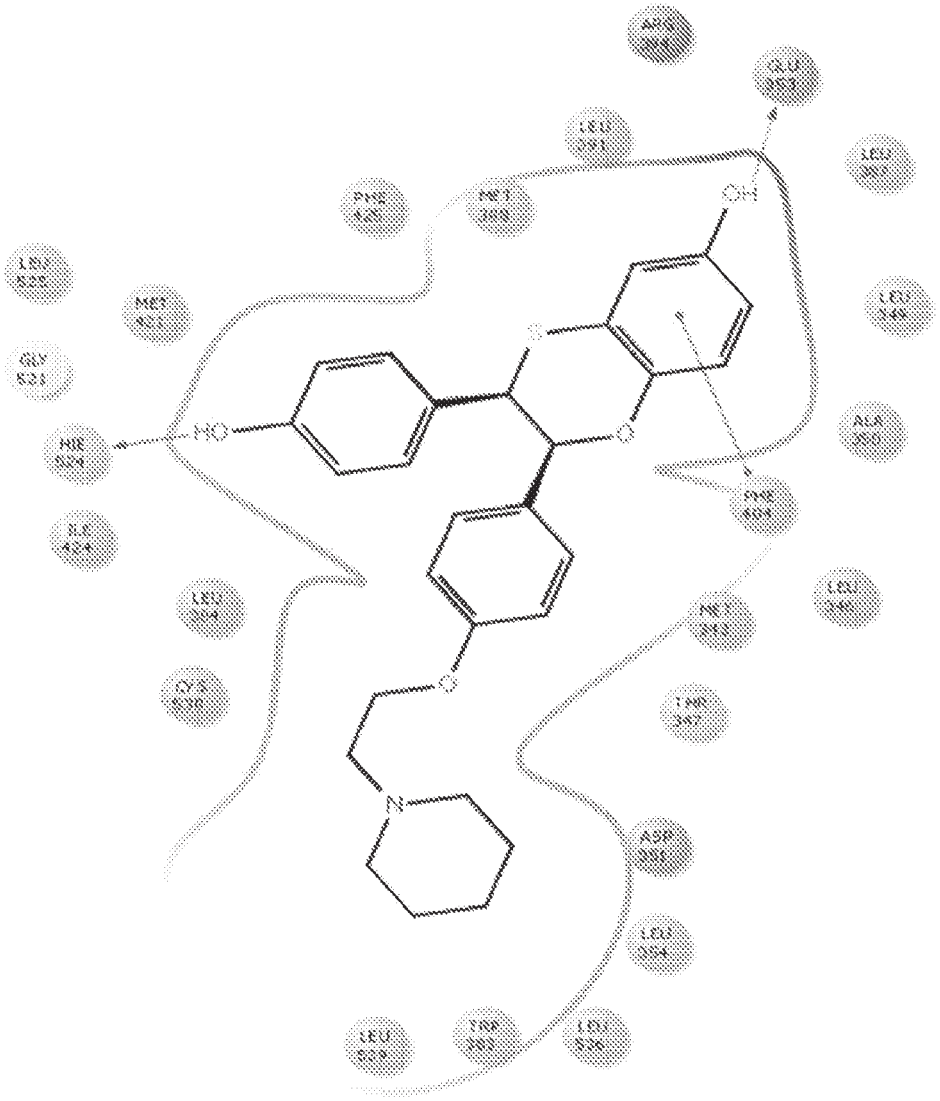


Fig. 30A

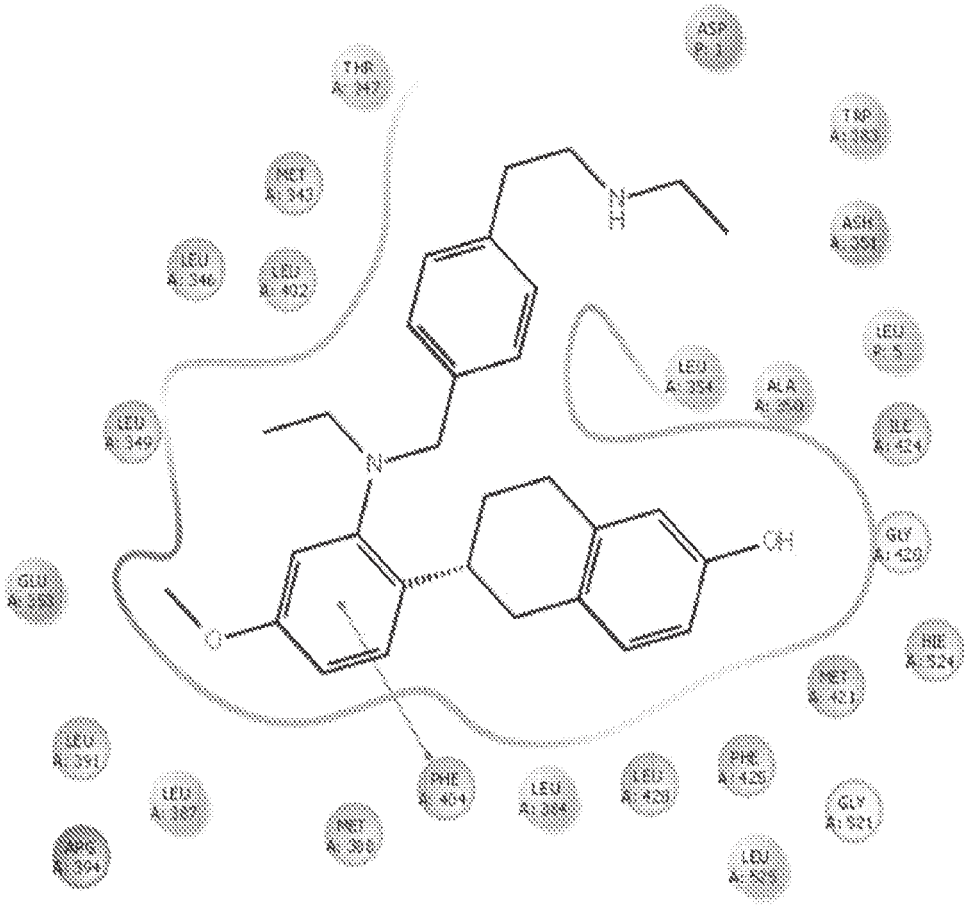

ASP
THR
TRP
MET
ASN
LEU
LEU
LEU
LEU
ALA
LEU
ILE
GLY
GLU
OH
N
MET
LEU
PHE
LEU
LEU
PHE
GLY
MET
LEU

Fig. 30B

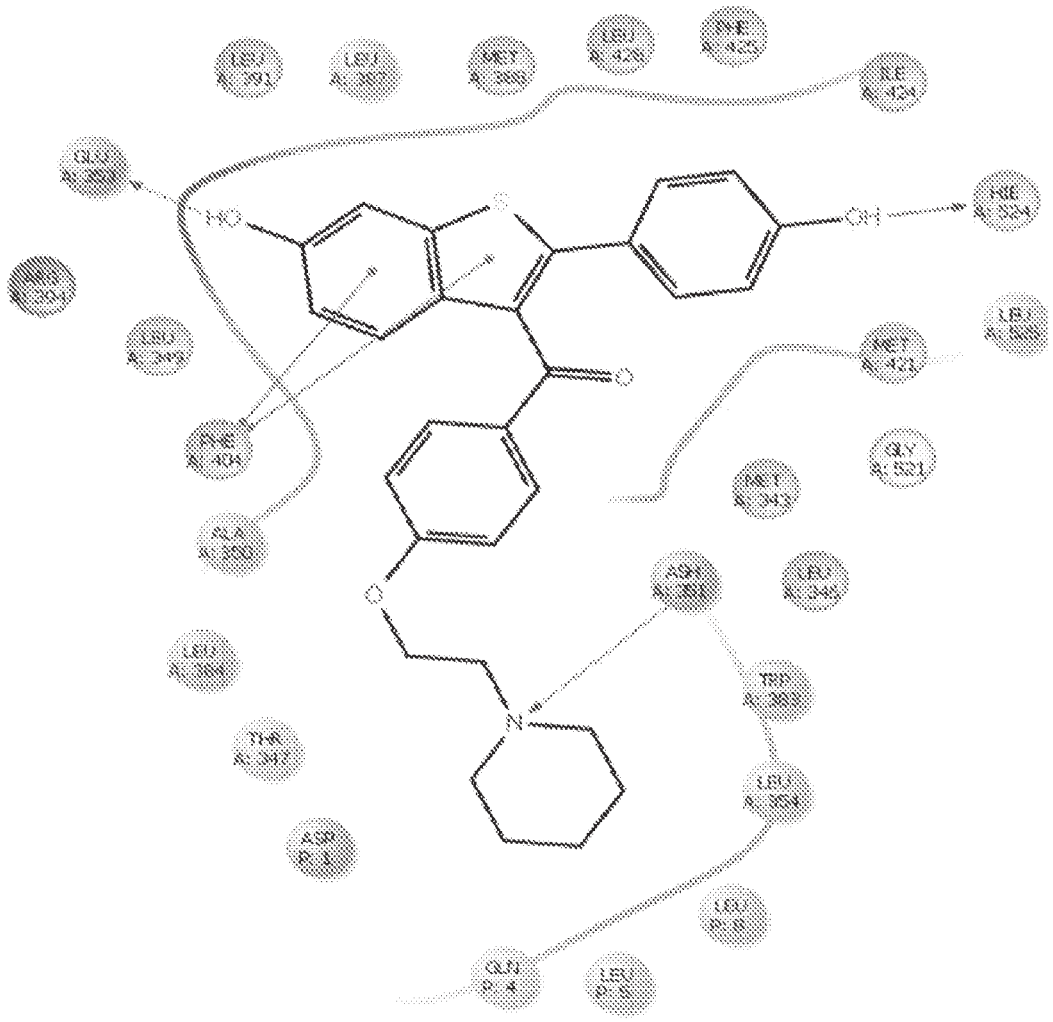


Fig. 31A

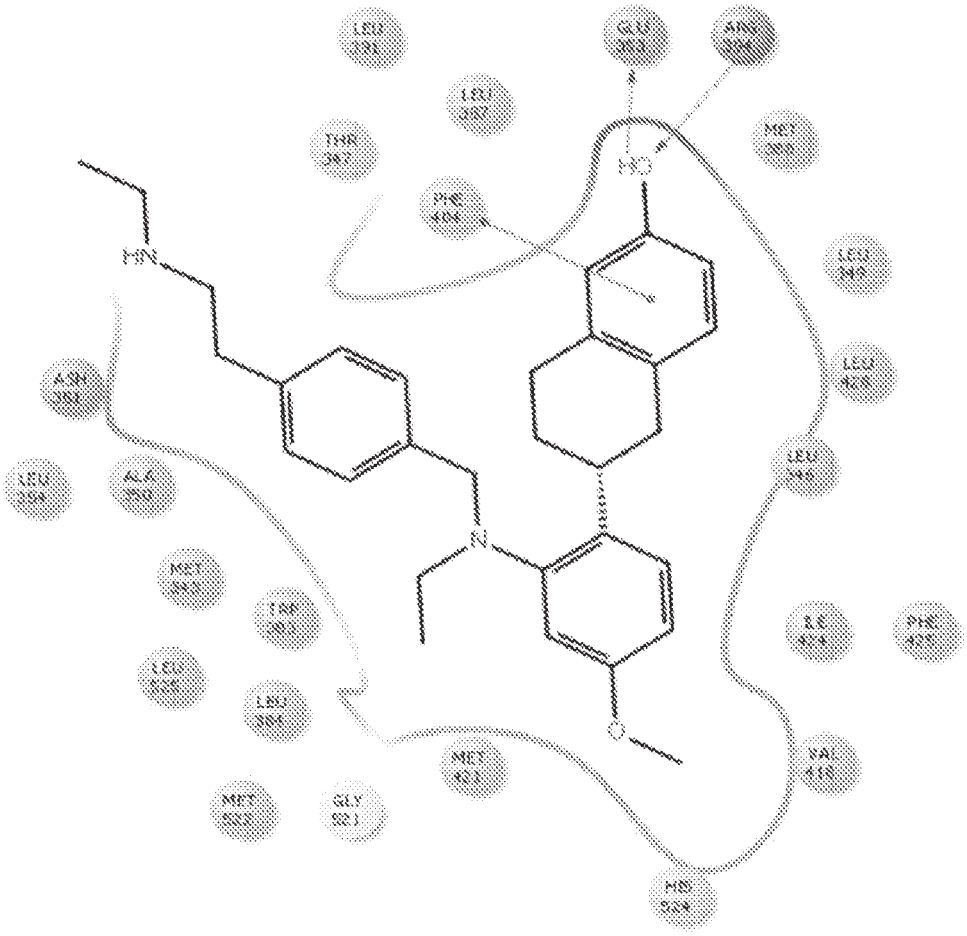


Fig. 31B

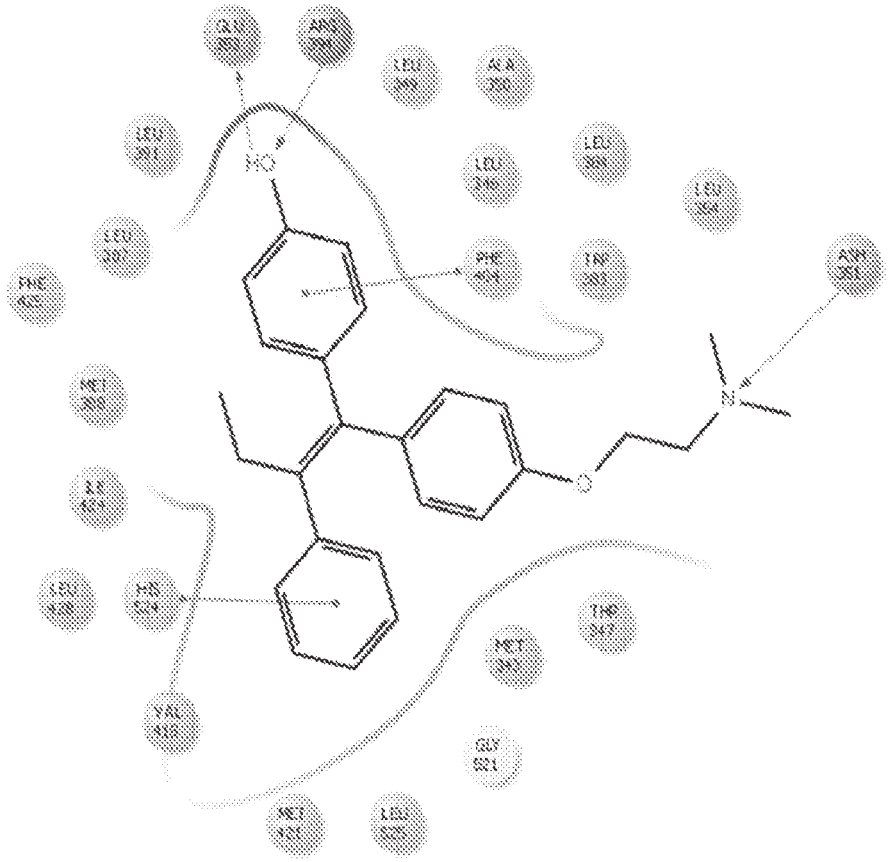


Fig. 32A

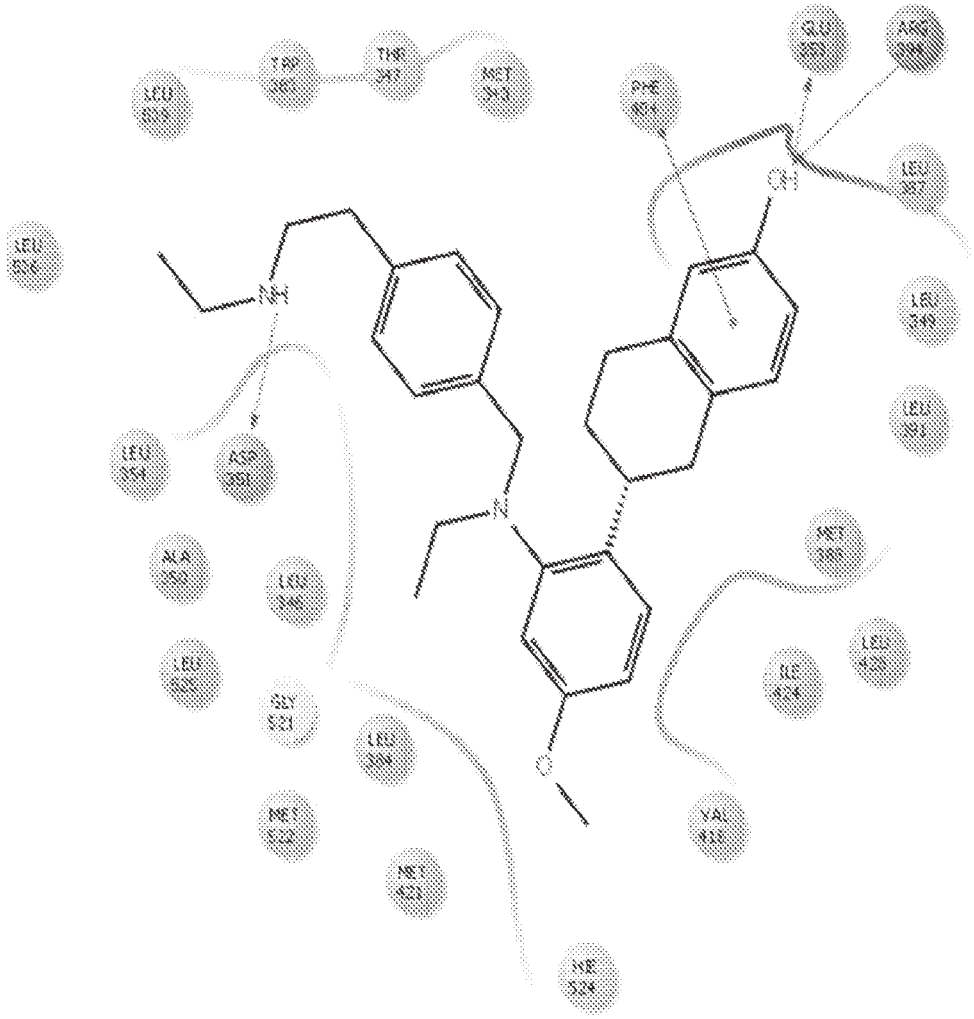


Fig. 32B

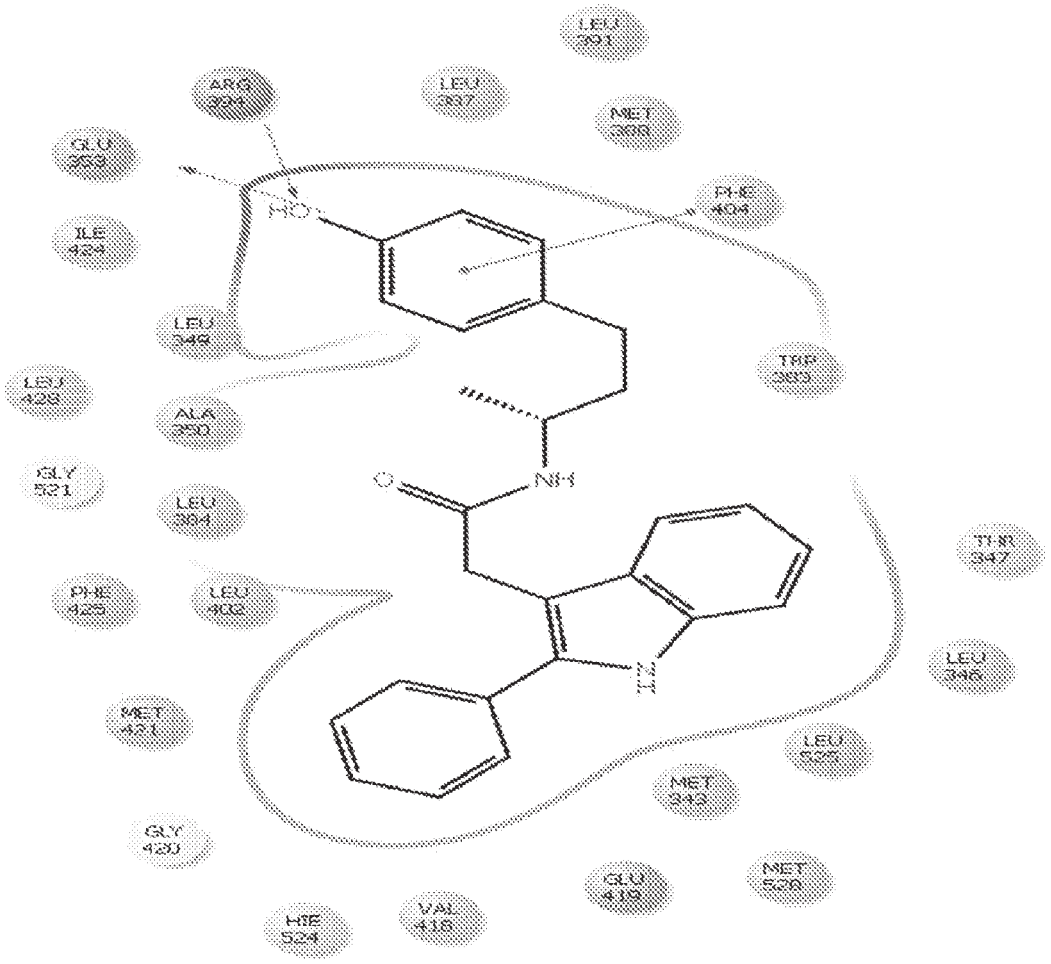

LEU 391
ARG 394
LEU 387
MET 388
GLU 389
PHE 404
HO
ILE 424
LEU 348
TRP 383
LEU 428
ALA 350
GLY 521
O
NH
LEU 384
TYR 347
PHE 429
LEU 402
LEU 346
MET 431
LEU 527
MET 343
GLY 420
GLU 419
MET 526
HIE 524
VAL 418

Fig. 33

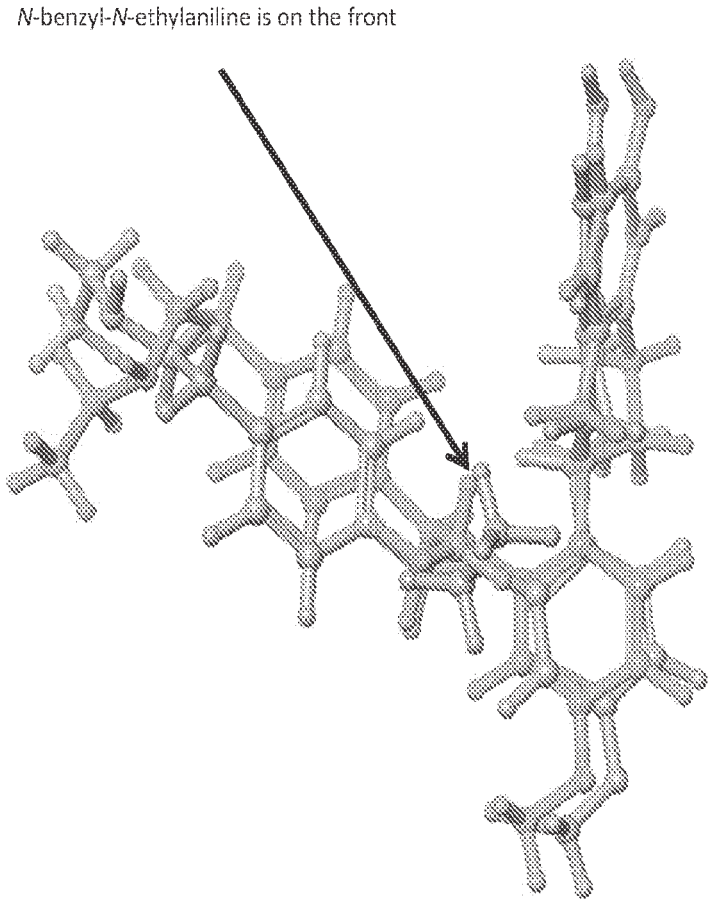


Fig. 34

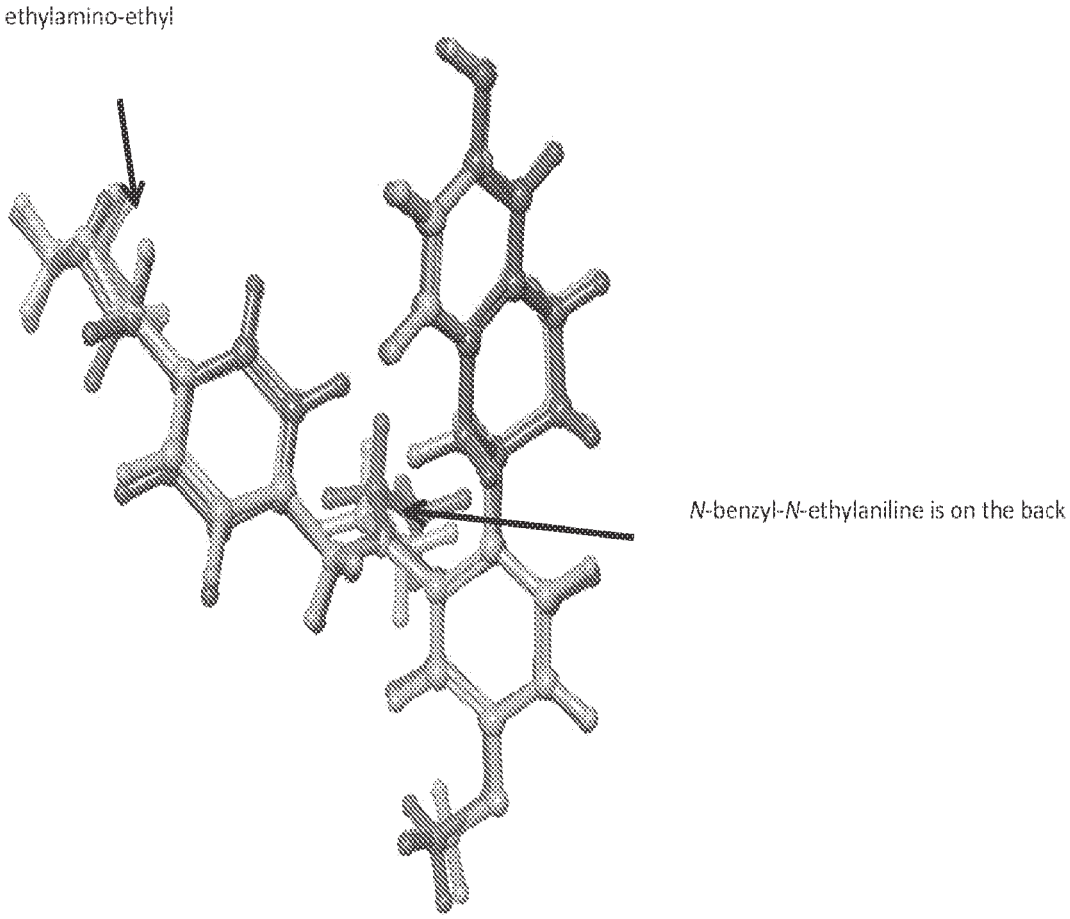


Fig. 35A

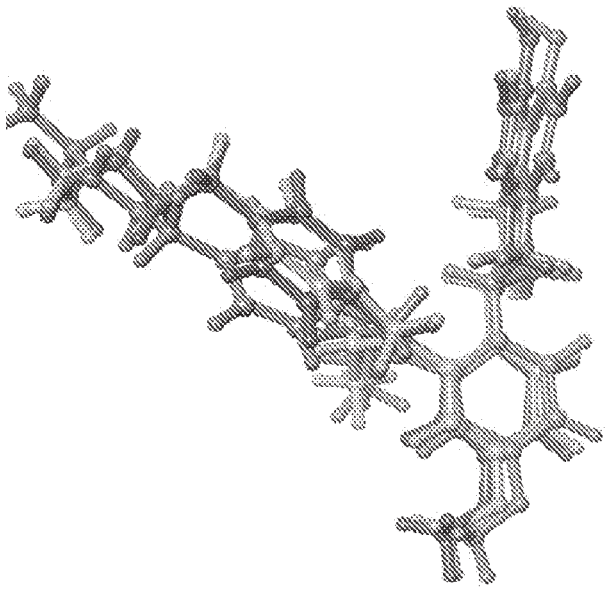


Fig. 35B

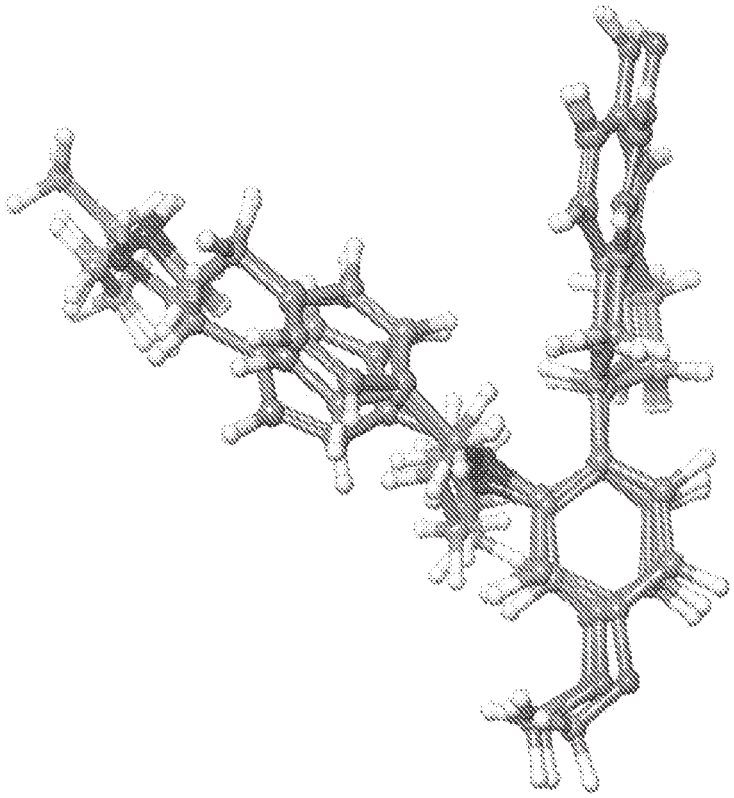


Fig. 36A

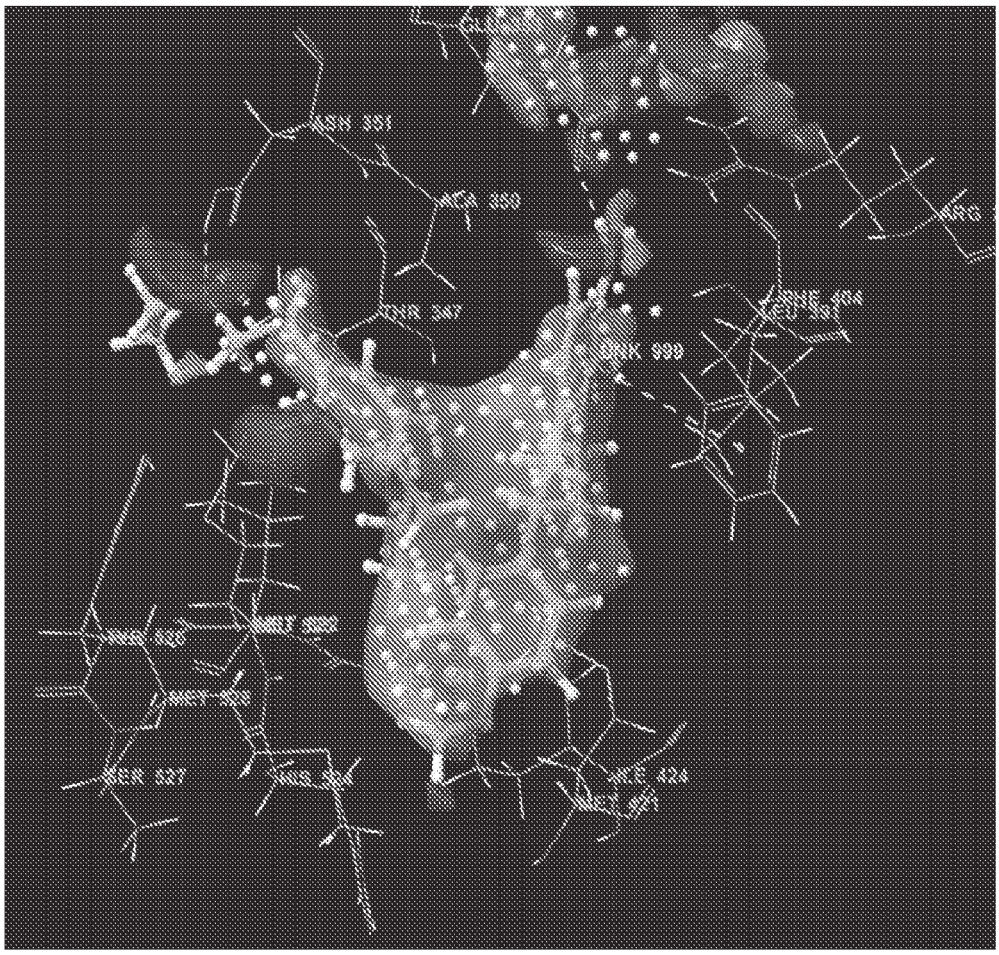


Fig. 36B

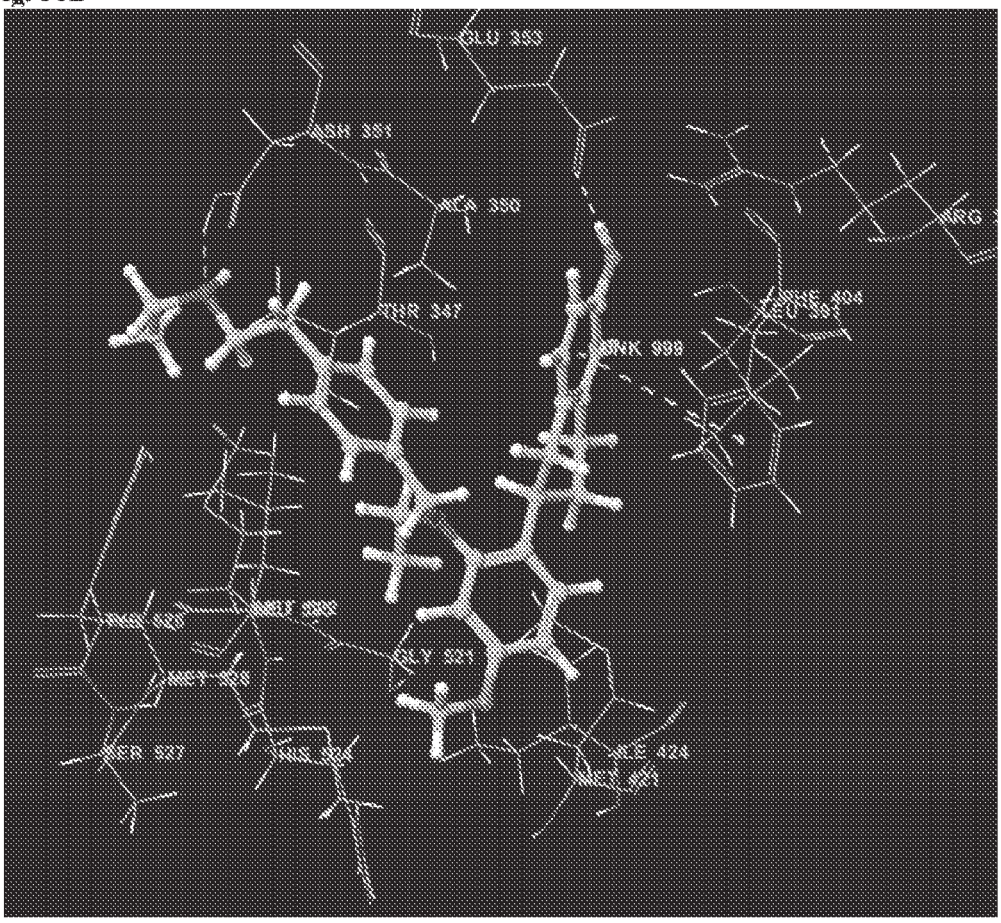


Fig. 36C

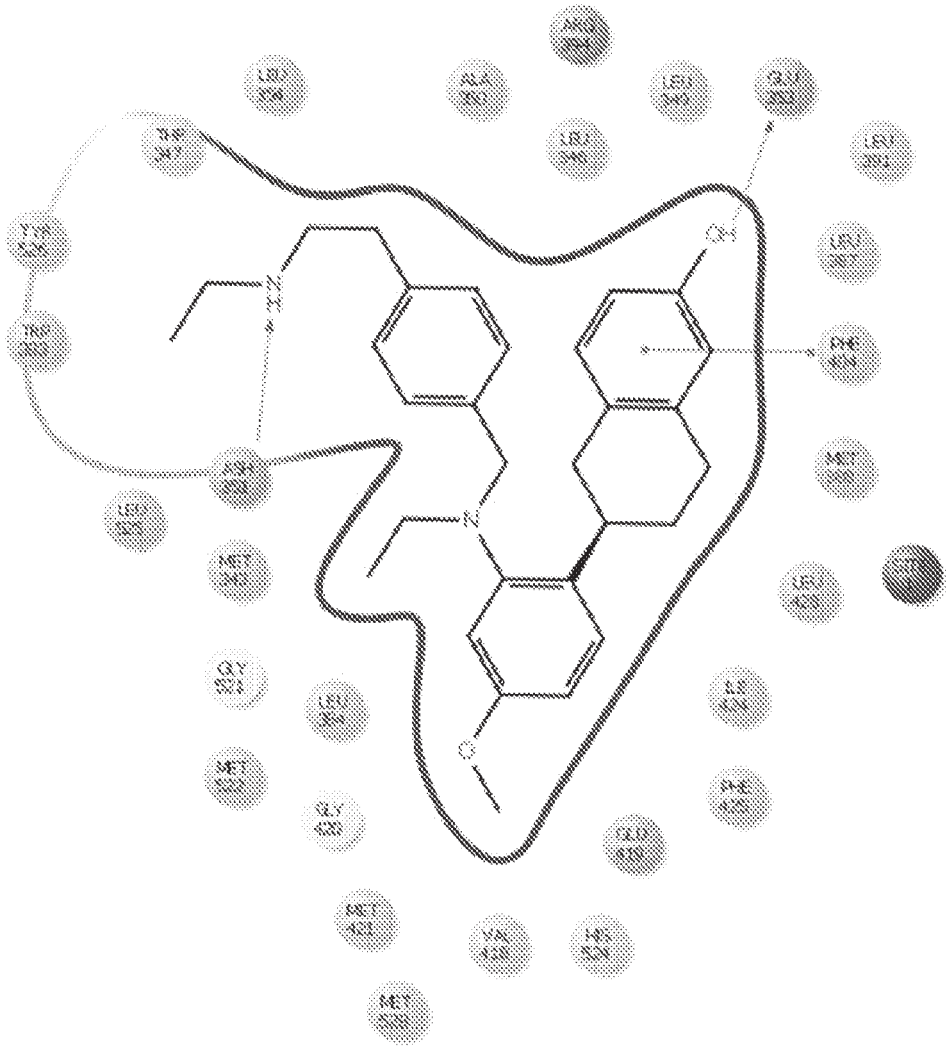


Fig. 37A

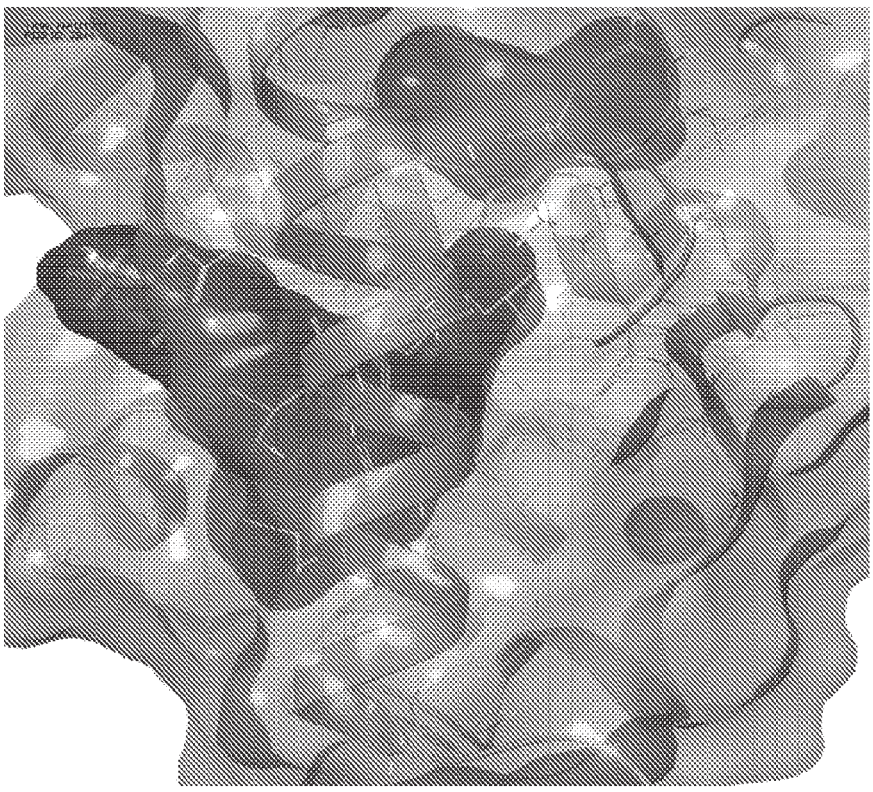


Fig. 37B

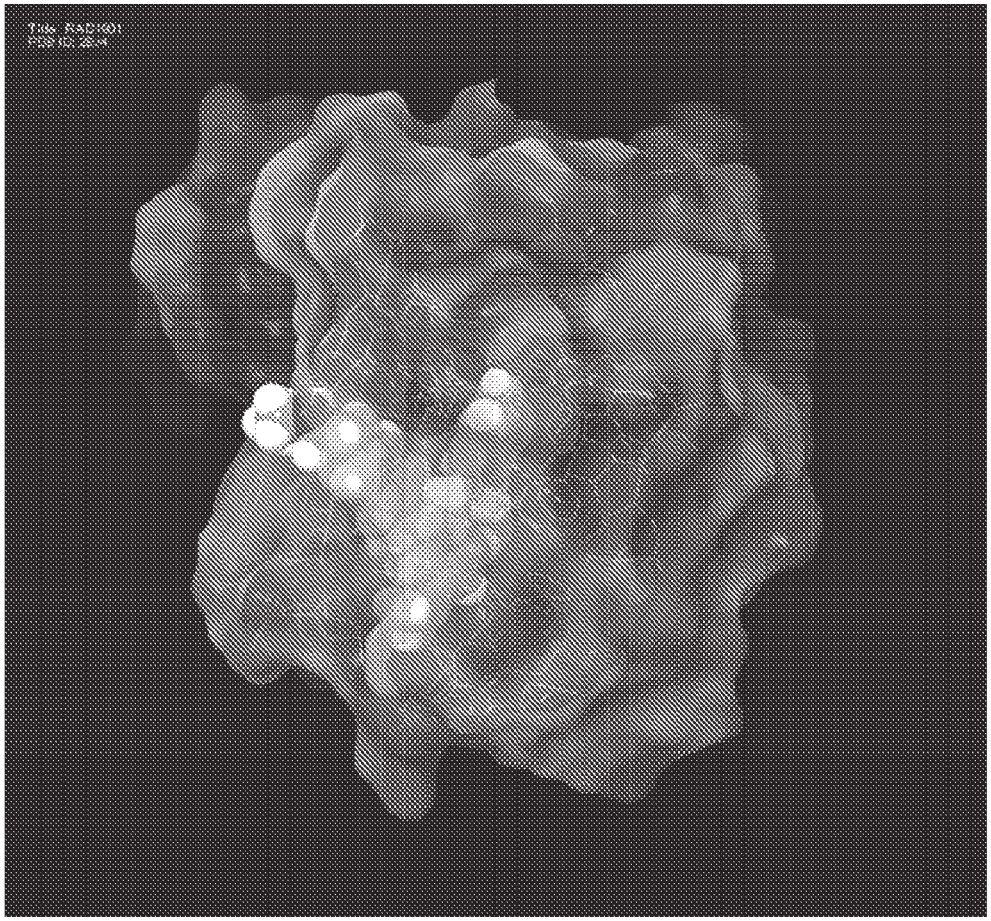


Fig. 37C

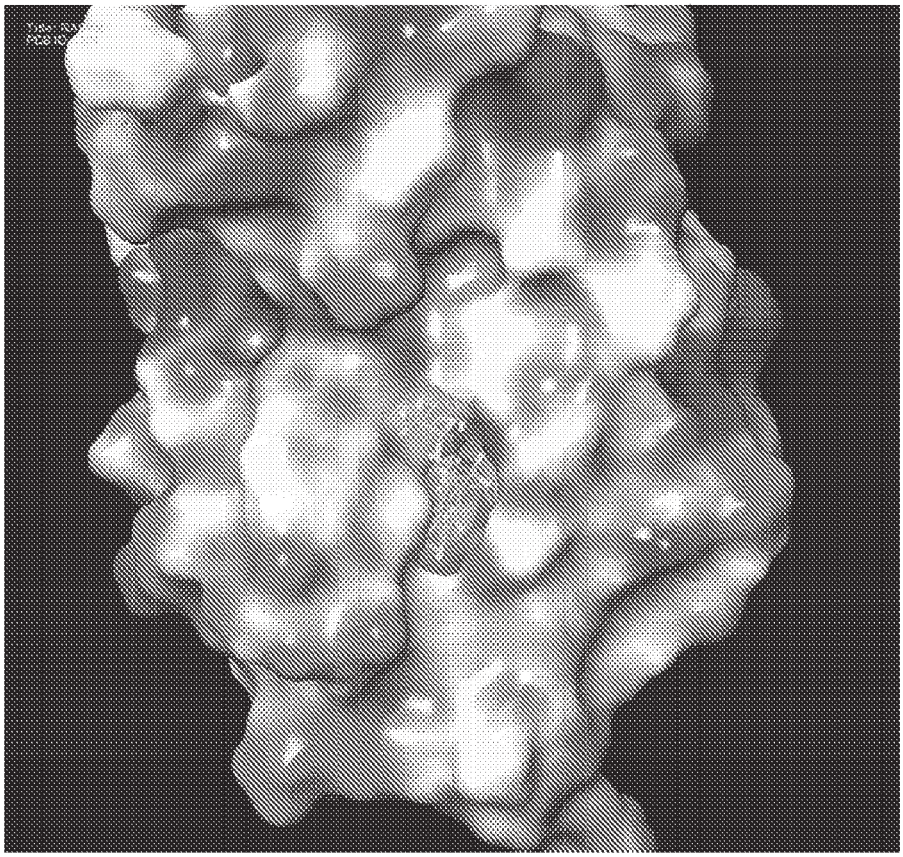


Fig. 38A

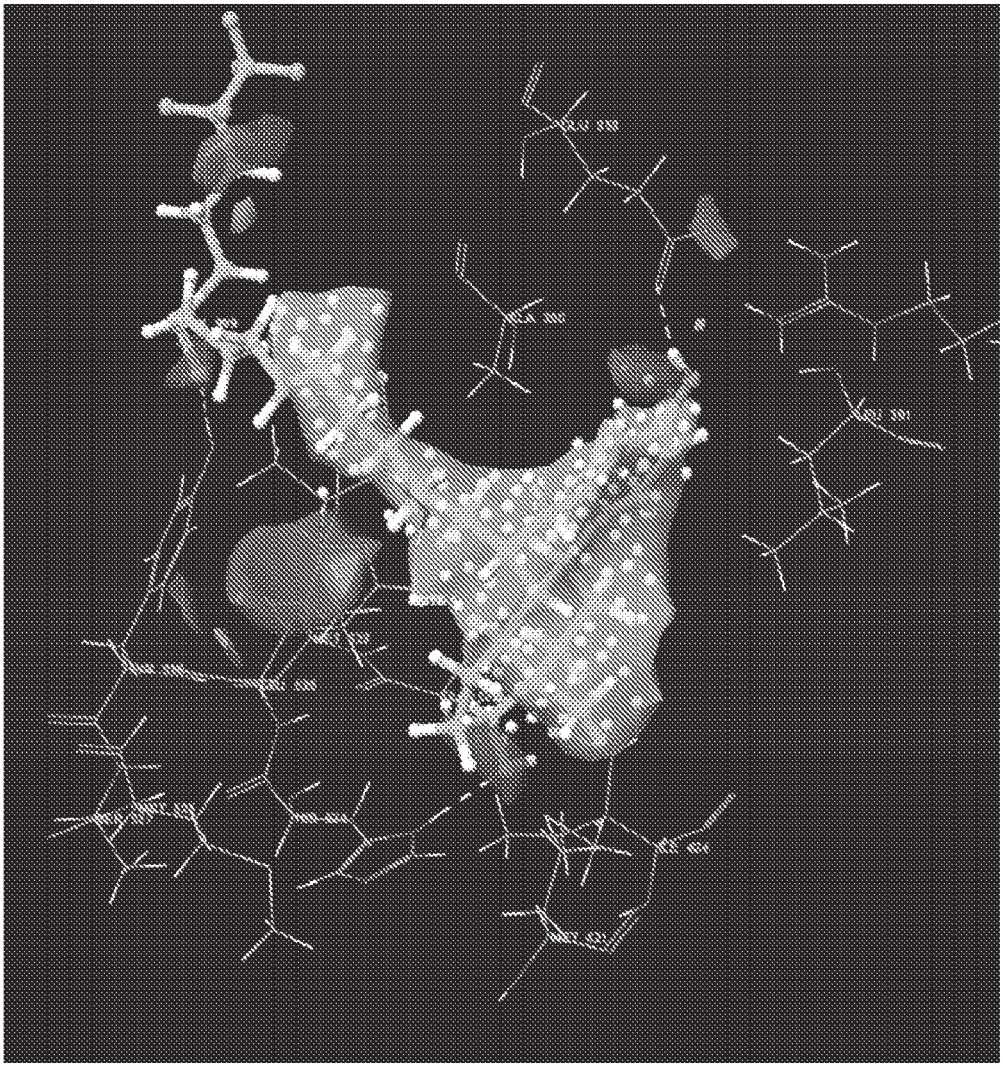


Fig. 38B

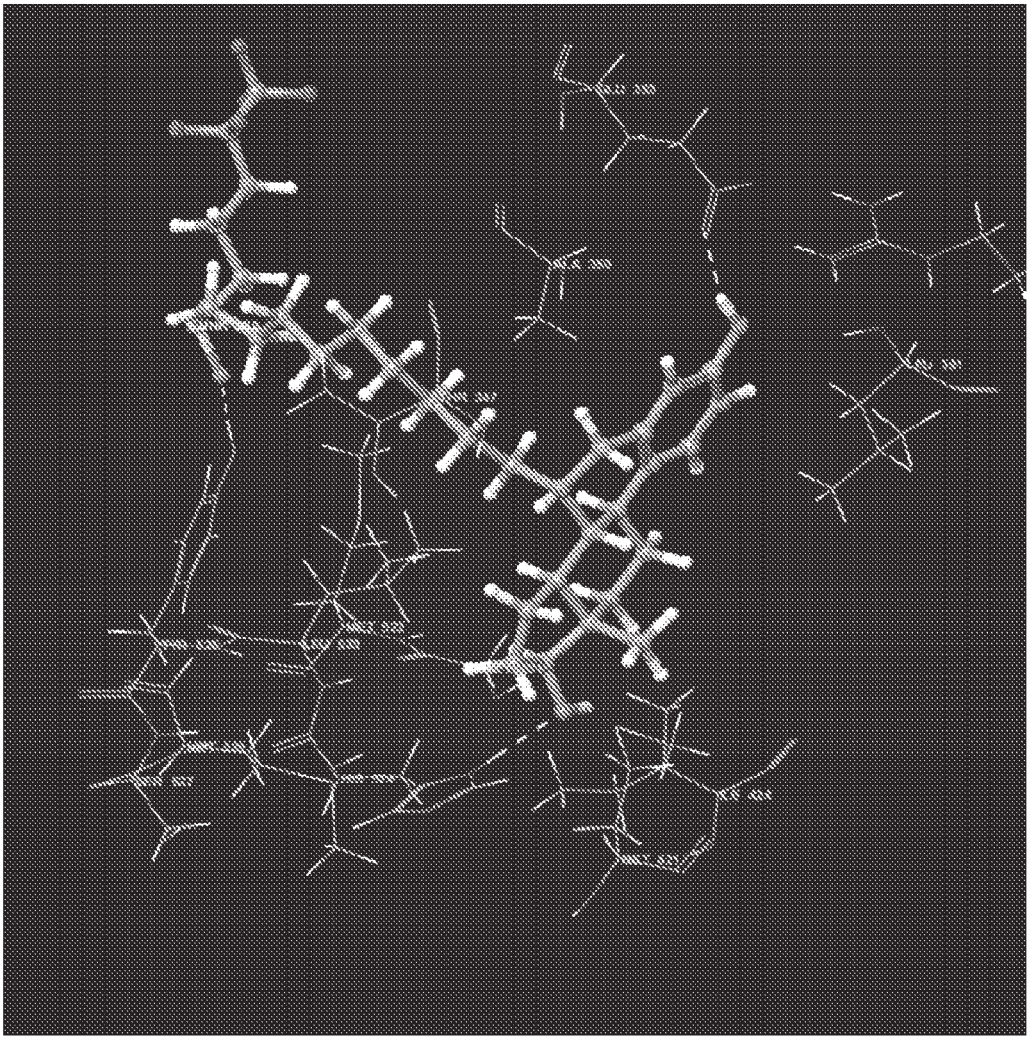


Fig. 38C

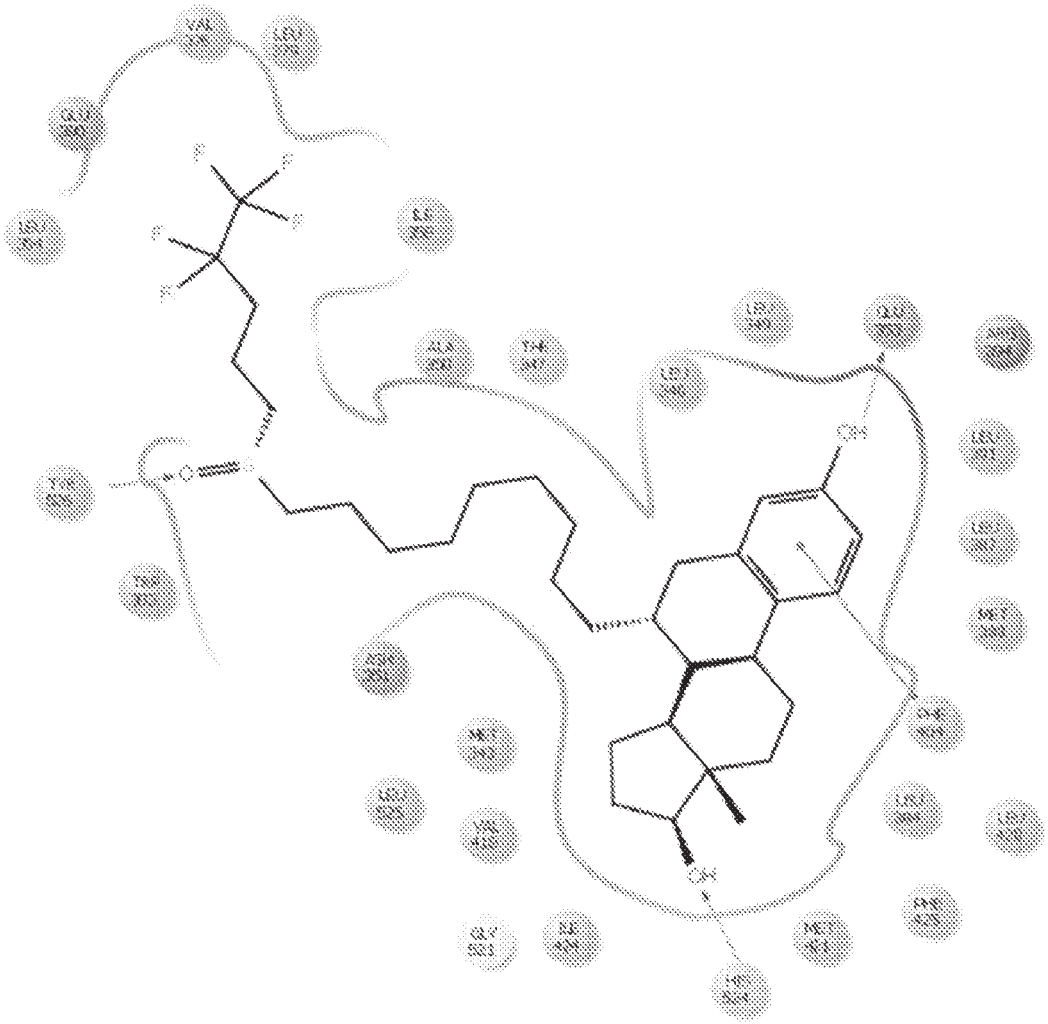


Fig. 39A

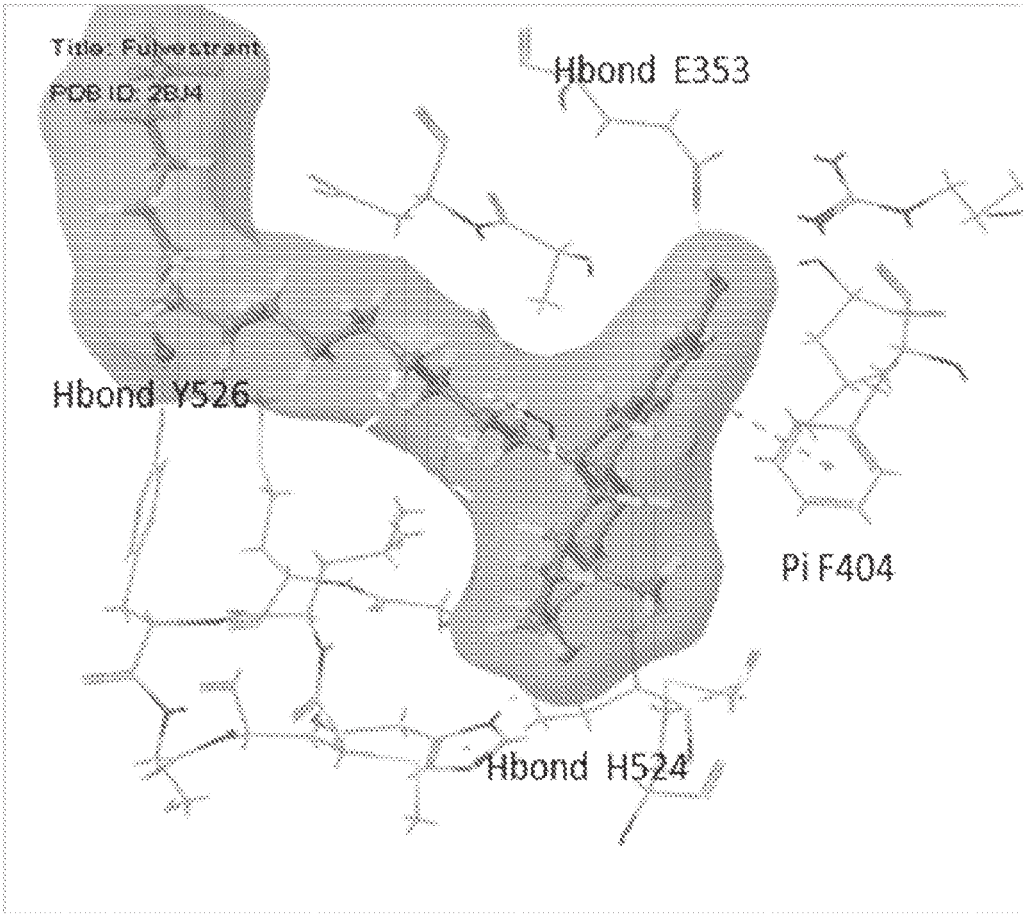

Title: Fulvestrant
PDB ID: 2FAI
Hbond E353
Hbond Y526
Pi F404
Hbond H524

Fig. 39B

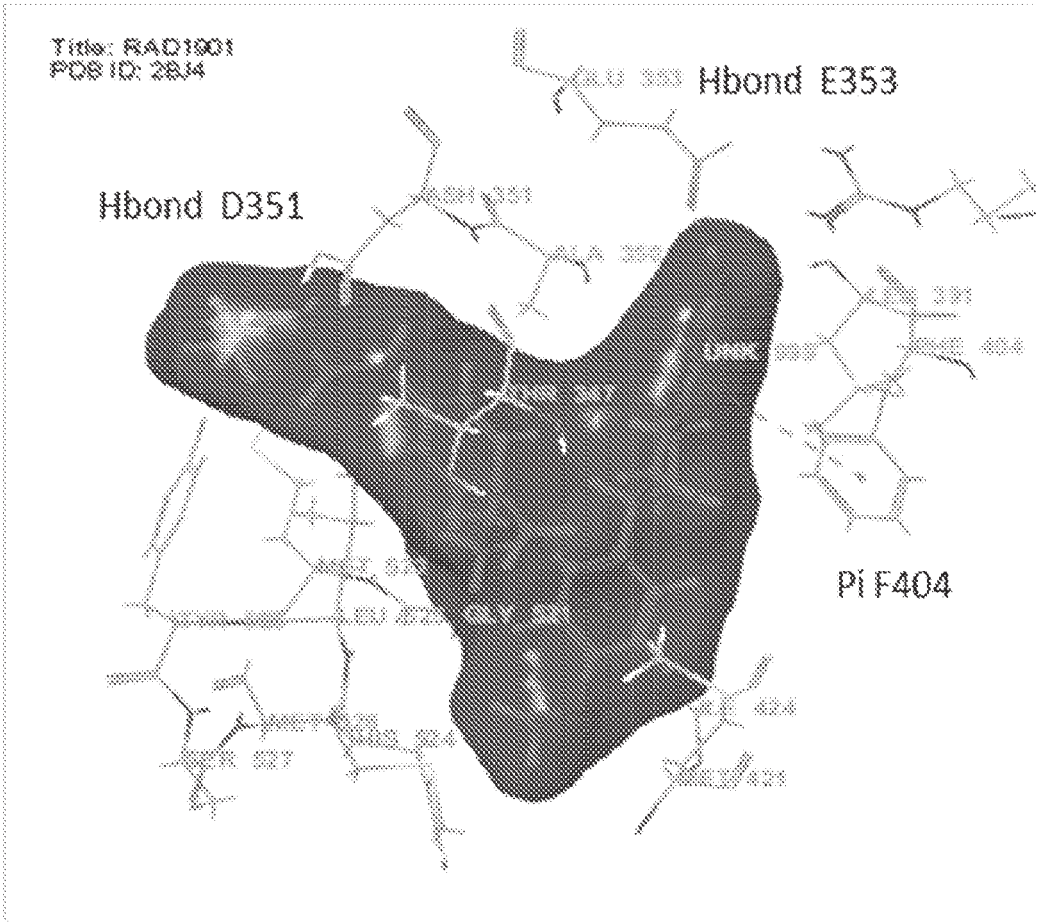


Fig. 40A

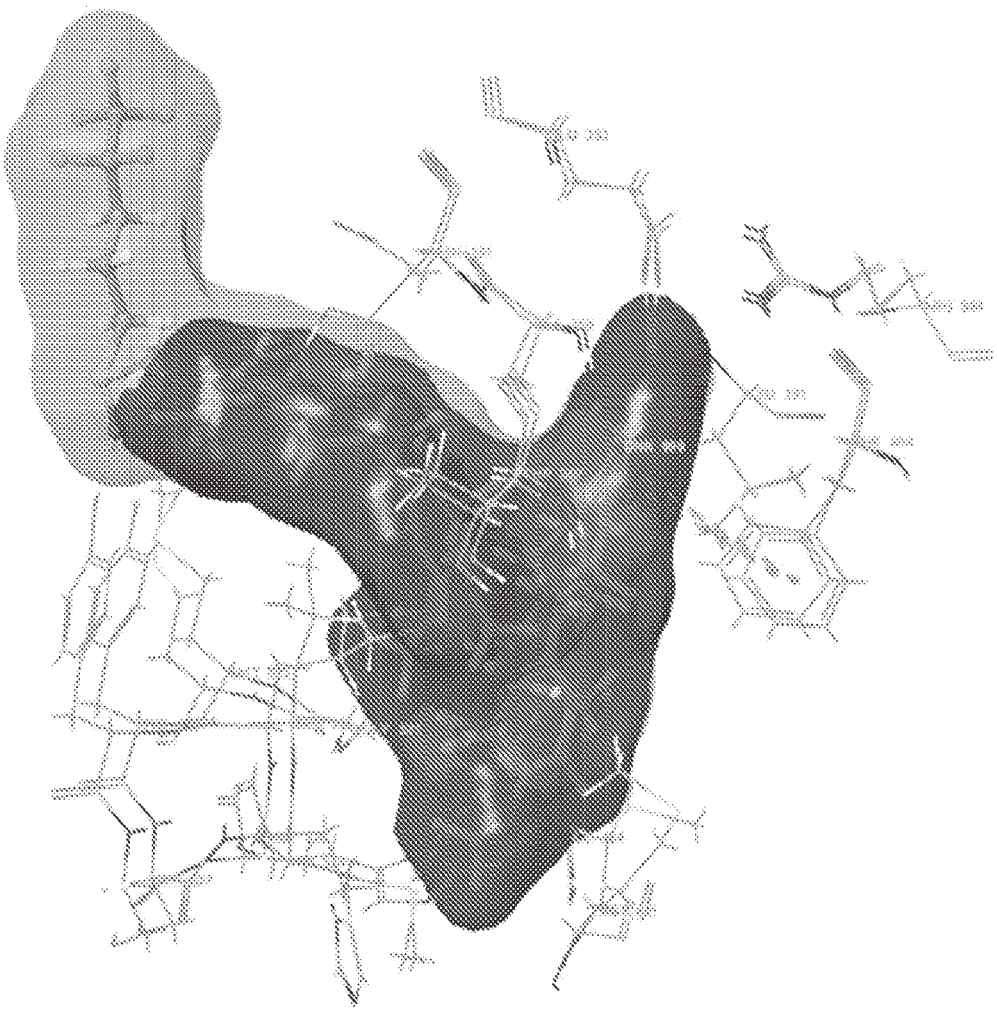
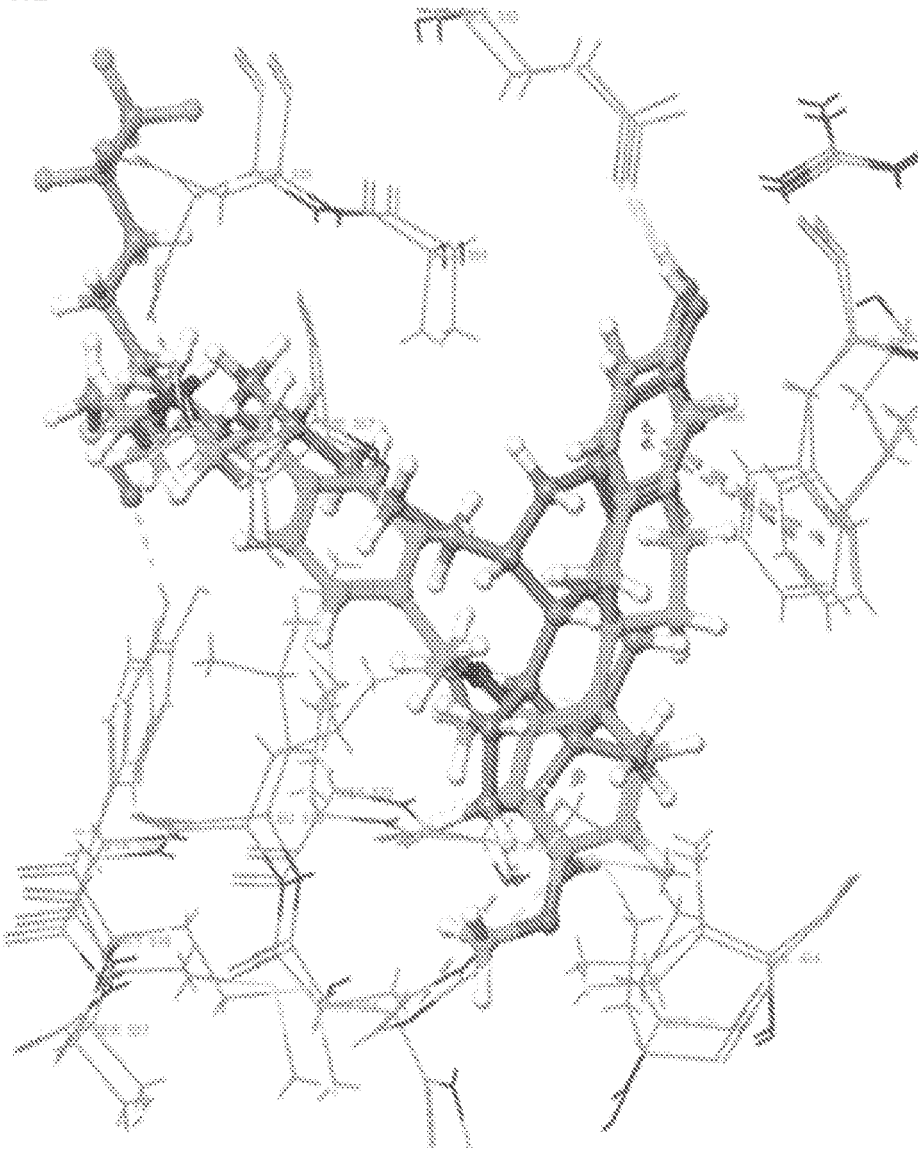


Fig. 40B



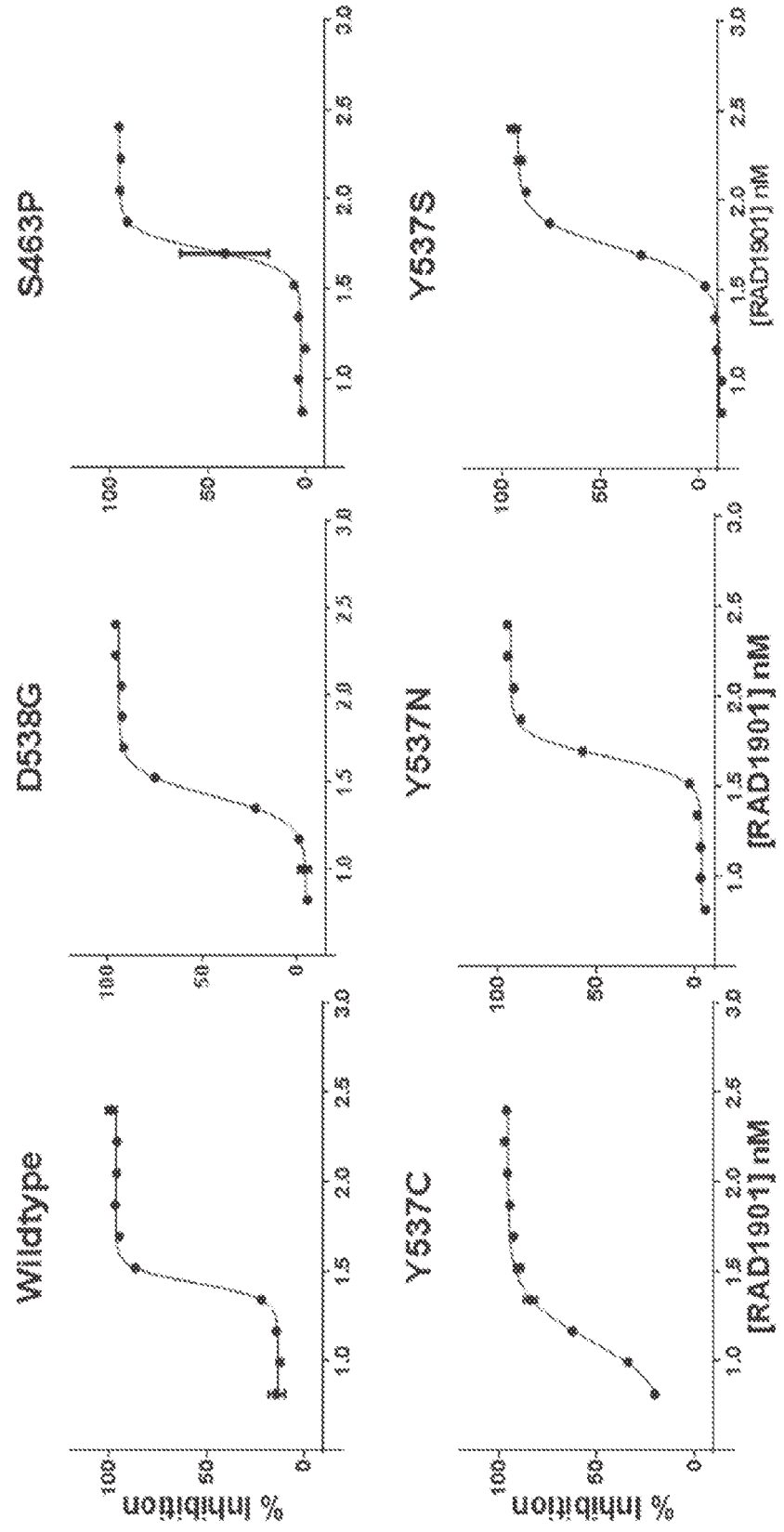

Wildtype
D538G
S463P
Y537C
Y537N
Y537S
% Inhibition
[RAD1901] nM
In vitro binding assay, 2nM fluoromone

Fig. 41

Fig. 42

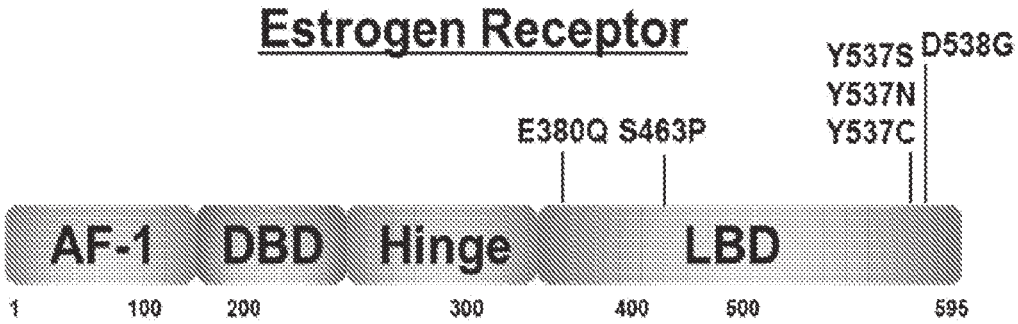

Estrogen Receptor
Y537S
D538G
Y537N
Y537C
E380Q
S463P
AF-1
DBD
Hinge
LBD
1
100
200
300
400
500
595

Table 1

Key baseline demographics of Phase 1 study of RAD1901 for the treatment of ER+ advanced breast cancer

	RAD1901 200 mg (N=4)	RAD1901 400 mg (N=4)	Total (N=8)
Mean age, years (range)	63 (55-74)	54 (43-70)	59 (43-74)
ECOG Performance Status, n (%)			
0	1(25)	2(50)	3(38)
1	3(75)	2(50)	5(62)

Table 2

Treatment related AEs in a Phase 1 study of RAD1901 for the treatment of ER+ advanced breast cancer

	200 mg N=4*			400 mg N=4			Total N=8		
Preferred term	Gr1	Gr2	Gr3	Gr1	Gr2	Gr3	Gr1	Gr2	Gr3
Dyspepsia	1	1	0	2	1	0	3	2	0
Nausea	1	0	0	2	0	0	3	0	0
Anemia	1	1	0	0	0	0	1	1	0
Headache	2	0	0	0	0	0	2	0	0
Abdominal pain	1	0	0	0	0	0	1	0	0
Asthenia	1	0	0	0	0	0	1	0	0
Constipation	0	0	1	0	0	0	0	0	1
Dermatitis acneiform	1	0	0	0	0	0	1	0	0
Diarrhea	1	0	0	0	0	0	1	0	0
Dizziness	1	0	0	0	0	0	1	0	0
Electrocardiogram QT prolonged	1	0	0	0	0	0	1	0	0
Eructation	1	0	0	0	0	0	1	0	0
Fatigue	1	0	0	0	0	0	1	0	0
Flatulence	1	0	0	0	0	0	1	0	0
Gastroesophogeal reflux disease	1	0	0	0	0	0	1	0	0
Hot flush	1	0	0	0	0	0	1	0	0
Hypokalemia	1	0	0	0	0	0	1	0	0
Esophageal spasm	1	0	0	0	0	0	1	0	0
Pain in extremity	1	0	0	0	0	0	1	0	0

Table 3

RAD1901 levels in plasma, tumor and brain of mice implanted with MCF7 cells after treated for 40 days.

	Dose (mg/kg)	Plasma (ng/mL)	Tumor (ng/mL)	Brain (ng/mL)	B/P Ratio	T/P Ratio
Vehicle		BLQ*	BLQ	BLQ	-	-
RAD1901	0.3	2	11	BLQ	-	
RAD1901	1	3	45	BLQ	-	
RAD1901	3	9	169	7	0.78	18.78
RAD1901	10	39	757	14	0.36	19.41
RAD1901	30	137	3875	72	0.53	28.28
RAD1901	60	334	11117	201	0.60	33.28

*BLQ: below the limit of quantitation

Table 4

SUV for uterus, muscle, and bone for a human subject treated with 200 mg dose PO once/day for six days

Dose	Uterus SUV % Change	Bone SUV % Change	Muscle SUV % Change
200 mg	-85%	16%	0%

Table 5

SUV for uterus, muscle, and bone for human subjects (n=4) treated with 500 mg dose PO once/day for six days.

Subject #	Scan	Mean Uterus SUV	Uterus SUV Change (%)	Mean Muscle SUV	Muscle SUV Change (%)	Mean Bone SUV	Bone SUV Change (%)
1	Baseline	3.88		0.33		0.36	
	Day 6	0.58	-85	0.31	-6	0.48	33
2	Baseline	6.47		0.25		0.49	
	Day 6	0.33	-86	0.42	68	0.55	12
3	Baseline	3.66		0.50		0.41	
	Day 6	0.58	-84	0.31	-38	0.47	-23
4	Baseline	3.35		0.30		0.40	
	Day 6	0.41	-88	0.24	-20	0.52	30
Mean			-86		1		13

Table 6

Effect of RAD1901 on BMD in ovariectomized rats.[a]

Treatment	Femur BMD (% change)	Lumbar Spine BMD (% change)
Sham	3.1 ± 2.4*	2.7 ± 5.0*
OVX+veh	-5.4 ± 5.1	-10.2 ± 12.8
OVX+E2	-0.5 ± 2.6*	-2.1 ± 12.2*
OVX+RAD1901	0.4 ± 2.8*	-1.1 ± 7.9*

[a]Adult female rats underwent either sham or ovariectomy surgery before treatment initiation with vehicle, E2 (0.01 mg/kg) or RAD1901 (3 mg/kg) once daily (n=20 per treatment group). BMD was measured by dual emission x-ray absorptiometry at baseline and after 4 weeks of treatment. Data are expressed as mean ± SD. *P < 0.05 versus the corresponding OVX+Veh control. BMD, bone mineral density; E2, beta estradiol; OVX, ovariectomized; Veh, vehicle.

Table 7

Effect of RAD1901 on femur microarchitecture in ovariectomized rats[a]

Treatment	BV/TV (%)	ConnD (1/mm^3)	TbN (1/mm)	TbTh (mm)	TbSp (mm)	ABD (mgHA/ccm)
Sham	0.394 ± 0.069*	138 ± 21*	5.2 ± 0.6*	0.095 ± 0.008*	0.175 ± 0.029*	456 ± 61*
OVX+Veh	0.234 ± 0.065	91 ± 32	3.5 ± 0.9	0.085 ± 0.011	0.307 ± 0.086	301 ± 69
OVX+E2	0.309 ± 0.079*	125 ± 25*	4.8 ± 0.8*	0.086 ± 0.008	0.204 ± 0.054*	379 ± 75*
OVX+RAD1901	0.300 ± 0.066*	113 ± 22*	4.5 ± 0.8*	0.088 ± 0.008	0.218 ± 0.057*	370 ± 66*

[a]Adult female rats underwent either sham or ovariectomy surgery before treatment initiation with vehicle, E2 (0.01 mg/kg) or RAD1901 (3 mg/kg) once daily (n=20 per treatment group). After 4 weeks, Bone microarchitecture was evaluated using microcomputed tomography. Data are expressed as mean ± SD. *P < 0.05 versus the corresponding OVX+Veh control. ABD, apparent bone density; BV/TV, bone volume density; ConnD, connectivity density; E2, beta estradiol; OVX, ovariectomized; TbN, trabecular number; TbTh, trabecular thickness; TbSp, trabecular spacing; Veh, vehicle.

Table 8

Key baseline demographics of Phase 1 dose escalation study of RAD1901

	Placebo (N=8)	RAD1901 200 mg (N=15)	RAD1901 500 mg (N=14)	RAD1901 750 mg (N=8)	RAD1901 1,000 mg (N=7)
Race white (% of the cohort)	8(100)	14(93)	10(71)	8(100)	7(100)
Mean age, years	64	62	59	64	64
Mean BMI, kg/m^2	26.1	25	24.4	24.9	26.7

Table 9

Most frequent (>10%) treatment related AEs in a Phase 1 dose escalation study of RAD1901

	Placebo N=8 n(%)			200 mg N=15 n(%)			500 mg N=14 n(%)			750 mg N=8 n(%)			1000 mg N=7 n(%)			Total Active N=44 n(%)			Total TEAE N=44
	Gr1	Gr2	Gr3	Gr1	Gr2	Gr3	Gr1	Gr2	Gr3	Gr1	Gr2	Gr3	Gr1	Gr2	Gr3	Gr1	Gr2	Gr3	All
Nausea	2 (25)	0	0	5 (33)	0	0	3 (21)	2 (14)	0	2 (25)	1 (13)	0	4 (57)	2 (29)	0	14 (32)	5 (11)	0	19 (43)
Dyspepsia	1 (13)	0	0	3 (20)	0	0	5 (36)	2 (14)	0	4 (50)	0	0	1 (14)	1 (14)	0	13 (30)	3 (7)	0	16 (36)
Vomiting	0	0	0	2 (13)	0	0	1 (7)	5 (36)	1 (7)	0	2 (25)	0	0	3 (43)	0	3 (7)	10 (23)	1 (2)	14 (32)
Hot flush	1 (13)	0	0	2 (13)	0	0	6 (43)	0	0	2 (25)	0	0	1 (14)	0	0	11 (25)	0	0	11 (25)
Abdominal pain	1 (13)	0	0	2 (13)	2 (13)	0	3 (21)	0	0	1 (13)	0	0	1 (14)	1 (14)	0	7 (16)	3 (7)	0	10 (23)
Oesophageal pain	0	0	0	0	2 (13)	0	1 (7)	3 (21)	0	1 (13)	0	0	1 (14)	1 (14)	1 (14)	3 (7)	6 (14)	1 (2)	10 (23)
Headache	0	0	0	3 (20)	0	0	1 (7)	1 (7)	0	3 (38)	0	0	2 (29)	0	0	8 (20)	1 (2)	0	10 (23)
Hiccups	0	0	0	1 (7)	0	0	4 (29)	0	0	2 (25)	0	0	2 (29)	0	0	9 (20)	0	0	9 (20)
Salivary hypersecretion	0	0	0	2 (13)	0	0	2 (14)	0	0	2 (25)	0	0	2 (29)	0	0	8 (18)	0	0	8 (18)
Diarrhoea	1 (13)	0	0	0	0	0	3 (21)	0	0	0	0	0	3 (43)	1 (14)	0	6 (14)	1 (2)	0	7 (16)
Dysphagia	0	0	0	0	0	0	1 (7)	2 (14)	0	3 (38)	1 (13)	0	0	0	0	4 (9)	3 (7)	0	7 (16)
Sensation of a foreign body	0	0	0	2 (13)	0	0	1 (7)	0	0	0	0	0	4 (57)	0	0	7 (16)	0	0	7 (16)
Abdominal distension	0	0	0	1 (7)	1 (7)	0	1 (7)	0	0	1 (13)	0	0	2 (29)	0	0	5 (11)	1 (2)	0	6 (14)
Odynophagia	0	0	0	2 (13)	0	0	1 (7)	1 (7)	0	0	0	0	1 (14)	1 (14)	0	4 (9)	2 (5)	0	6 (14)
Dizziness	2 (25)	0	0	1 (7)	0	0	2 (14)	0	0	1 (13)	0	0	1 (14)	0	0	5 (11)	0	0	5 (11)
Abdominal discomfort	0	0	0	3 (20)	0	0	0	0	0	1 (13)	1 (13)	0	0	0	0	4 (9)	1 (2)	0	5 (11)
Flatulance	0	0	0	2 (13)	0	0	2 (14)	0	0	1 (13)	0	0	0	0	0	5 (11)	0	0	5 (11)
Myalgia	1 (13)	0	0	2 (13)	1 (7)	0	0	1 (7)	0	1 (13)	0	0	0	0	0	3 (7)	2 (5)	0	5 (11)

Table 10

Pharmacokinetic parameters in a Phase 1 dose escalation study of RAD1901 (Day 7)

Parameter	Statistic	200 mg N=15	500 mg N=11	750 mg N=6	1000 mg N=3
C_{max} (ng/mL)	Geo-Mean Min, Max	49.8 30.6, 85.5	197 105, 316	322 248, 420	540 481, 602
t_{max} (h)	Median Min, Max	3.00 2.00, 6.00	4.00 2.00-6.02	3.00 3.00, 4.00	4.00 3.00, 6.00
$AUC_{0\text{-}tau}$ (h*ng/mL)	Geo-Mean Min, Max	670 418, 1181	2927 1562, 5460	4614 3209, 7183	8292 7281, 8947
$t_{1/2}$ (h)	Geo-Mean Min, Max	38.3 27.7, 51.4	37.5 33.8, 41.3	38.4 34.6, 46.4	42.3 38.7, 49.4

Table 11

Frequency of LBD mutations

	Frequency (%)
D538G	29.5
Y537S	25.0
Y537N	13.6
Y537C	9.1
E380Q	6.8
S463P	4.5
L536R	2.3
L536Q	2.3
P535H	2.3
V392I	2.3
V534E	2.3

Table 12

Differences of ER-α LBD-antagonist complexes in residue poses versus 3ERT

Residue #/ PDB	**L1-3/Helix 8**		**Helix 11**							**Helix 5**	**Helix 12**	
	M421	I424	E521	M522	H524	L525	Y526	S527	M528	E380	Y537	L540
2BJ4	x	x		x	x		x		x	x	NA	
2JFA	x	x		x	x		x	x	x		NA	
1SJ0	x	x	x	x	x		x	x	x			
2JF9		x		x	x	x	x	x	x		NA	
1YIM	x	x		x	x		x		x			
1R5K	x	x		x	x		x	x	X		x	x
1UMO	x	x		x	x							
1ERR	x	x			x	x	x	x				
2IOK	x	x			x		x	x	x		x	x
3UUC	x	x			x		x	x	x	x	x	
1YIN	x	x	x	X	x	x	x	x	x			
2AYR	x			X	x				x			
2OUZ	x	x				x			x			

Table 13

Evaluation of structure overlap of ER-α LBD-antagonist complexes by RMSD calculations:

	3ERT	2BJ4	2JFA	1SJ0	2JF9	1Y1M	1R5K	1UOM	1ERR	2IOK	3UUC	1Y1N	2AYR
RMSD													
3ERT													
2BJ4	0.804												
2JFA	1.196	0.554											
1SJ0	0.786	0.637	1.115										
2JF9	1.177	0.411	0.415	1.186									
1Y1M	0.978	0.687	1.118	0.276	1.072								
1R5K	1.483	0.759	0.52	1.307	0.892	1.342							
1UOM	0.739	0.761	0.723	0.489	0.909	0.499	1.115						
1ERR	1.12	0.483	0.595	1.016	0.851	1.112	1.208	0.918					
2IOK	0.824	0.689	0.787	0.899	0.897	0.854	1.208	0.736	0.838				
3UUC	1.024	0.915	0.896	1.03	0.888	1.036	1.228	1.012	0.873	0.929			
1Y1N	0.749	0.683	1.105	0.432	1.061	0.318	1.293	0.557	1.076	0.744	1.015		
2AYR	0.659	0.682	0.95	0.792	1.124	0.777	1.391	0.491	1.118	0.071	1.031	0.581	

Table 14

Analysis of ligand binding in ER-α LBD-antagonist complexes

	Ligand: Binding to	**EC_{50} (μM)**	**Comments**
3ERT	OHT: E353, R394	0.010	Flipped amine, F404 was too far from the phenol thus there were no pi-interactions
2BJ4	OHT: E353, R394, pi F404	0.010	
2JF9	OHT: E353, D351, H524, pi F404	0.010	
2JFA	RAL: E353, D351, H524 and pi F404 x2	0.002	
1ERR	RAL: E353, D351, R394 and pi F404 x2	0.002	Phenol flipped for H524
1YIM	CM3: E353, H524,D351 pi F404	0.0015(IC_{50})	D351-carboxyle oriented well with pyrrolidine
1YIN	CM3: E535, H524 pi F404	0.001	
1SJ0	E4D: E353, H524, pi F404 x 2	0.0008(IC_{50})	
1R5K	GW5: D351 pi F404	0.039(IC_{50})	No anchor bond with E353
1UOM	PTI: E353, H524 pi F404	NA	
2IOK	IOK: E353 pi F404	0.001	
3UUC	OD1: E353, R394, T347	NA	Very small compound
2OUZ	C3D :E353, pi F404	0.003	
2AYR	L4G: E353, pi F404 x2	0.0107	

Table 15

Model evaluation for RAD1901 docking

	EC_{50}(μM)	EF_{50} (=predictive power)	Can model predict crystal structure?	Ligand docking score	RAD1901 docking score
1ERR	0.001		No	-11.452	-7.912
3ERT	0.002		No	-12.175	-8.151
3UCC	NA	8474	Yes	-9.278	NA
2IOK	0.001		Yes	-11.952	-10.478
1R5K	0.039	6100	Yes	-11.518	-12.102
1SJ0	0.001	7511	Yes	-12.507	-9.816
2JFA	0.001	6780	Yes	-11.480	-11.055
2BJ4	0.002	5642	Yes	-9.727	-11.971
2OUZ	0.003	--	Yes	-11.789	-9.611

Table 16

Induced Fit Docking Score of RAD1901 with 1R5K, 1SJ0, 2IFA, 2BJ4 and 2OUZ

ER-α Crystal Structure	RAD1901 IFD Docking Score
1R5K	-14.1
1SJ0	-13.1
2JFA	-13.9
2BJ4	-13.8
2OUZ	-13.4

INTERNATIONAL SEARCH REPORT

International application No.
PCT/US 16/30317

A. CLASSIFICATION OF SUBJECT MATTER
IPC(8) - A01N 57/00; A01N 57/10 (2016.01)
CPC - A61K 31/66; A61K 31/685; C07F 9/1651
According to International Patent Classification (IPC) or to both national classification and IPC

B. FIELDS SEARCHED

Minimum documentation searched (classification system followed by classification symbols)
IPC(8): A01N 57/00; A01N 57/10 (2016.01)
CPC: A61K 31/66; A61K 31/685; C07F 9/1651

Documentation searched other than minimum documentation to the extent that such documents are included in the fields searched
USPC: 514/133; 514/146

Electronic data base consulted during the international search (name of data base and, where practicable, search terms used)
PatBase; Keyword limited: Mutant/drug-resistant/estrogen receptor alpha; RAD1901; breast/uterine/ovarian/pituitary/metastatic cancer; postmenopausal/relapsed/previous treatment AI/SERM/aromatase/anti-estrogen/antiestrogen

C. DOCUMENTS CONSIDERED TO BE RELEVANT

Category*	Citation of document, with indication, where appropriate, of the relevant passages	Relevant to claim No.
Y	WO 2014/203129 A1 (OLEMA PHARMACEUTICALS, INC.) 24 December 2014 (24.12.2014), entire document, especially: para [0003]; para [0037]; para [0049]; para [00104]; para [00127]; para [00150].	1-17
Y	US 2011/0124617 A1 (LYTTLE et al.) 26 May 2011 (26.05.2011), entire document, especially: para [0007]; para [0008], Formula I; para [0057]; para [0071]; para [0074]; para [0076]; para [0077]; para [0084]; para [0130].	1-17
Y	(ALLURI et al.) "Estrogen receptor mutations and their role in breast cancer progression"Breast Cancer Research . 2014. Vol. 16, pg 494, 8 pages, entire document, especially: abstract; pg 4, col 1, para 2; pg 4, col 2, para 1.	5-6

☐ Further documents are listed in the continuation of Box C. ☐

* Special categories of cited documents:
"A" document defining the general state of the art which is not considered to be of particular relevance
"E" earlier application or patent but published on or after the international filing date
"L" document which may throw doubts on priority claim(s) or which is cited to establish the publication date of another citation or other special reason (as specified)
"O" document referring to an oral disclosure, use, exhibition or other means
"P" document published prior to the international filing date but later than the priority date claimed
"T" later document published after the international filing date or priority date and not in conflict with the application but cited to understand the principle or theory underlying the invention
"X" document of particular relevance; the claimed invention cannot be considered novel or cannot be considered to involve an inventive step when the document is taken alone
"Y" document of particular relevance; the claimed invention cannot be considered to involve an inventive step when the document is combined with one or more other such documents, such combination being obvious to a person skilled in the art
"&" document member of the same patent family

Date of the actual completion of the international search	Date of mailing of the international search report
27 June 2016 (27.06.2016)	04 AUG 2016
Name and mailing address of the ISA/US Mail Stop PCT, Attn: ISA/US, Commissioner for Patents P.O. Box 1450, Alexandria, Virginia 22313-1450 Facsimile No. 571-273-8300	Authorized officer: Lee W. Young PCT Helpdesk: 571-272-4300 PCT OSP: 571-272-7774

Form PCT/ISA/210 (second sheet) (January 2015)

摘要

本文公開了在具有耐藥性雌激素受體α陽性癌症或突變型雌激素受體α陽性癌症的受試者中抑制腫瘤生長或產生腫瘤消退的方法。該方法需要向受試者施用治療有效量的、具有結構(I)的RAD1901或其鹽或其溶劑化物。